uh

THE PROPAGATION OF SOUND IN FOAMS

a thesis submitted for the degree of

Doctor of Philosophy

in the

University of London

and for the

Diploma of Imperial College of Science and Technology

by

George Anthony Vignaux, B Sc., A.R.C.S.

Acoustics Group

Royal College of Science

June, 1961

ABSTRACT

An apparatus has been constructed with which it is possible to produce, in a tube, constant and uniform foams with controllable density and bubble size. The sound source is situated at one end of the tube and a probe microphone is used as detector.

It has been found that owing to a series of transverse modes occurring in the frequency range used, measurements of the bulk properties of the foam were difficult to make except at low frequencies.

A hypothesis to explain both the existence of these modes and the discrepancy between the measured and theoretical values of the compressional sound velocity is proposed in terms of the existence of a foam shear modulus.

Theoretical analysis of the propagation of waves in an elastic medium which is confined in a rigid cylinder and of the thermal damping in a foam are contained in appendices.

ACKNOWLEDGEMENTS

The author is indebted to Dr. R.W.B. Stephens for his interest and guidance during the course of this work and to past and present members of the Acoustic Group, Royal College of Science, for their help and encouragement. He also wishes to thank Professor P.M.S. Blackett for allowing him laboratory facilities and to the Admiralty for the provision of a research grant. Finally he wishes to thank Mrs. M. Hartnup who typed the manuscript.

CONTENTS

CHAPTER 1

INTRODUCTION

Because foams are so easy to form and require no elaborate apparatus to make observations upon them, and also because of their intrinsic interest, they have been studied since the beginnings of science.

Foams are important not only to the engineer who used them in flotation or the fireman who fights fires with them, but because of their unique physical and chemical properties they have interest for the physical chemist, the rheologist and the physicist.

Professor G. Quincke of Heidelberg was once quoted as saying "Alle ist Schaum", a phrase which can have two possible interpretations, pointing out that everything in this world is evanescent, eventually reverting to dust, or alternatively that everything is made up of small cells, each one a separate entity yet forming a whole when clustered together. Both interpretations illustrate important characteristics of foams, their eventual collapse once they have been formed and the fact that they are composed of bubbles packed closely together forming cells whose shape depends upon the physical conditions.

However, foams also have a number of other unique properties which are interesting to the scientist. Their relatively large air content together with the aggregate effect of the separate

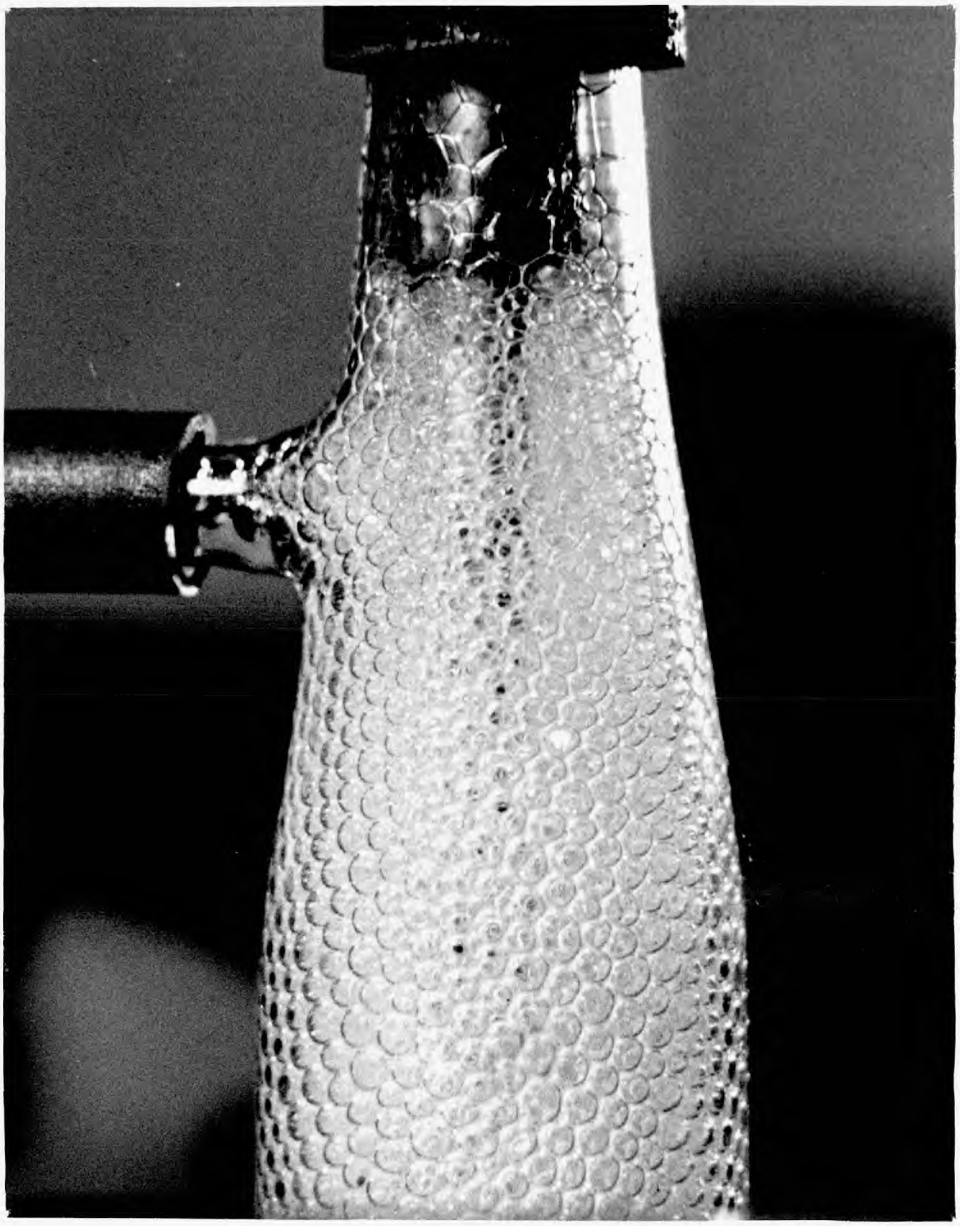

Fig. 1.1 A monodisperse foam produced in the Apparatus described in Chapter 7 (X 2.83)

bubbles results in a very low thermal conductivity; their relatively large surface area means that rapid transmission of substances from the gas to the liquid can take place easily and their surface active properties have led to their use in froth flotation.

But probably the most interesting attribute is their possession in some part of all the essential physical properties of solids, liquids and gases. When the foams are light and contain much gas then their compressional behaviour approximates to that of a gas; when they are dense they behave like liquids, and when the films are rigid they form a solid structure. Yet they are easily penetrated by measuring probes without breaking, they conduct electricity and transmit light. Thus they offer to a physicist a unique opportunity to study the propagation of waves through a solid using techniques already developed for liquids.

Most of the work that has been done on the propagation of waves in these media has been concerned with sound propagation in water containing bubbles and has confirmed the theoretical analysis of the properties for the case where the bubbles are widely spaced. It was felt that the investigation of foams of different densities would give some information about the properties of the intermediate region.

The first few chapters deal with the theoretical or measured mechanical properties of foams followed by discussion of the propagation of vibrations through the foam medium, particularly when it is monodisperse. A description is then given of the apparatus that has been developed to produce uniform monodisperse foams and to investigate their propagation characteristics for continuous acoustic waves. Finally, the results of the measurements made with the apparatus are examined critically in the light of the theories developed earlier.

The appendices include the author's theories for thermal and viscous damping in foams, a discussion of the propagation of waves in an elastic material contained in a cylinder and a glossary of important parameters that have been used to describe foams.

CHAPTER 2

FOAM PARAMETERS AND STRUCTURE

2.1. PARAMETERS USED IN DESCRIBING FOAMS

The most important mechanical properties of a foam are its bubble size and its density; they both play a great part in determining its physical properties.

The density of a foam can vary from nearly zero to about half that of the liquid composing the foam. Because of this large range, many different quantities have been used as a measure of density for maximum convenience in a particular range. Some of those used by various authors are listed in Appendix 1. In this report only a few of them are used: the density $\bar{\rho}$, defined in the normal way as the mass of unit volume of foam; the expansion ratio E defined as the ratio of the volume of foam to that of the liquid forming it; and the gas (or air) volume factor x.

Some relations between these parameters are set out below:

Foam density $\quad \bar{\rho} = \frac{\rho_L}{E}\left(1 + \frac{\rho_G}{\rho_L}(E-1)\right)$

Expansion Ratio $\quad E = \frac{1}{1-x}$

Gas volume factor $\quad x = \frac{E-1}{E}$

where ρ_G and ρ_L are the densities of gas and liquid respectively.

The value of density usually quoted is the mean density of the whole foam mass but owing to the phenomenon of drainage the density is not sufficient to describe these properties, for it will vary with both height above the base of the foam and with time. The rate of variation depends on the density, bubble size, viscosity of the solution (and hence on temperature), surface tension and density of the solution. It should be emphasised here, that as Bikerman points out, drainage and persistance of foams are entirely different phenomena, and should not be confused.

The problems associated with drainage will be examined in a later section, where the control of the foam parameters will be discussed.

The bubble size is, of course, most simply described by the bubble volume or radius, assuming that it is spherical. For a polydisperse foam, i.e. a foam with a wide distribution of bubble sizes, which are not only most common in nature but also have been studied more often, a distribution of function of bubble sizes must be constructed to give complete information on this aspect. However this has rarely been attempted not merely because of the labour entailed but also because in such a foam, the bubble sizes vary with time. This was demonstrated by Clark and Blackman (1948) who pointed out that, in such a foam, the pressure in the smaller bubbles is higher than that in the larger ones. This pressure difference leads to diffusion of gas through the bubble walls, the smaller bubbles decreasing in size and the larger ones increasing. The foam becomes more polydisperse as it becomes older.

As a measure of bubble size these authors used a quantity known as the "specific surface". This is defined as the area of interface between the disperse and the continuous phase included in unit volume of foam, and has the dimensions of $(\text{length})^{-1}$ (see Clark (1947)(6)).

Clark and Blackman showed that the specific surface, which was found to have an importance in considering the shear strength of foams, could also be estimated from measurements of light transmission through the foam. It must be pointed out here that Matelon (1953) (12) misquoted Clark (1948) (13) when he stated that the specific surface could be estimated from the conductivity. In fact Clark states that the conductivity ratio "... appears to be independent of the nature of the foaming agent and of the specific surface of the foam ...". This conclusion is partially confirmed by experiments made by the author, over a small range of bubble sizes, in connection with the measurement of the density of the foams used in the work to be described later.

If the foam is monodisperse*, the description of bubble size is simple. It is easily shown that the specific surface is given by the relation

$$S = \frac{3}{a}\,\frac{E-1}{E} = \frac{3\left(\frac{4}{3}\pi\right)^{\frac{1}{3}}}{v^{1/3}}\,\frac{E-1}{E}$$

where a is the bubble radius

and v is the bubble volume.

In this report, the bubble volume is used because it is this

---

* i.e. a foam made up of bubbles of uniform size.

quantity that is measured in the experimental work

2.2. THE STRUCTURE OF FOAMS

The shape of foam cells and the structure of foams have interested observers over a long period. The structure is of general theoretical interest since it demonstrates a solution of minimal area problems, but in particular for the purpose of this thesis it is of importance in the propagation of vibrations in the medium.

Foams can vary in density from comparatively light, rigid structures to heavy liquid masses of bubbly water. This range of physical properties leads to a change in relative importance of the different factors which combine to give the stability conditions affecting the foam structure.

For very light foams, the surface tension of the liquid lamellae is of overriding importance. There are two conditions to consider, the statics of the forces at each junction of lamellae and at each junction of the bounding lines between them; and the fact that, because of surface energy considerations the most stable configuration is that with minimum interfacial area.

The first of these conditions leads to the conclusion that for stability the angle between lamellae at their junctions (the Plateau Borders) must be 120°, and that four Plateau Borders must meet forming angles of 109° between them. If we examine the regular solid shapes whose packing repetition fills all space and

Fig 2.1 The possible theoretical forms of a completely Regular foam cell.

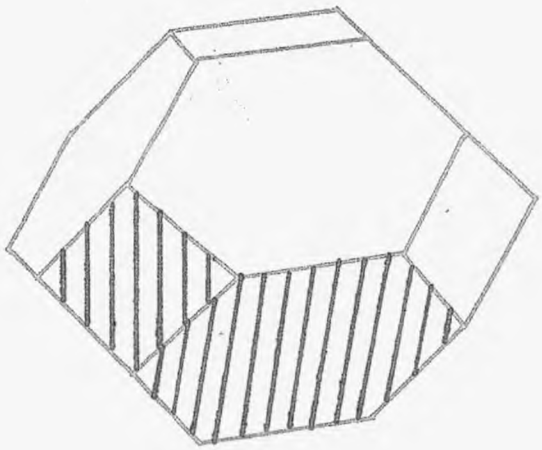

Tetrakaidecahedron (minimum area)

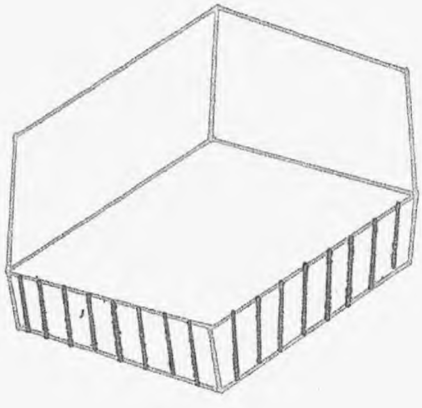

Rhombic Dodecahedron (face-centred cubic packing) whose geometry approximates to these conditions, we are left with the 12-sided Rhombic and Pentagonal Dodecahedra. The former body satisfies these conditions exactly.

The second condition is that the area of interface should be as small as possible. Lord Kelvin examined the most general solution for the homogeneous division of space and also the solution that gave the minimum partitional area. He showed that the Tetrakaidecahedral (or 14-hedral) cell which has 14 walls, in general not plane, satisfies these criteria. In this body there are 8 hexagonal and 6 quadrilateral walls. In the minimal area body, the squares which are plane are of two sizes, and the hexagons have curved faces.

In contrast, very dense monodisperse foams will approximate in structure to the packing of spheres. There are two closest packings of equal density for non-deformable spheres known as hexagonal and face-centred cubic packing. If we examine the shapes of the cells, each of which contains a sphere or bubble, we find that in the latter type of packing the cell shape is a regular Rhombic dodecahedron. If we allow the bubbles in a dense foam, packed in this way, to expand at the expense of the liquid, the air-space will approximate more and more to this shape.

The shape of foam cells have been investigated experimentally as well as theoretically. Desch examined the form of cells in gelatine, soap and rosin foams and concluded that the most common shape was that of the pentagonal 12-hedra. Matzke counted the faces of cells in a monodisperse foam, and showed that they had a mean number of 13.7 faces, consisting mainly of non-regular pentagons. In these experiments the structure was not regular.

These experiments agree with those carried out by various authors on the shapes of packed peas and lead shot after compression. Bernal has recently repeated these investigations, using plasticene lumps, in connection with theories of liquid structure. Mean numbers of faces of about 13.5 were found, although there was a large variation.

The similarity between the cell structures of living organisms and that of froths was observed soon after the invention of the microscope. D'Arcy Thompson suggested that similar forces, i.e. surface stresses and minimum areas are involved in the two cases. The cells of bees have caps which are sections of the surface of regular Rhombic 14-hedra and satisfy the requirements of minimum quantities of wax to enclose given volumes.

Summarizing therefore, it appears that for light foams the most stable structure (i.e. that which balances all the surface forces and which has minimum partitional area) should be one composed of non-regular 14-hedra and they are controlled essentially by surface tension forces alone.

In the case of dense monodisperse foams, gravity control is more important than surface tension forces and the structure will be face-centred cubic packing, giving a rhombic cell shape. This structure is directly observable.

As a foam drains, there must be a change in the most stable configuration from a cell shape of 12-hedra to one of 14-hedra as the surface forces become more important than the gravitational. This change cannot be undertaken merely by means of a smooth transition because the whole lattice shape must be modified, and we would expect in practice to find a mixture of packing types with a mean number of cell faces lying between 12 and 14. For light foams this mean will probably be nearer to 14. For polydisperse foams the change over of shape would be easier because the structure is less integrated.

CHAPTER 3

THE COMPRESSIBILITY OF FOAMS

3.1. BULK MODULUS AND COMPRESSIBILITY

A simple estimate of the compressibility of foams or masses of bubbles in a liquid can be made by considering the fractions of the two components together with their compressibilities. We may therefore write for the compressibility $\bar{\beta}$ for a foam

$$\bar{\beta} = x\beta_G + (1-x)\beta_L \qquad 3.01$$

where β_G and β_L are the compressibilities of the gas and liquid respectively

x is the gas volume ratio.

Now the compressibility of the gas phase β_G is calculated by differentiation of the equation of state of the gas

$$pv = RT \qquad 3.02$$

to substitute in the defining equation for compressibility

$$\beta_G = -\frac{dv}{v\,dp} \qquad 3.03$$

But the compressibility also depends on whether adiabatic or isothermal conditions prevail in the gas. Thus we obtain

$$\beta_G = \frac{1}{\bar{\gamma} p} \qquad 3.04$$

where $\bar{\gamma}$ lies between the extreme values of 1.00 for isothermal conditions in the gas, and 1.40 for adiabatic conditions.

Upon substitution for β_G into equation 3.01 we have

$$\beta_G = \frac{x}{\bar{\gamma} p} + (1-x)\beta_L \qquad 3.05$$

the compressibility of the liquid may be assumed to change little with the gas pressure.

This relation for the compressibility was obtained by Mallock (1910) (1), Wood (1955) (2), and Karplus (1958) (3) in connection with the velocity of sound in water containing bubbles.

Now for most mixtures, the compressibility due to the liquid can be ignored in comparison with that due to the gas and, making this approximation, we arrive at the simple relation

$$\bar{\beta} = \frac{x}{\bar{\gamma} P} \qquad 3.06$$

This will not be valid in the limiting case of very few bubbles, where $x \to 0$.

Comparison between 3·04 and 3·06 leads to the recognition of an analogy between the compressibility of a foam and that of a gas with the difference of the gas volume ratio. As x becomes nearer 1 this comparison is closer, as would be expected since the foam is then made up almost entirely of gas and very little liquid.

Penney and Blackman (1943) (4) showed that foams obeyed Boyle's Law of compression in a static experiment. Previously, Seihr (1938) (15) had anticipated the experiment but, as Matelon points out, owing to a limited pressure range, came to the conclusion that the foam behaved linearly, i.e. as an elastic solid. Penney and Blackman also demonstrated that compression takes place isothermally in foams (i.e. $\bar{\gamma} = 1{\cdot}00$) and this observation was verified for bubbly liquids by Karplus (1958). This leads naturally to a discussion of the thermal conditions inside the gas in the foam.

3.2. THE THERMAL CONDITIONS IN THE FOAM

There are two factors which must be taken into account when dealing with the heat conditions inside a foam subject to compressional stresses.

The first point is that the liquid, in our case water, has a much greater heat capacity than the gas (air) but it is the gas that is compressed the most. If we assume that the foam is completely dispersed (i.e. we may neglect the structure of the foam) and that the frequencies are high enough for no heat flow to take place between adjacent areas, then the effective specific heat ratio $\bar{\gamma}$ must lie somewhere between 1.00, its value for water, and 1.40, its value for air.

If, however the frequencies are low, or static compression is taking place, then isothermal conditions apply and the effective specific heat ratio will be 1:00 for all values of density.

In 1942, Heinrich (4) in a little known paper, proposed a theory for the equation of state for a foam or intimate mixture of a liquid and a gas, and derived a relation for $\bar{\gamma}$ in terms of his mixing ratio, z (see Appendix 1):

$$\bar{\gamma} = \frac{z C_p + C_L}{z C_v + C_L} \qquad 3.07$$

where C_p and C_v are the gas specific heats

C_L is the specific heat of the liquid, and where adiabatic conditions are assumed.

This relation has been tabulated (Table 3.1) for an air/water mixture, and is plotted against expansion ratio in fig 3.1. The table shows how different ways of expressing the foam density have different regions of effectiveness. It also demonstrates that the value of $\bar{\gamma}$ differs from 1.00 only for very light foams (i.e. $\rho < 0{\cdot}01$ or $E > 100$).

The second factor affecting the thermal conditions in the foam is the structure. If the frequency was such that, in a free gas, adiabatic conditions would prevail, for large bubbles the value of $\bar{\gamma}$ for the gas would be near 1.40. If the same amount of gas was distributed throughout the foam in the form of small bubbles, the water, being in better contact with the gas, would act as a heat sink and the conditions would be more nearly isothermal. In an intermediate case, where the bubble size is such that time is taken for conduction through the gas to the bubble wall, a phase lag between pressure change and volume change would be introduced and thermal damping would occur.

This phenomenon was investigated theoretically by Pfriem (1940) (16), but even in the simple case that he considered, that of a single bubble in an infinite medium, calculation of the damping factor and the variation in compressibility is tedious. This work is summarised in reference (17) where figures are given showing the variation of log decrement and resonant frequency of a bubble as a

(cont on p24)

TABLE 3.1 VALUES OF THE EFFECTIVE SPECIFIC HEAT RATIO OF A FOAM FOR VARIOUS DENSITIES

Showing also the relations between the different foam density parameters.

Density gm cm^{-3}	Air Volume Ratio	Heinrich's (Mass) Mixing Ratio	Expansion Factor	Effective Specific Heat Ratio
$\bar{\rho}$	x	z	E	$\bar{\gamma}-1$
1.00	0	0	1.00	0
0.667	0.333	0.613 10^{-3}	1.50	
0.500	.501	1.232 10^{-3}	2.005	
0.200	.801	4.94 10^{-3}	5.025	<0.5 10^{-3}
0.100	.902	0.0113	10.2	0.76 10^{-3}
0.050	.952	0.024	20.8	1.65 10^{-3}
0.010	.991	0.141	111	9.2 10^{-3}
5.0 10^{-3}	.996	0.330	250	21.3 10^{-3}
3.3 10^{-3}	.998	0.570	500	35.5 10^{-3}
2.0 10^{-3}	>.9995	1.600	1292	90 10^{-3}
1.67 10^{-3}		2.81	2268	0.145
1.426 10^{-3}		6.14	5000	0.208
1.326 10^{-3}		12.26	10^4	0.275
1.246 10^{-3}		61.4	5 10^4	0.368
1.236 10^{-3}		122.6	10^5	0.385
1.226 10^{-3}				0.402

The specific heat ratios were calculated for an intimate mixture of air and water at STP from Heinrich's formula, using the following values for the constants

ρ_L = 1.00 (gm cm^{-3})

ρ_G = 1.226 10^{-3} (gm cm^{-3})

γ = 1.402

C_L = 1.00 (cals $gm^{-1} deg^{-1}$ C)

C_p = 0.242(cals $gm^{-1} deg^{-1}$ C)

C_v = 0.175(cals $gm^{-1} deg^{-1}$ C)

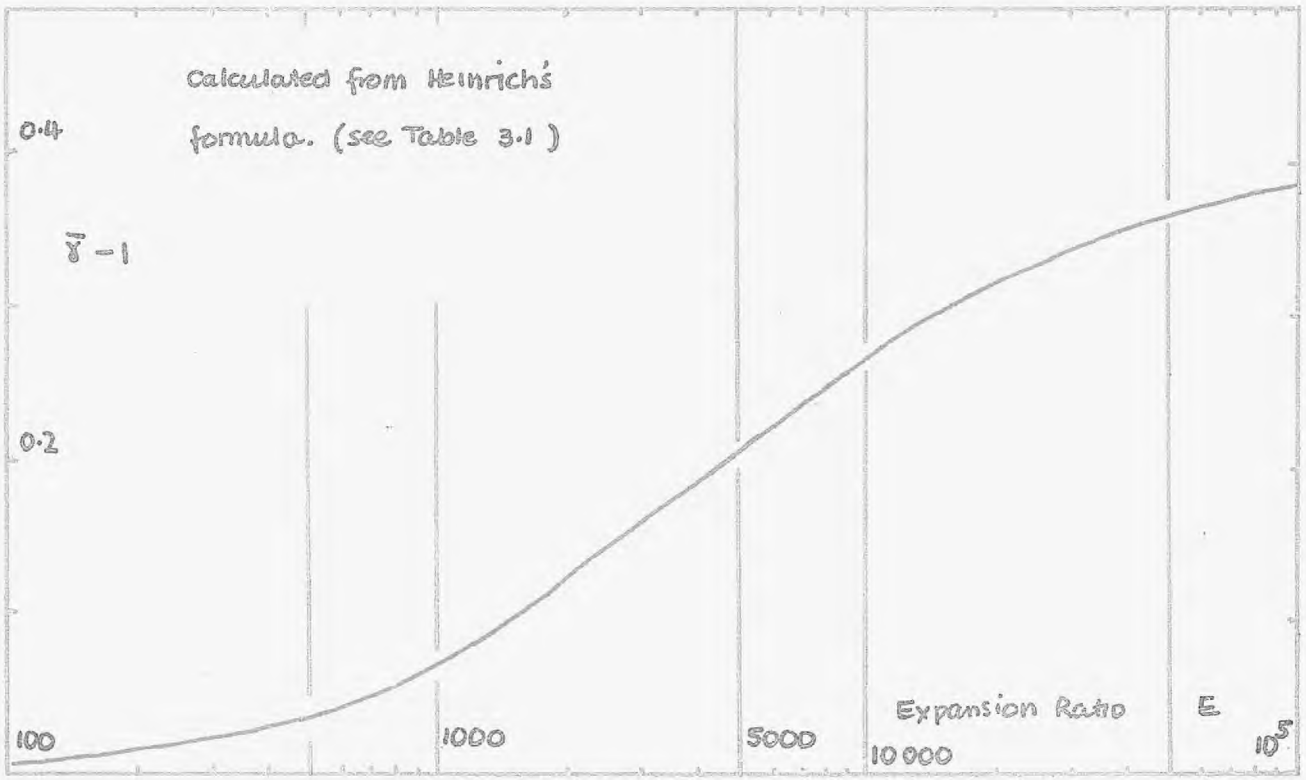

Fig 3.1 Effective Specific Heat Ratio $\bar{\gamma}$ as a function of Expansion Ratio

function of the quantity $2a\sqrt{\dfrac{\omega}{2b}}$

where b is the thermal diffusivity (definition in appendix)

a is the bubble radius

ω is the angular frequency

For a dense foam, the thermal conditions will be similar to those found in the above case, i.e. the liquid can be considered to be an infinite heat sink so that the temperature of the bubble walls will remain constant and independent of variations in the gas. If however, the foam is light, the bubble walls will vary in temperature slightly as the gas temperature changes during a pressure cycle. This means that the simple Pfriem theory is no longer valid.

A simple theory is proposed (Appendix 2) which takes into account the effect of the mass of the water. If we take first the simple case of very low frequency it shows that the real part of the bulk modulus of the gas in the foam is given by the relation

$$\bar{K}' = P\,\frac{\gamma(1+X)}{1+\gamma X} \qquad 3.08$$

where γ is the specific heat ratio of the gas and

$$X = \frac{\rho_L C_L}{\rho_G C_p}\,\frac{1}{E-1} \qquad 3.09$$

rearranging this expression and substituting in terms of Heinrich's mixing ratio, z, we have:

$$\bar{K}' = P\,\frac{zC_p + C_L}{zC_v + C_L} \qquad 3.10$$

or

$$\bar{\gamma} = \frac{zc_p + C_L}{zc_v + C_L} \qquad 3.07$$

which is the expression derived by Heinrich (4), and quoted above for the effective specific heat ratio for a foam.

Taking the case of very high frequencies or large bubble sizes we obtain from the theory the real part of the bulk modulus of the gas in the foam,

$$\bar{k}' = \gamma P \left[1 - 3\frac{\gamma - 1}{a}\sqrt{\frac{b}{2\omega}} \right] \qquad 3.11$$

which tends to the normal adiabatic case as the frequency tends to infinity.

At intermediate values of the frequency-bubble size function $2a\sqrt{\frac{\omega}{2b}}$ the bulk modulus has values lying between the extremes calculated at the limits. The damping becomes a maximum at an intermediate frequency, the value of the logarithmic decrement reaching about 0.35 for the dense foams but dropping when the foam expansion ratio becomes greater than about 100.

The derivation of these functions according to the simple theory proposed is set out in appendix 2 . Graphs and diagrams are drawn for both the effective specific heat ratio and the thermal logarithmic decrement, for certain values of expansion ratio.

3.3 THE EFFECT OF BUBBLE SIZE

A foam comprising very small gas bubbles will behave like a gas at a pressure above atmospheric. This excess pressure arising from capillary forces, will however be negligible, in the foams used, in comparison with the hydrostatic and atmospheric pressures already acting upon the bubbles.

The capillary pressure P_c is given by the relation

$$P_c = \frac{T}{a}$$

where T is the surface tension of the liquid*.

For $T \simeq 70$ (dyne cm^{-1}) and for a bubble radius $\simeq 0.5$ mm which was typical for the foams used in this work, we find that

$$P_c \simeq 1400 \text{ (dyne cm}^{-2}\text{)}$$

whereas $P \simeq 10^6$ (dyne cm^{-2}) is the atmospheric pressure

thus $\frac{P_c}{P} \simeq 0.2\ \%$

and it is clear that this effect may be neglected for the purpose of the present work.

Deryagin (1933) (18) pointed out that since the compression of the foam deforms the lamellae, the compressibility should be different from that of the gas phase. The same result is obtained by Bikerman (1953) p. 118 (10) and the bulk modulus was found to be

$$\bar{K} = P + \frac{2}{3} P_c$$

where P_c, as before, is the capillary pressure. The difference from atmospheric pressure is less than the capillary pressure since

---

* This may also be written in terms of the specific surface S if the foam may be assumed to be monodisperse

$$P_c = \frac{TS}{3} \frac{E}{E-1}$$

decreasing the volume of the bubble increases the capillary pressure and hence some of the pressure increase is taken up in this way rather than in decreasing the volume.

The same arguments used above may be applied to show that the difference is negligible when compared with the accuracy of measurement obtained in the experimental work.

3.4 COMPRESSIBILITY AND SHEAR MODULUS OF A FOAM

The previous analysis of compressibility or its reciprocal, bulk modulus, has been based on the assumption that the foam is a mixture of fluids which have no elastic shear modulus. If the structure of the foam results in a shear elasticity, then by definition, there will be an increase in bulk modulus.

We have

$$K = \lambda + \frac{2}{3}\mu \qquad 3.12$$

where K is the bulk modulus

λ, μ are Lamés constants, μ being the shear modulus.

3.5 CONCLUSION

We have shown that a suitable expression for the bulk modulus of a foam is

$$\bar{K} = \frac{\bar{\gamma} P}{x} + \frac{2}{3}\bar{\mu} \qquad 3.13$$

where we have assumed that the contribution due to the liquid compressibility is negligible and where $\bar{\gamma}$ is a function of frequency, bubble size and density but which can be considered to be near 1.00 for dense foams. $\bar{\mu}$ is the foam shear modulus which will be considered in the next section.

CHAPTER 4

THE SHEAR PROPERTIES OF FOAMS

4.1 THE BINGHAM MODEL

Penney and Blackman (1943) (14) first suggested that foams might behave as a Bingham body (19), (20) when they showed that foams possessed a critical shearing stress, beyond which, they behaved as liquids and below which they approximated to solids. However it is also true that foams exhibit some viscosity below this critical or yield stress and it is probable that in this region they act somewhat like a visco-elastic solid having the properties of creep under constant stress.

The properties of the Bingham body as a model for foams are illustrated in the diagram fig 4.1. The simple Bingham body, where $\eta_2 = \infty$ behaves according to the equations

$$\sigma = \mu\epsilon \qquad |\sigma| < |\theta|$$
$$\sigma - \theta = \eta_{pl}\frac{\partial\epsilon}{\partial t} \qquad |\sigma| \geq |\theta|$$

where σ is the applied shear stress

θ is the critical or yield stress

ϵ is the shear strain

μ is the shear elasticity or rigidity modulus

η_{pl} is the "plastic viscosity"

The diagram shows a plot of strain rate versus shear stress as a straight line, corresponding to the constant "plastic" viscosity, passing through the yield stress at zero strain rate.

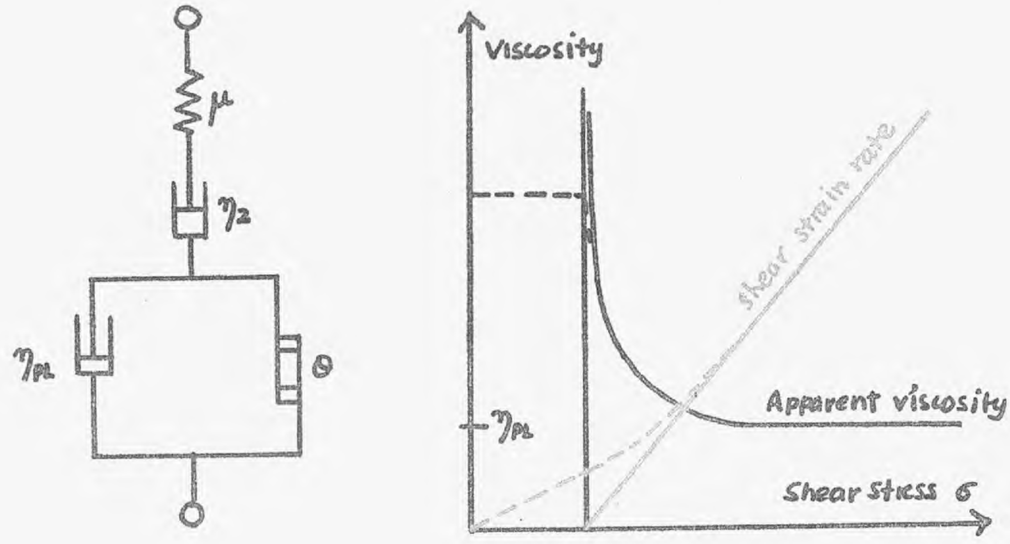

Fig 4.1 The Bingham Body as a model for the behaviour of a Foam in shear. With the visicosity η_2 in series

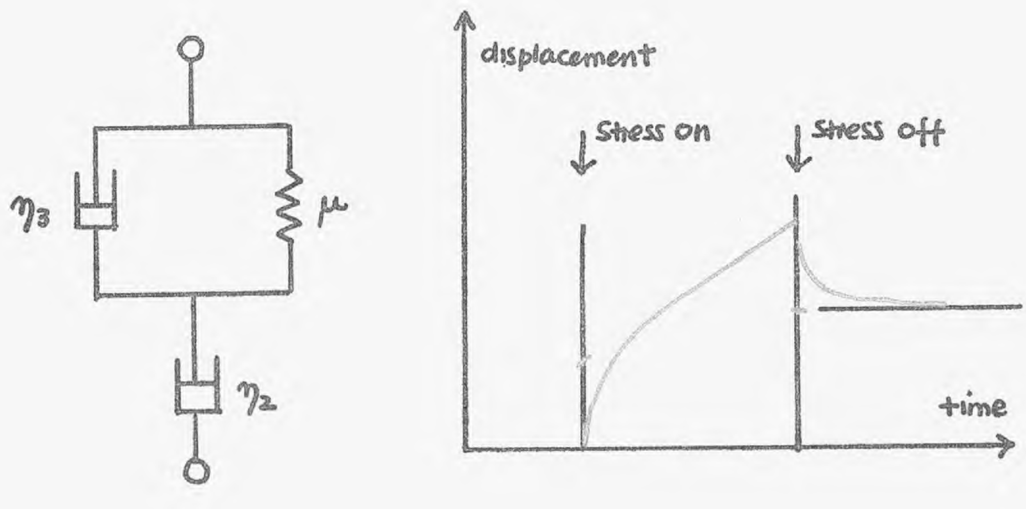

Fig 4.2 The lethersich Body as a model of the Foam below the yield stress and its responce to a step stress pulse.

The apparent viscosity, defined as the ratio of stress to strain rate becomes infinite at the yield stress.

If there is, in addition, a viscosity below the critical shear stress, the graphs would correspond more to the dashed curves in the diagram. It is probable that the viscosity would in any case be dependent on the stress amplitude.

4.2 THE ELASTIC SHEAR MODULUS OF FOAMS

Deryagin (1933) (18) first attempted to calculate the shear modulus of foam. He showed that by integrating for all possible inclinations of the surface containing surface tension forces, μ should be given the expression

$$\mu = 0.4 \, P_c$$

Deryagin and Obukhov (1934) tested this equation by measuring the shear modulus using a circular plate partly immersed in the foam and the value of P_c by measuring the increase in pressure caused by the collapse of the foam. Shear moduli of the order of 800–4500 (dyne-cm^{-2}) and values of $\frac{\mu}{P_c}$ of 0.23–0.70 are reported for 0.002% saponin solution. However, for 0.1% saponin solution $\mu \sim$ 22,000 and $\frac{\mu}{P_c}$ of 8.1 were found, showing a marked deviation from theory. It is probable that the plastic properties of saponin films make foams of this substance inappropriate for testing a theory based on the assumption of elastic surface forces only.

Blackman (1944) (23) showed that, below the yield stress, at least part of the displacement observed is elastic, and therefore recoverable but he quotes no values of the shear modulus.

4.3. THE VISCO-ELASTIC BEHAVIOUR OF FOAMS

Blackman demonstrated that foams exhibited visco-elastic behaviour in shear. Examination of the diagrams given (see (12) p. 337) indicates that a suitable model for behaviour at stresses less than the critical, would be the Lethersich body.(37) This model is indistinguishable in behaviour from the Jeffreys body and both are described in detail in ref. (20) p. 467 ff. The diagram fig. 4.2 shows this model and its response to a unit stress step on and off. Comparison with fig. 5, p.337 ref. (12) indicates that for this particular experiment this is a reasonable hypothesis to use in discussing the motion of the foam. (see fig. 4.3).

The equation governing the shear strain for this body is

$$\bar{\epsilon} = \bar{\sigma}\left[\frac{1}{p\eta_2} + \frac{1}{\eta_3\left(p+\frac{1}{\tau_1}\right)}\right]$$

where p is the operator $\frac{\partial}{\partial t}$ and

τ_1 is the retardation time of the Voigt-Kelvin part of the Lethersich body, given by $\tau_1 = \frac{\eta_3}{\mu}$. There also is a relaxation time τ_2 associated with this body, given by $\tau_2 = \frac{\eta_2+\eta_3}{\mu}$ and it can be shown that the stress relaxes with this time.

If we assume this hypothesis, we can approximate the behaviour of the foam by fitting the theory to the experimental curve found

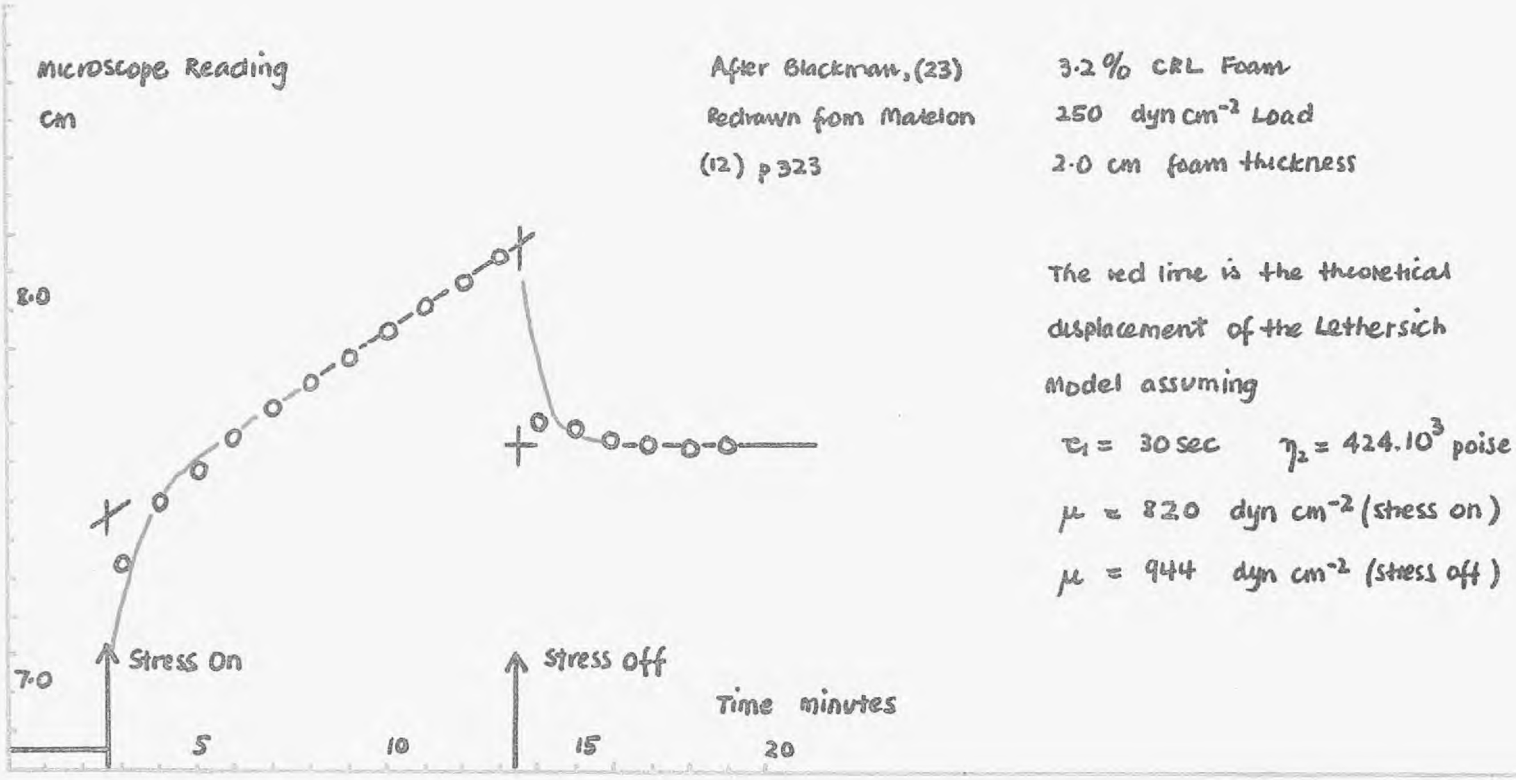

Fig 4.3 Horizontal Displacement of a sheared slab of Foam as a function of time

by Blackman (1944), (see fig 4.3). Using appropriate values of the parameters. The retardation time τ_1 , is shown to be about 30 secs., but the exponential form of the retardation appears to be only approximate. In addition to this, that part of the displacement which one would assume to be elastic is found not to be completely recoverable, and hence the Lethersich model does not completely describe the behaviour of the foam.

However, it seems to be indicated that this hypothesis is suitable for the general description of foam shear properties, needing at the most five parameters including the critical shearing stress and the plastic viscosity.

The Lethersich model has been described as representing the behaviour of an elastic sol, where elastic particles are assumed to be dispersed in a non-elastic viscous medium; forces are transmitted to the dispersed elastic medium by the flowing liquid. The Jeffreys body, which is the same in behaviour, was originally suggested to describe the rheological behaviour of the earth's crust, and represents a relaxing gel, a dispersion of viscous liquid in a continuous elastic solid. The Lethersich model serves well as a simple definition of a foam if each bubble if considered as a "particle" which is imbedded in a viscous liquid and which has a shear modulus measured by its resistance to distortion.

H. Fröhlich and R. Sack (1946) (26) examined theoretically the case of a dispersion of elastic spheres in a viscous liquid; they assumed that the concentration of the dispersion was very small and arrived at the following system of equations, where p represents the operator $\frac{\partial}{\partial t}$.

$$(1 + \tau_2 p)\,\bar{\sigma} = \eta^* (1 + \tau_1 p)\, p\, \bar{\epsilon}$$

η^* is the viscosity of the whole medium and is assumed to be given by Einstein's equation (1911)

$$\eta^* = \eta_m \left(1 + \tfrac{5}{2} x\right)$$

where it is assumed that the particles are rigid,

$$\tau_1 = \frac{3\eta_m}{2\mu_p}\left(1 - \tfrac{5}{2} x\right)$$

and

$$\tau_2 = \frac{3\eta_m}{2\mu_p}\left(1 + \tfrac{5}{3} x\right)$$

τ_1 and τ_2 are the relaxation and retardation times respectively, and η_m is the viscosity of the liquid (which is assumed to be Newtonian)

μ_p is the shear modulus of the material of the particles

x is the volume concentration of the particles.

Now ~~for~~ the Fröhlich-Sack system of equations is easily shown to be identical with those of the Lethersich Body if we put the following equivalents:

$$\eta_2 = \eta^*$$

$$\eta_3 = \frac{6}{25}\,\frac{\eta^*}{x}\left(1 - \tfrac{5}{2} x\right)$$

$$\mu = \frac{4}{25}\,\mu_p\left(1 + \tfrac{5}{2} x\right)$$

These equations are, of course, only valid for media where the concentration of the dispersed media is very small, but comparison of their properties with those of foams may be informative even though the concentrations of the latter may be near 100%. It suggests, for example, that the Lethersich lumped constant model is suitable for the description of the properties of dense foams and bubbly liquids and the extension to lighter foams is supported by the experiments described above by Blackman.

4.4 THE VISCOSITY OF FOAMS

Sibree (1934) (24) measured the apparent viscosity in a cylindrical viscometer for various shear rates. He showed that the apparent viscosity is a decreasing function of the shear rate tending to a limiting value which corresponds to our plastic viscosity. It was considered to be a characteristic of the foam, and was found to follow the Hatschek (1911) formula for emulsions except that a correction had to be made to the value of the concentration

$$\eta_2 = \frac{\eta_m}{1 - (1.3\ x)^{\frac{1}{3}}}$$

Grove (1951) et al. also measured the viscosity and again showed that it increased with the air volume. Blackman (1944) also found that it varied with the stress.

There is no suitable theory to explain the variation of viscosity with air volume of foams, because of the high values of concentration. It is reasonable to suppose that the following general principles apply:

1. that at very low concentrations, i.e. bubbly liquids, the viscosity should tend to that of a viscous liquid containing

elastic spheres, e.g. it should be given by a relation similar to that of Einstein's equation.

2. At high concentrations the viscosity below the yield stress should become very large. At the densest packing where the bubbles are unable to move relative to one another, the flow viscosity should become infinite.

Mooney's (1951) (28) equation satisfies these two principles

$$\eta_2 = \eta_m \exp\left(\frac{\frac{5}{2}x}{1-kx}\right)$$

where k is the "self crowding factor" and $1{\cdot}35 < k < 1{\cdot}91$ the limits representing the extremes of packing densities.

The variation of viscosity with stress and with shear rate is explained by the Bingham model, the material yielding at a certain value of stress. We consider this value, the critical shear stress, in the next section.

4.5 THE CRITICAL SHEAR STRESS

At a particular value of the stress the viscosity of some foams decreases suddenly. This value is known as the critical shear stress or, from comparison with the Bingham Model, the yield stress. It is the existence of this effect that makes the pumping of foams through tubes and pipes easy. Simple experiments show that a plug of foam subject to a small pressure difference moves slowly; as the pressure is increased the foam begins to flow easily and the apparent viscosity drops sharply.

Penney and Blackman (1943) (14) investigated this effect in connection with fire fighting foams, they measured the critical shear stress using an arrangement of rectangular zinc gauze plates, noting the stress at which the foam yielded. This apparatus was found to be useful with solid foams, but it was unsuitable for soap and other liquid foams. Blackman (1944) (23) repeated the experiments using a cylinder rotating in a box containing the foam. He showed that the viscosity drops suddenly from a value of the order of $10^5 - 10^9$ poise to about 1 poise for "solid" foams, but that with a soap foam no such liquefaction occurred because the foam structure collapsed before the critical shear stress was reached.

That the critical shear stress depends on the concentration and physical properties of the surface active agents in the foaming solution and also upon the specific surface of the foam, was demonstrated by Clark (1947). He found experimentally that this relation is obeyed:

$$\theta = (2.0 \pm 0.2).\theta_L.S.$$

where θ is the critical shearing stress

θ_L is the surface shearing stress of the liquid surface

and S is the specific surface of the foam.

The simple rupture theory that he proposed gave the constant as 1.00 but otherwise was identical with the empirical formula.

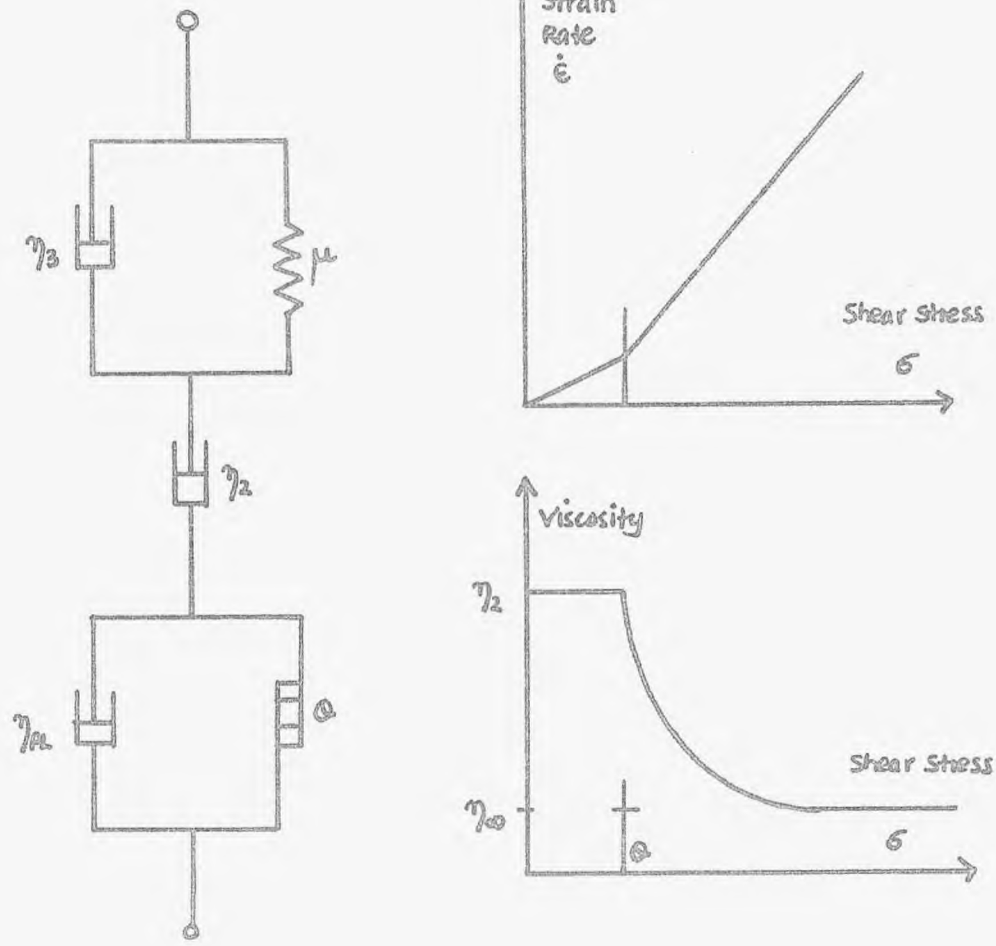

Fig 4.4 The Suggested Lethersich-Bingham Model for a Foam

4.6 CONCLUSIONS

We suggest that the shear properties of a foam can be described approximately by a combination of the Lethersich model together with a yield element, as suggested by Blackman, to form a complex Bingham Body. (see the diagram fig. 4-4).

Foams have a small elastic shear modulus and exhibit visco-elastic behaviour with a strain retardation time τ_1 . τ_1 was demonstrated to be of the order of 30 seconds for one foam. Values have not yet been predicted theoretically.

Foams have a viscosity which allows them to shear continuously. As yet, there is no acceptable theory for the viscosity as a function of foam density or bubble size, but it is known that it becomes greater for very light foams.

Most foams yield at a certain value of the stress; this value being a function of the yield stress of the surface film and the specific surface of the foam. Above this value, the viscosity is very low and the foam behaves as a liquid. Some foams have no specific value of yield stress and others, e.g. light soap foams, are destroyed before the yield stress is reached.

CHAPTER 5

THE VELOCITY OF VIBRATIONS IN A FOAM

5.1 INTRODUCTION

The classical theory of elasticity shows that there are two types of distortion that can be transmitted in a solid of infinite extent; the compressional wave, or P wave, characterised by the bulk modulus and involving volume changes in the medium, and the shear wave, or S wave in which there are no volume changes. All vibrations in the infinite medium must separately satisfy the two wave equations describing these waves.

However at the confines of the medium the boundary conditions must be satisfied as well. Rayleigh, and Love waves are examples of waves propagated under these conditions. Similarly other specific types of waves propagate along cylinders and rods; the equations for solid, infinitely long rods with completely free surfaces have been solved by Pochammer and Chree. In a later chapter we will be particularly interested in the propagation of waves in a solid cylinder with a rigid surface.

All of the equations which have been derived for the velocities of these special types of wave, however, involve the two velocities c_1 the P-wave and c_2 , the S-wave and we now go on to consider these two waves for the particular medium of interest.

5.2 COMPRESSIONAL WAVE VELOCITY AT VERY LOW FREQUENCIES

The velocity of compressional waves at infinite wavelength is given by the normal relation

$$c_1^2 = \frac{\bar{\lambda} + 2\bar{\mu}}{\bar{\rho}} = \frac{\bar{k} + \frac{2}{3}\bar{\mu}}{\bar{\rho}} \qquad 5.01$$

and substituting from the expressions already obtained, we have

$$c_1^2 = \frac{E^2}{E-1}\,\frac{\bar{\gamma}P}{\rho_L}\,\frac{\left[1 + 2\frac{E-1}{E}\frac{\bar{\mu}}{\bar{\gamma}P}\left(1 + \frac{\bar{\gamma}P}{E-1}\frac{1}{K_L}\right)\right]}{\left(1 + \frac{1}{E-1}\frac{\bar{\gamma}P}{K_L}\right)\left(1 + \frac{\rho_G}{\rho_L}(E-1)\right)} \qquad 5.02$$

where we have neglected the effect of the surface tension of the liquid upon the compressibiliby of the gas in the constituent bubbles of the foam. K_L is the bulk modulus of the foam liquid, approximately 2.10^{11} (dyn.cm^{-2}) for water.

Neglecting the foam shear modulus, $\bar{\mu}$, or in other words ignoring the structure of the foam,equation 5.02 reduces to

$$c_0^2 = \frac{\frac{E^2}{E-1}\,\frac{\bar{\gamma}P}{\rho_L}}{\left(1 + \frac{1}{E-1}\frac{\bar{\gamma}P}{K_L}\right)\left(1 + \frac{\rho_G}{\rho_L}(E-1)\right)} \qquad 5.03$$

This relation has been studied by Karplus (1958) (3) who considered different values of expansion ratio, E, and derived simple expressions for the velocity in different regions. Mallock (1910) (1) and Wood (1955) (2) have also derived this expression for mixtures of liquids with particular reference to gas bubble clouds in water.

Heinrich (1942) (4) in considering the propagation of sound in an intimate mixture, also derived an expression for $\bar{\gamma}$ as a function of the specific heat of the liquid and the mixture density. His method was to establish the equation of state of the mixture and

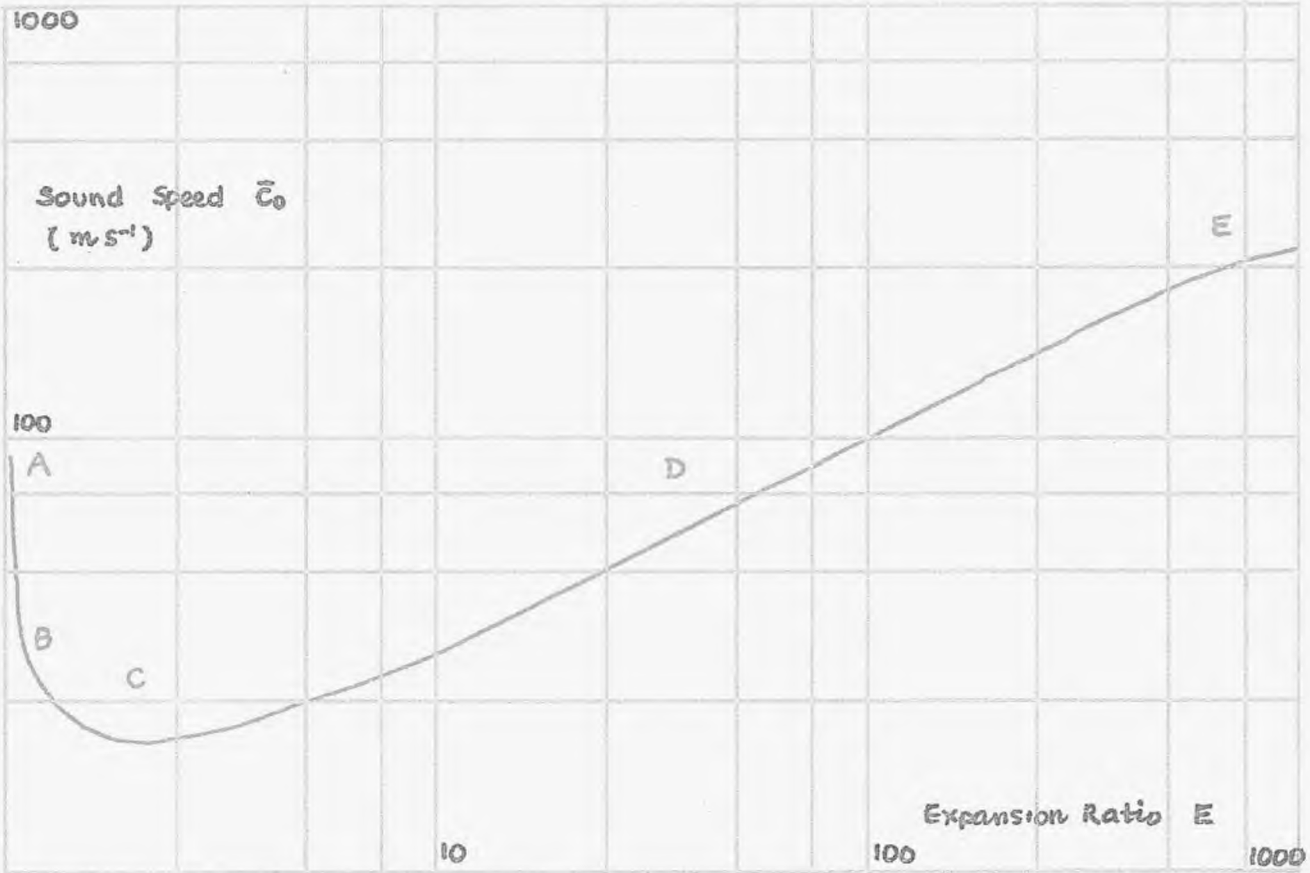

Fig 5.1 The Velocity of Sound in a Foam

(At constant pressure, at STP and neglecting the shear modulus and the liquid compressibility) to derive the velocity by differentiating the pressure with respect to the density. Evaluating equation 3 and plotting the calculated sound velocity as a function of the expansion ratio E, we arrive at figure 3.1 where we have used the numerical values for air and water at room temperature, and have assumed that the foam is, in fact, a homogeneous mixture of air and water; structural effects having been neglected.

In dense bubbly water ($E \leqslant 1.5$) Region A, the velocity decreases rapidly with expansion ratio from the velocity of sound in pure water, about 1500 ms^{-1}, as the compressibility increases without having a great effect upon the density of the medium.

In region B the effect of the increasing amount of air in the mixture curves the velocity line towards the minimum velocity region C.

The minimum velocity, about $20ms^{-1}$ occurs at a density of 0.5 $gm\ cm^{-3}$ ($E = 2$) for a water-air mixture. This low velocity exists because the medium there has half the compressibility of air together with half the density of water. Heinrich pointed out that the existence of this minimum implies a very low critical pumping speed for mixtures of these densities, a fact that might become important for high speed transport of foams. Under certain conditions of density and pumping rate it is possible to visualise that the foam will only be passing with high amplitude variations of density, since the mean density will be unstable.

As the amount of air increases, the velocity increases and is in this region proportional to E giving a straight line of slope 0.5 on the logarithmic graph. Since it is in this region, $(2 < E < 200)$, Region D, that most of the experimental work was done, this method of plotting is most convenient.

For very light foams, Region E $(E > 200)$ the density of the air becomes important in determining the sound velocity. The velocity curve flattens off towards the velocity in air, about 330 ms^{-1}.

Again equation 3 indicates that the sound speed is a function of the static pressure whereas this is not the case in either pure air or pure water (except to a second order). This effect is most important in region C, that of minimum velocity. Karplus showed from this observation that shock waves should be formed very easily and rapidly in bubbly mixtures. Cambell and Pitcher (1958) (35) have investigated the propagation of shock waves through mixtures of glycerine and water of these densities.

If there is a shear modulus, $\bar{\mu}$, the velocities will be higher than those given by this expression; the increase can be written in terms of the shear wave velocity

$$\bar{c}_1^{\,2} = \bar{c}_0^{\,2} + 2\bar{c}_2^{\,2} \qquad 5.04$$

where $\bar{c}_1$ is the compression wave velocity

$\bar{c}_0$ is the velocity assuming zero shear modulus as calculated from equation 3.

$\bar{C}_2$ is the shear wave velocity where

$$\bar{C}_2^{\,2} = \frac{\bar{\mu}}{\bar{\rho}} = \frac{\bar{\mu} E}{\rho_L} \qquad 5.05$$

for the case where the air density can be neglected.

5.3 THE FREQUENCY DISPERSION OF COMPRESSION WAVES

There are two mechanisms possible to explain a frequency dispersion of velocity. The first is that due to thermal or viscous relaxation effects giving rise to an increasing velocity with increasing frequency and to attenuation which passes through a maximum at a certain frequency. The second is a resonant mechanism, similar to that found in bubbles in water, or like the cut-off phenomenon in a low pass filter. This type of dispersion has been discussed at length by Brillouin; its general character is one of anomalous dispersion, the velocity dropping towards regions of maximum attenuation.

1. Relaxation Effects

(i) Thermal Relaxation

The thermal relaxation effect has already been discussed in the previous chapter and has been considered more thoroughly in the appendix. The velocity rises from that given by isothermal conditions to that given by adiabatic conditions as the effect of the liquid in the bubble walls becomes less important. This effect is best described in terms of the effective specific heat ratio, $\bar{\gamma}$.

The velocity ratio is then given by

$$\frac{C_{hi}}{C_{low}} = \left[\frac{\gamma(z + \frac{C_L}{C_V})}{\gamma . z + \frac{C_L}{C_V}}\right]^{\frac{1}{2}} \qquad 5.06$$

where $z = \frac{\rho_G}{\rho_L}(\epsilon - 1)$, is Heinrich's mixing ratio, and where the suffixes refer to high and low frequencies. The greatest rate of change of velocity with frequency coincides with the maximum value of damping, and occurs at a frequency-bubble size factor of

$$2a\sqrt{\frac{\omega}{2b}} \simeq \frac{3}{2}\pi$$

Other types of damping mechanisms in the medium will also produce velocity dispersion. In particular, we visualise effects due to viscosity in the liquid surrounding the bubble producing an out-of-phase component in the compressibility.

(ii) Visco-inertial relaxation

Nesterov (1959) (31) considered dispersion and attenuation in highly concentrated suspensions. His method was to imagine the suspension, not as spheres each in a cell of its own which is the usual approach, but as a regular lattice of packed cylinders of liquid. Each liquid cell contained a small cylinder of solid with the diameter equalling the height and having the same volume as the suspension particle. Calculation using this model gave an estimate of sound velocity and attenuation in a concentrated emulsion or suspension.

He presented the concept of a density which was frequency dependent and gave rise to dispersion and energy loss in waves travelling through the medium. He used the term "dynamic density" to describe this. The mechanism for the frequency dependence is that the movement of the solid plug will be different from that of the liquid surrounding it. This relative movement will be opposed by the viscosity, η , of the liquid.

Now we assume that this reasoning is equally applicable to the case of gas bubbles dispersed in a liquid. We therefore make the gas bubble equivalent to Nesterov's solid particle.

At low frequencies the solid particle (or gas bubble) and the liquid will move almost as one and therefore the cylindrical cell will have an effective density given by

$$Re[\bar{\rho}_{low}] = \frac{\rho_L}{E} + \frac{\rho_G}{E-1} \qquad 5.07$$

for frequencies where $\left[\frac{\omega \rho_L}{2\eta}\right]^{\frac{1}{2}} \delta \ll 1$

where δ is the mean gap width between particles. This, of course is the normal static density of the mixture, the masses of the components simply adding together.

At high frequencies, however, the particles (or bubbles) will tend to move independently. The frequency is then assumed to be so high that there are many wavelengths of the viscous wave across the cylindrical cell. (This has the corresponding case in the thermal damping example, where under adiabatic conditions there are many wavelengths of the thermal wave across the bubble). Under these conditions, the masses of the components add in a complicated manner to give the real part of the complex density. For foams, this will be given by

$$Re[\bar{\rho}_{hi}] = \rho_L \left\{ 1 + \frac{\frac{E-1}{E}(\rho_G - \rho_L)(2E-1)}{\rho_G + \rho_L(2E-2)} \right\} \qquad 5.08$$

$$\text{for} \left[\frac{\omega \rho_L}{2\eta}\right]^{\frac{1}{2}} \delta \gg 2$$

There is a transition region where the rate of change of velocity and the losses will be a maximum and this occurs when

$$\left[\frac{\omega \rho_L}{2\eta}\right]^{\frac{1}{2}} \delta \simeq 1.5$$

Assuming that the compressibility remains constant, the ratio of velocities for foams is given by

$$\frac{c_{hi}}{c_{low}} \simeq \sqrt{2}$$

where the distance between bubbles is assumed to be small.

2. Resonance Dispersion

There are two ways of approaching this problem, we may consider the foam as a mass of bubbles and examine the behaviour of this medium as a function of frequency, or conversely we may consider it as a loaded network comprising a three dimensional system of alternate layers of gas and liquid.

(i) Resonances of a gas bubble in a foam

Only the strongest resonance of a gas bubble, i.e. the volume resonance that is mainly responsible for the scattering and attenuation of sound waves passing through water containing bubbles, is considered here. The surface and other modes of resonance will be of importance at higher frequencies in the cut-off region but since, in the experimental work, it was not possible to reach these frequencies, these higher modes are here ignored.

Minnaert (1933) (29) first gave the frequency of this fundamental resonance as

$$\omega = \frac{1}{a}\sqrt{\frac{3\bar{\gamma}P}{\rho_L}} \tag{5.09}$$

where a is the bubble radius.

This phenomenon has received much attention since the beginning of the War, in connection with the propagation and attenuation in sea water containing bubbles (see for example references 1, 15, 16, 17, 30). However only the properties of single bubbles or of bubble clouds with spacing large enough so as not to interfere with the liquid flow between them have been considered. Foldy (1945) (32) examined the effect of wave scattering between bubbles. Macpherson (1956) (33) measured the reflection from and attenuation through lattices of bubbles with close spacing. He used Foldy's theory to interpret his results. The resonances in these systems were as predicted by theory.

It was shown that as the volume ratio of the gas in a bubbly liquid increases, the attenuation-frequency curve becomes closer to that displayed by a low pass filter. This statement is consistent with the properties suggested in the next section when we examine the Brillouin method.

When bubbles get very close together, the normal scattering theory is, of course, no longer applicable. It might, however, be possible to consider the resonance of a bubble in the midst of

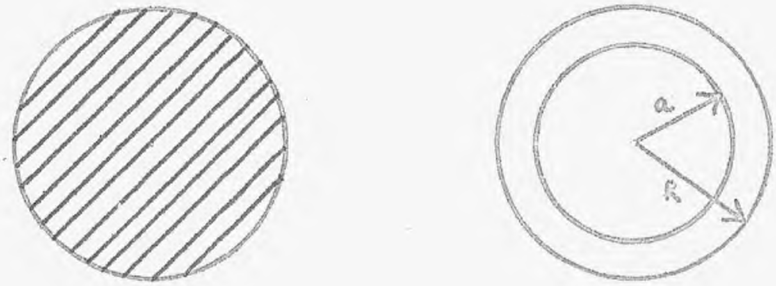

Foam medium , $\bar{K}$, $\bar{\rho}$

Cell of foam containing a bubble

The Models used in the Calculation

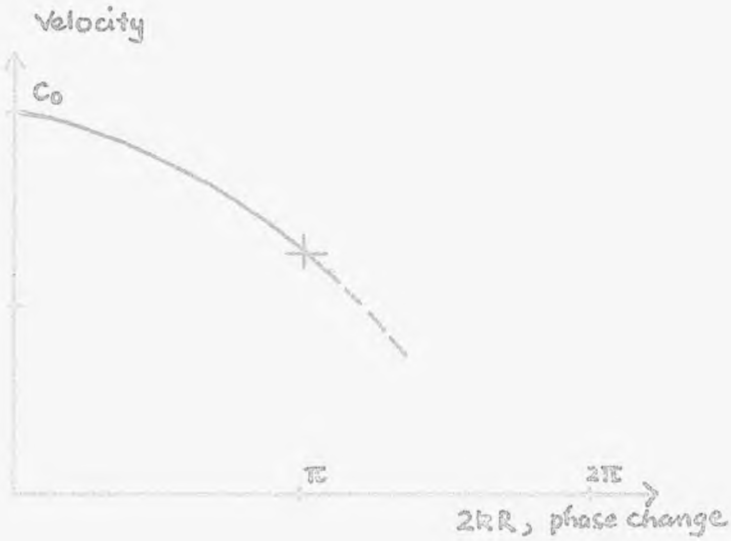

Phase velocity as a function of wavelength.

Fig 5.2 The Velocity of sound in a foam using the cell Method a mass of foam, using a method similar to that used by Fröhlich and Sack to examine the compressibility of such a cell. This method would give the impedance and velocity of the continuous medium having the same properties as the cell, but it would be invalid for wavelengths short enough for scattering to occur.

This method has been used for the case of a foam, where we assume that there is no wave structure in the liquid surrounding a bubble, i.e. the foam is light and the liquid film thin.

The analysis shows that the velocity drops gradually as the frequency is increased until the cut-off frequency is reached. This is given by

$$\omega_c^2 = \frac{3\bar{\gamma}P}{a^2\rho_L}(E-1)\left[\left(\frac{E-1}{E}\right)^{\frac{2}{3}}+1\right]^{-1} \qquad 5.10$$

and the velocity is then $\frac{2}{\pi}$ of the velocity at low frequency. The cell radius, R , is then equal to $\frac{\lambda}{4}$ (see fig. 5.2).

Beyond this frequency, according to the theory, the attenuation rised rapidly and the velocity drops still further. But in these regions, the assumption of infinite wavelength is no longer valid, and the equations do not necessarily give the correct velocity. Nevertheless it might be pointed out that the general behaviour is similar to that of the Brillouin lattice discussed in the next section.

(ii) The Brillouin Method

Brillouin* considered the propagation of waves in periodic

---

* see for example Brillouin, Leon "Wave Propagation in Periodic Structures" McGraw-Hill Book Co Inc. (1946).

Fig 5.3 The one-dimensional foam with Mechanical and Electrical Analogues

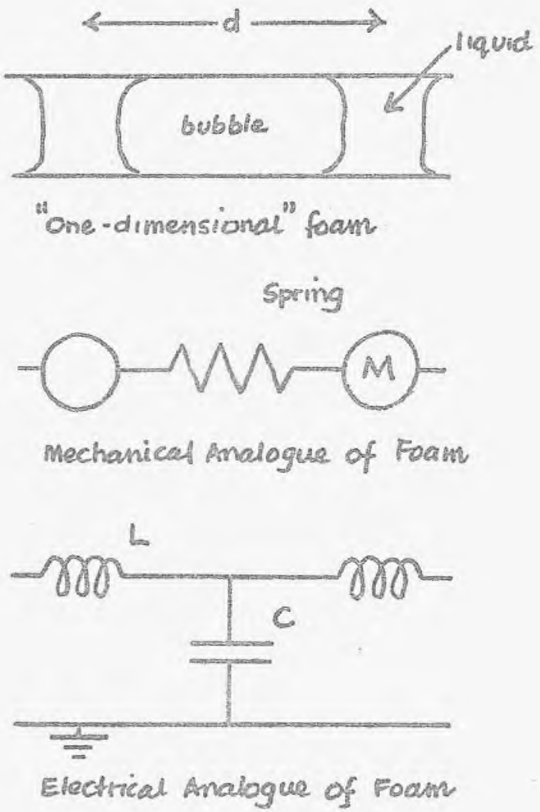

Fig 5.4 The corresponding Reciprocal Lattice for the one-dimensional Foam showing the first and second zones

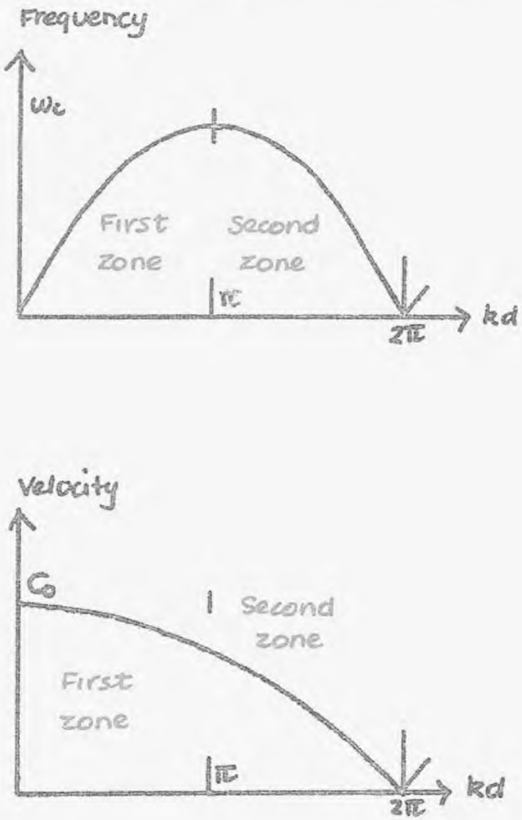

structures and introduced the concept of zones into discussion of these problems. This section deals with similar problems and uses his methods.

A light foam can be thought of as being made up of alternate layers of gas and liquid (fig. 5.3). If we accept this model, there is an obvious analogy with a low pass filter consisting of springs and masses set out in series. The behaviour of this system - a "one-dimensional foam" is shown in the diagram (fig. 5.4) where ω and c are plotted, in the reciprocal lattice, against kd, the phase change across a cell. In the usual crystal lattice case, it is found that the frequency is a periodic function of the wave number, thus at any one frequency there is ambiguity in the wavelength. In practice, then, the wave number is restricted to an interval containing one period of the frequency, and this interval is called the first zone. The limits of the first zone correspond to the longest wavelength possible at the cut-off frequency. Other zone limits, in the reciprocal lattice, correspond to successively shorter wavelengths (each one like modes, just fitting into the cell in the real lattice).

The behaviour of the Brillouin model is like that described in the previous section; there is a cut-off frequency and corresponding cut-off wavelengths and the velocity decreases towards the boundary of the first zone in the reciprocal lattice.

The equivalence between inductance and mass and between

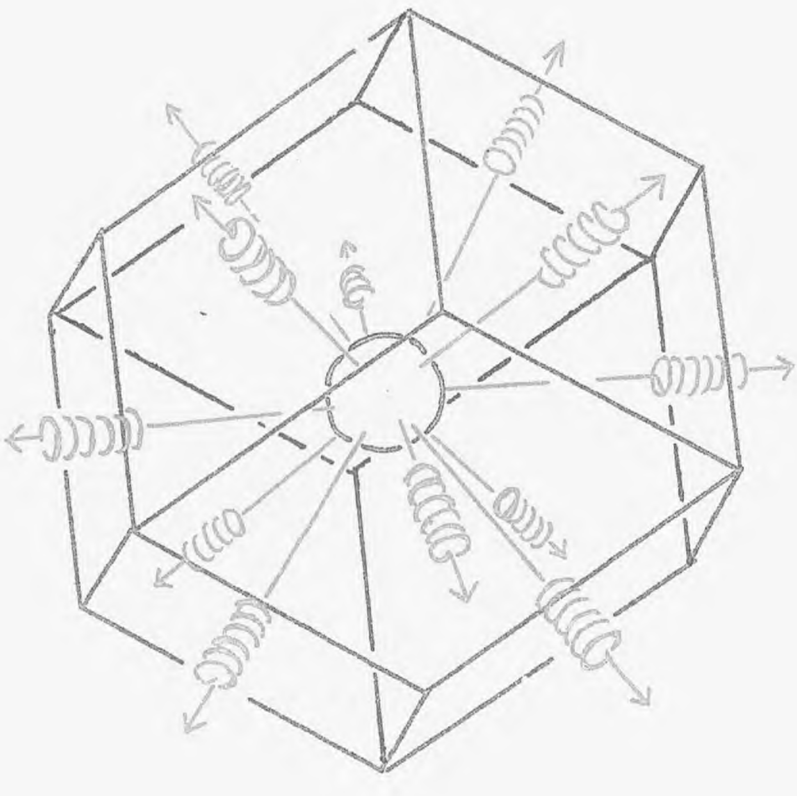

Fig 5.5 The Three dimensional Lumped Constant Model for a Foam.

capacitance and reciprocal of stiffness can be employed to make easier the visualisation of the problem, and we can extend the model into two or three dimensions using this method.

In the diagram, fig. 5.5, an attempt has been made to set up a model for the structure of a foam cell, based upon the face centred cubic packing. The conditions under which this type of packing is likely have been discussed previously (Chapter 2), and shown to be satisfied in the case of dense foams. It has the further advantage of mathematical simplicity.

The inductances represent the mass of liquid in the cell divided among the 12 faces of the rhombic dodeca-hedron and the sphere represents the capacity of the gas bubble.

This model behaves similarly to the uni-dimensional case, having a cut-off wavelength which varies with the direction of propagation of the wave relative to the lattice and the velocity decreasing towards the outside of the first zone which here takes the form of a regular 14-hedron.

(iii) Propagation beyond "cut-off"

We should expect on the basis of these models that vibrations will be attenuated rapidly at frequencies beyond the cut-off frequency. However, we have assumed that the liquid component is devoid of compressibility and that the gaseous component is devoid of mass, in addition to the assumed absence of damping.

The existence of these effects will lead to marked changes in behaviour. In particular, we visualise that the attenuation beyond cut-off will be less than would be predicted by the simple theories.

For example, at frequencies so high that the wavelength in air is much smaller than the bubble diameter, sound could propagate through the medium as through a series of separate rigid partitions, suffering heavy attenuation by reflection in the process. At intermediate frequencies, resonances within the enclosure of the bubble are to be expected.

Conversely, vibrations could be transmitted through the film structure with minor perturbations due to the air in the bubbles. Resonances due to surface vibrations in the cell walls would then be expected at certain frequencies.

3. Conclusion

On the basis of two simple models we are led to expect that the velocity of compressional waves in an infinite foam medium will drop as the frequency approaches the cut-off frequency. Estimates for this differ but it corresponds approximately to the frequency when the bubble diameter is one wavelength.

This decrease in velocity will probably be compensated to some extent by an increase in velocity due to relaxation effects arising from thermal and viscous processes.

5.4 SHEAR WAVE VELOCITY

The formula for the shear wave velocity is

$$\bar{c}_2^{\,2} = \frac{\bar{\mu}}{\bar{\rho}} = \frac{\bar{\mu}}{\rho_L} E \qquad 5.11$$

where $\bar{\mu}$ is the assumed shear modulus.

Since so little is known about the shear modulus of foams, an estimate of velocity cannot easily be made. We can predict from this equation, however, that if the shear modulus remains reasonably constant with density (and this is in doubt) the velocity should increase as $E^{1/2}$.

The frequency variation of velocity can be discussed with no greater confidence. We expect, from the discussion of the shear modulus in Chapter 4, that if the Lethersich model is assumed, the real part of the shear modulus will be given by the relation

$$\bar{\mu}' = \bar{\mu} \frac{\omega^2 (\tau_2 - \tau_1)^2}{(1 + \omega^2 \tau_2^2)} \qquad 5.12$$

where the symbols are the same as those used before (see also fig 6.1). This equation gives a rising velocity with frequency; over the same range the attenuation passes through a maximum.

A decrease in velocity with frequency is predicted by a cut-off mechanism identical to that examined in 5.2.2, the cut-off wavelength being, again, of the order of bubble size.

CHAPTER 6

THE ATTENUATION OF VIBRATIONS IN A FOAM

6.1 GENERAL PRINCIPLES

Attenuation of vibrations in any infinite medium is due to the presence of damping mechanisms which can be represented by imaginary components in the elastic moduli governing the motion. The attenuation of compressional waves in the foam is therefore most easily studied in terms of the ratio of imaginary to real parts of the bulk modulus and similarly that of shear waves in terms of the ratio of imaginary to real parts of the shear modulus.* This ratio is often expressed in terms of the logarithmic decrement, Δ, of the type of wave and damping considered and is given by

$$\Delta = \pi \omega \frac{K''}{K} \qquad 6.01$$

where K is the appropriate elastic modulus.

The various logarithmic decrements may, if they are small, be added together to give the total damping effect for the wave and hence the attenuation from the relation

$$\alpha = \frac{\omega}{2\pi C} \Delta_{total} \quad \text{nepers cm}^{-1} \qquad 6.02$$

where C is the velocity of the wave considered.

In this chapter we consider the different damping mechanisms that could give rise to attenuation of sound and shear waves in the foam medium.

---

* see for example H. Kolsky "Stress Waves in Solids" Oxford (1953) p.99 ff.

6.2 VISCO ELASTIC DAMPING

The shear properties of a foam below the critical shear stress have been discussed at length and the Lethersich Body was suggested as a model for its behaviour. The equation for this model under sinusoidal oscillation was shown to be

$$\bar{\epsilon} = \bar{\sigma}\left\{\frac{1}{i\omega\eta_2} + \frac{1}{\eta_3\left(i\omega+\frac{1}{\tau_1}\right)}\right\}$$

where the symbols have already been defined. We can find a complex shear modulus $\bar{\mu}$, given by

$$\frac{\bar{\sigma}}{\bar{\epsilon}} = \bar{\mu} = \frac{\omega^2\eta_2^{\,2}}{\mu(1+\omega^2\tau_2^{\,2})} + i\omega\eta_2\frac{1+\omega^2\tau_1\tau_2}{(1+\omega^2\tau_2^{\,2})}$$

We can simplify this expression by making some assumptions, for example we may assume that η_3 and hence τ_1 is very small. Then we find that

$$\bar{\mu} \simeq \mu\left[\frac{(\omega\tau_2)^2}{1+(\omega\tau_2)^2} + i\frac{(\omega\tau_2)}{1+(\omega\tau_2)^2}\right] \qquad 6.03$$

The real and imaginary parts of this expression are sketched in fig. 6.1. Hence the decrement for compressional waves will be

$$\Delta_V = \frac{4}{3}\,\frac{\pi\mu}{\bar{K}}\,\frac{\omega\tau_2}{1+(\omega\tau_2)^2} \qquad 6.04$$

where $$\tau_2 = \frac{\eta_2}{\mu}$$

and $\bar{K}$ is the foam bulk modulus.

From this expression the attenuation due to visco-elastic causes alone is found to be

$$\alpha = \frac{4}{3}\,\frac{\omega^2}{\bar{c}_1^{\,3}\,\rho}\,\frac{E\eta_2}{1+(\omega\tau_2)^2} \qquad \text{nep.cm}^{-1}$$

Similarly the decrement for shear waves, assuming the shear properties are as described here, will be approximately

Fig 6.1 The Shear Modulus of foams assuming the Lethersich Model. Assuming η_3 is negligible

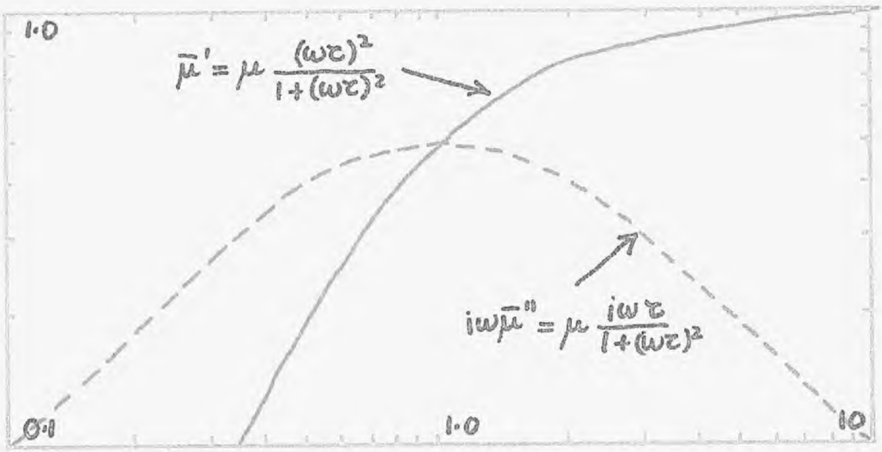

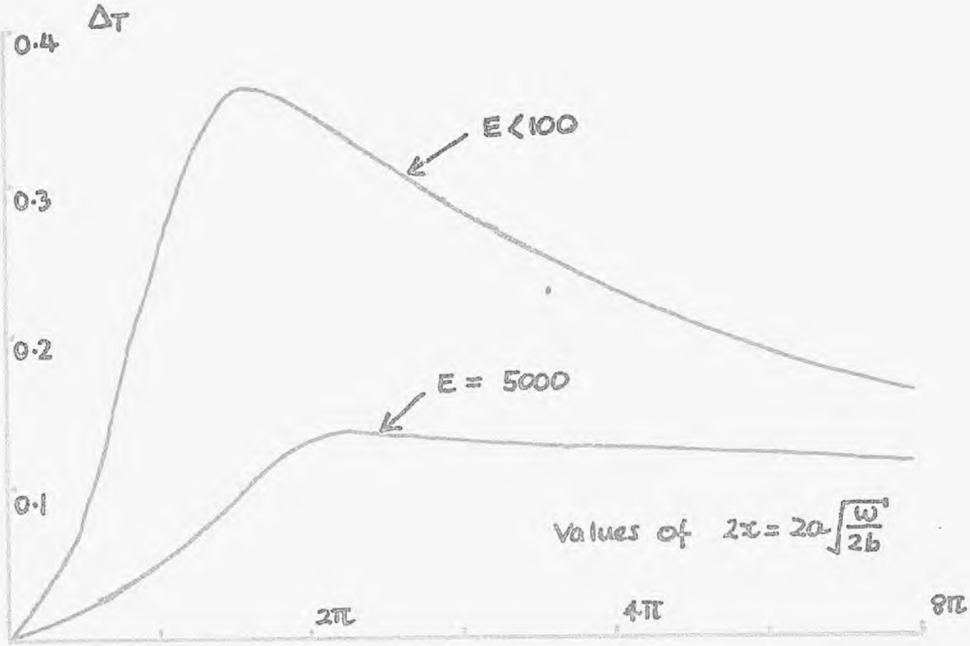

Fig 6.2 Values for the logarithmic damping decrement Δ_T

$$\Delta_V(\text{shear}) = \pi\omega \frac{1}{(\omega\tau_2)} = \frac{\pi}{\tau_2} \qquad 6.05$$

and hence the attenuation

$$\alpha_V(\text{shear}) = \frac{\omega}{2\bar{c}_2}\frac{1}{\tau_2} \qquad \text{nep-cm}^{-1}$$

6.3 VISCO-INERTIAL DAMPING

The dispersion due to this phenomenon, the longitudinal motion of the particles, in this case bubbles, parallel to the wave direction and against the action of the liquid viscosity, has been considered in a previous chapter. We are now interested in the attenuation that this might cause. Nesterov (1959) (31) gives complicated expressions for the imaginary part of the moduli for two cases which are similar to those quoted for the thermal damping case. The expressions are even more complicated if we no longer allow the frequency to be either very high or very low.

For our purposes, we are interested in effects at long wavelengths and low frequencies. Under these conditions, we find that

$$\Delta_{V1} = \frac{3\pi}{16}\frac{\omega^2}{\eta_L}(0.439\, b\, \rho_L)^2 c_{low}\left(\sqrt{\frac{2E-1}{2(E-1)}}-1\right)^2 \frac{2(E-1)^2}{2(2E-1)^2} \qquad 6.06$$

where we have substituted in terms of the expansion ratio for the foam and c_{low} is unaffected by the frequency and corresponds to the velocity calculated by the mixture method.

The decrement is inversely proportional to the liquid viscosity, but is proportional to the square of the frequency. It becomes very large as E becomes near 1 and tends to zero as E becomes large, as one would expect since there is then very little space for the bubble to move in.

6.4 THERMAL DAMPING

This section and the following one deal with damping processes that affect only the compression modulus, λ .

We have already discussed the mechanism of thermal damping, a fuller account is given in the appendix. The value of Δ_T which is predicted by the theory varies with the vibration frequency, foam density and bubble size but a maximum value of about 0.35 for dense foams is found (see fig. 6.2).

Over most of the range of variables the expressions for Δ_T are complicated, but at the limits simple analytical expressions can be derived.

For very low frequencies Δ_T reduces to

$$\Delta_T = \frac{\omega\pi}{5}\,\frac{\gamma-1}{\gamma}\,\frac{a^2}{b}\,\frac{\gamma X^2}{(1+X)(1+\gamma X)} \qquad 6.07$$

where the symbols are defined in the Appendix; and

$$X = \frac{\rho_L c_L}{\rho_G c_p}\,\frac{1}{E-1}$$

Now for very dense foams, when the ratio X becomes very large this expression reduces to that derived by Pfriem (1940) (16) for a single bubble oscillating in an infinite liquid;

$$\Delta_T = \frac{\omega\pi}{15}\cdot\frac{\gamma-1}{\gamma}\,\frac{a^2}{b} \quad (\omega \text{ small}) \qquad 6.08$$

The other simple case that can be considered is that for high frequency or large bubble size when Δ_T reduces to

$$\Delta_T = \pi \frac{3\frac{\gamma-1}{a}\sqrt{\frac{b}{2\omega}}}{1+\frac{3\gamma-1}{a}\sqrt{\frac{b}{2\omega}}} \qquad 6.09$$

which tends to that given by Pfriem in a similar way.

For intermediate ranges of frequency and bubble size, the values of Δ_T have been plotted for some values of E in the Appendix.

6.5 DILATATIONAL VISCOSITY DAMPING

A viscous resistance to pure expansion and contraction can be visualised for a foam and an attempt has been made in appendix 3 to obtain an expression for the decrement due to this. We find that

$$\Delta_D = \frac{4\pi\omega}{3} \cdot \frac{\eta_L}{\bar{\gamma} P \ E} \qquad 6.10$$

Δ_D becomes small as the foam gets lighter and the amount of liquid in each cell becomes small. This expression is similar to that suggested by Taylor's theory which is based upon the concept of independent bubbles rather than of cells, but the variation with foam density is different.

6.6 DISLOCATIONAL DAMPING

A foam, particularly when it is dense and approximates to a collection of elastic spheres, can be thought of as a sort of crystal. As such, loss of energy due to movement of bubbles in the lattice might be visualised. This will have a connection with the visco-inertial damping mechanism since the bubbles are moving against the action of the liquid viscosity, but it will only occur at high amplitudes of vibration. Bubbles are forced from one site to another in the lattice, the process giving rise to energy loss.

6.7 THERMAL ATTENUATION

At short wavelengths, there will be effects due to heat conduction parallel to the wave direction. A range of states from the isothermal to the adiabatic similar to that described in the "radial" thermal damping case, and a similar relaxation absorption peak would be expected.

The decrement will be

$$\Delta_{TL} = \frac{\pi \omega}{c_1^2} \frac{\bar{\gamma}-1}{\bar{\gamma}} \bar{b} \qquad 6.11$$

where $\bar{b}$ is the thermal diffusivity of the foam medium (see appendix 2).

6.8 CONCLUSION

We have discussed some of the different mechanisms that could give rise to energy absorption in foam. The most important effects are those due to foam viscosity, bubble movement inside the cell, heat flow inside the bubble and dilatational viscosity, and as a general rule they become greater for dense foams and for high frequencies.

The total attenuation for compressional waves will be given, for small decrements, by the relation

$$\alpha_c = \frac{\omega}{2\pi C_1} \left(\Delta_V + \Delta_{V1} + \Delta_T + \Delta_D \right) \qquad 6.12$$

and for shear waves

$$\alpha_S = \frac{\omega}{C_2 . 2\pi} \Delta_V (\text{shear}) \qquad 6.13$$

CHAPTER 7

THE FOAM-MAKING APPARATUS

7.1 EXPERIMENTAL REQUIREMENTS

So many of the properties of foams depend on bubble size and density that in order to make useful measurements both of these parameters must be specified exactly as functions of space and time.

The theoretical and experimental problems are simplified if monodisperse foams are used. They have several advantages over the polydisperse foams, notably spacial uniformity of structure and physical properties, constant drainage rate, constant bubble size with time and the possibility of the simple mathematical description of their structure and parameters. They suffer from the possible disadvantage of having a crystal-like structure (see chapter 2) which may affect the velocity of waves propagating in different directions. This effect will not be so marked if "polycrystalline" foams are used.

For our purpose it is not only necessary to be able to restrict the bubble size to within close limits but also to be able to change this size between runs so that foams of different properties may be investigated, and also it must be possible to measure the bubble volume as they are made.

The velocity and attenuation of foams also depends to a great extent upon the density. It will be a great advantage if we can

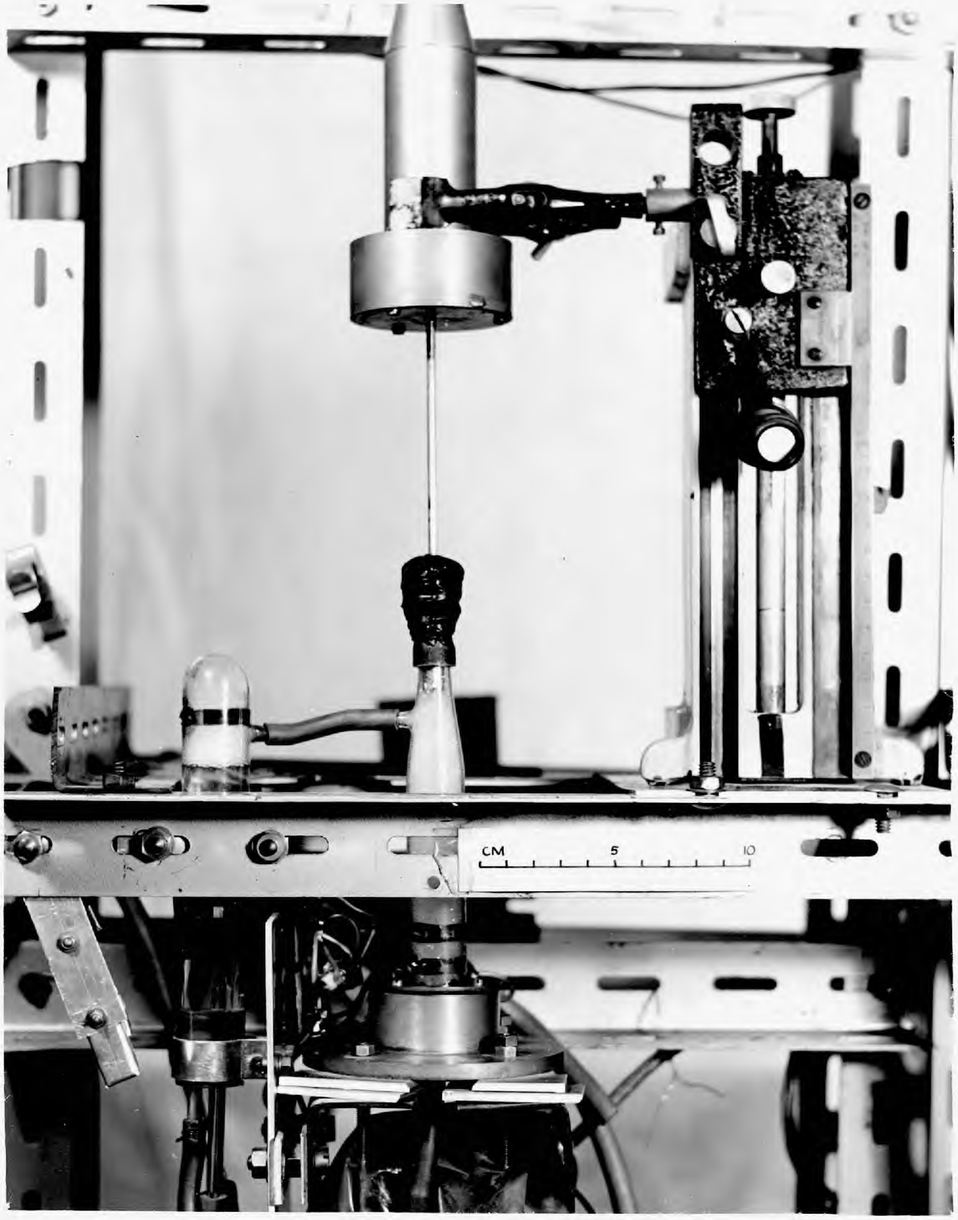

Fig. 7.1 The Apparatus in use with the large diameter tube fitted

make foams with a constant density in time and also in space. This is difficult even with monodisperse foams due to drainage, but an attempt has been made to restrict density variations as much as possible. It is convenient to be also able to change the foam density at will between runs, and it would be convenient to be able to measure it in situ.

The temperature has some effect on sound propagation and it is necessary to keep it constant during a run.

Lastly, the propagation of the vibrations in the foam so made must be measured to the accuracy desired and sound absorbers and anti-vibration mountings are needed to keep spurious signals to a minimum.

These requirements have led to the development of the apparatus to be described. Each section is described in some detail but we start with a short general account.

7.2 A GENERAL DESCRIPTION OF THE APPARATUS

A monodisperse foam is produced by bubbling air under constant pressure and at a constant rate through a single capillary into a solution of stergene and distilled water. The solution is supplied from a reservoir by a gear pump driven by a servo-motor whose speed is controlled automatically to keep the solution at the required level in the formation tube.

Foam is continuously extracted and forced through a narrow

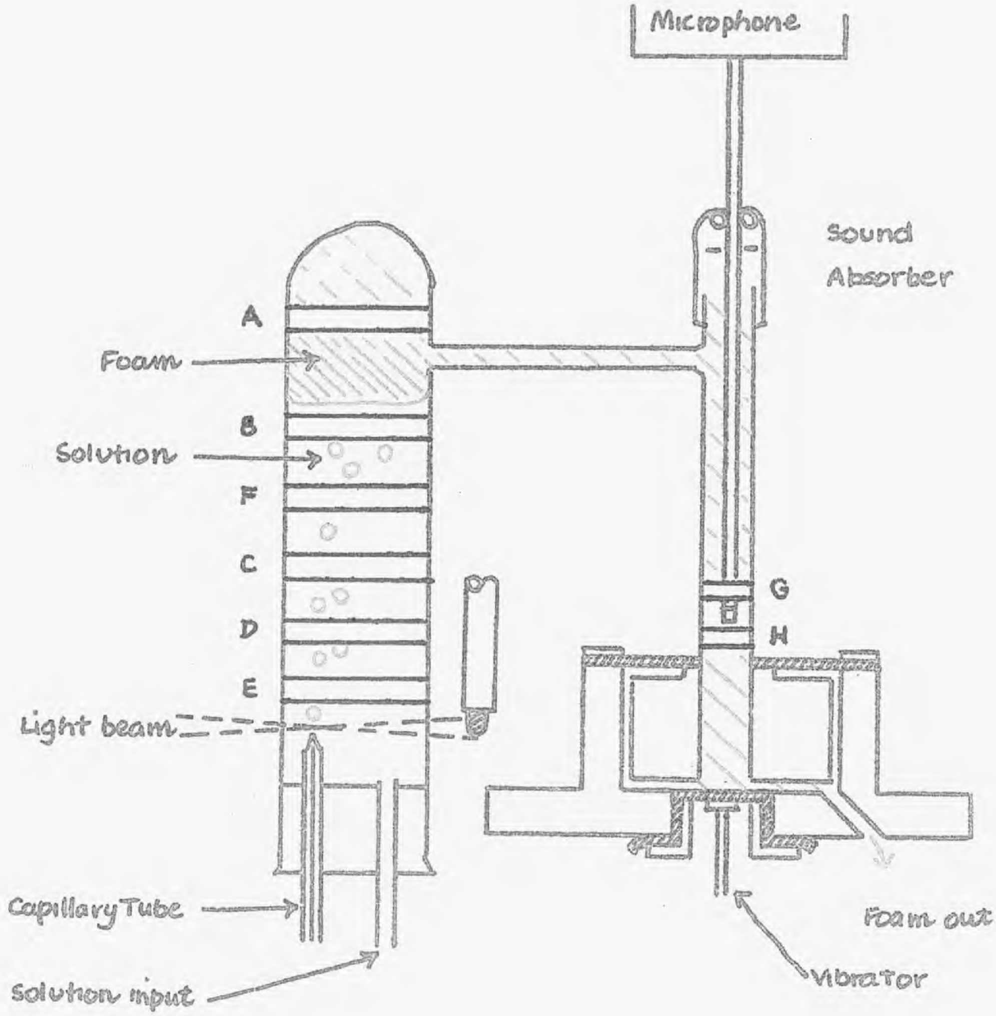

Fig 7.2 The foam Production and Measurement Apparatus, with small diameter tube fitted

connecting pipe (figs 7.1 and 7.2) into the propagation tube, down which it passes, flows out at the bottom and is collected in the reservoir.

A Goodmans electromechanical vibrator oscillates a rubber diaphragm at the base of the measurement tube and the sound waves pass up this tube to be absorbed at an attenuator at the top. A moveable probe microphone passes through the attenuator and down the axis of the tube and the phase and amplitude of the waves are measured as a function of position.

The bubble size is estimated from the air flow rate and the bubble emission frequency, and the foam density by using an electrical conductivity method.

7.3 THE BUBBLE FORMATION SYSTEM

It was decided to form bubbles from a single capillary tube as previous experiments had shown that bubbles of constant size can be produced by this simple system, provided that the gas pressure and flow rate are kept constant.

The air is supplied either by way of a pressure reducing valve from a cylinder or directly from the compressed air supply. A needle valve controls the flow rate into a large capacity bottle which serves to smooth out fluctuations in pressure caused by bubbling from the flow-off tube.

This is an arrangement consisting of a glass tube dipping beneath the surface of water contained in a wider tube. The depth beneath the surface can be varied at will and this controls the pressure in the system, since any excess pressure causes bubbling. During a run this tube is kept bubbling slowly to ensure a constant pressure. At this point it is possible to release the system to atmospheric pressure using the tap provided.

The air passes via a small capillary tube resistance to the flowmeter. This is another length of capillary tube across which is connected a water monometer measuring the drop in air pressure across it. The flowmeter can be cut-out while adjustments are made to the rest of the system. It is capable of an accuracy of about 5% with the most common flow rates (this accuracy could be improved if a commercial device like a rotameter were available).

The pressure relative to atmospheric is then measured using a mercury manometer but in practice this is used only as a check on the stability of the system. It was visualised that if the experimental accuracy had improved it would be necessary to correct the calculated bubble size for the pressure excess in the system (c.f. Clark (1948) (13)).

The air then passes by way of pressure tubing to the capillary tube bubbler at the bottom of the foam tube. The tubes are made by narrowing down standard capillary tubing. About twenty are made at a time, each one is given a number and they are stored in a stoppered bottle. When one is to be used, the drawn out tube is carefully broken off at a suitable point to obtain the orifice size required, usually about 0.1 mm. This system is successful in keeping the capillaries free from dust and grease.

After a period of use the tubes become partially or completely blocked with a white soapy deposit at the orifice. It is interesting to note that Karplus (1958) (3) p.83 found a similar deposit in his apparatus when he used detergent in the water. This blocking occurs sooner with the large bore capillaries than with the very thin ones, and it seems to be connected with the sucking back of the solution when the air pressure is reduced. This sucking back was observed frequently, particularly, as one would expect, with the wider capillaries.

The effect of partial blockage is to produce the so-called double-bubbling mode in which the bubbles are formed alternately one side and the other of the orifice. If the pressure is constant, this mode is stable but it is eliminated if the pressure is changed either up or down. It occurs also with supposedly normal capillaries at certain pressures. The bubbles produced are smaller in size than those produced in the normal mode and it is reasonable to suspect that the bubbles, produced as they are in pairs, are of two sizes, but simple observation using a stroboscope and photographing failed to detect any difference. Because of this, this mode was often used in practice for producing small bubbles.

By choosing capillary tubes of the correct diameter a whole range of bubble sizes can be produced. Bubble volumes in the range from 2 to 12 μL have been formed, but those of about 8 μL are used most often. The long term variations of air pressure, volume flow and temperature of the solution give rise to slow changes in the mean bubble volume within a range of about 10% during a run, but the variation from this mean over short periods of time is estimated to be less than 1%.

Having attempted to make bubbles of a constant volume, it is necessary to be able to measure their size continuously as they are being formed. The method used is discussed next.

7.4 BUBBLE SIZE MEASUREMENT

The bubble volume is estimated from the air volume flow rate and the frequency of bubble emission. The former quantity is found from the reading of the flowmeter, described above, after it had been calibrated.

To measure the rate of bubble emission, a D.C. galvanometer lamp is focussed onto the bubble stream, just above the orifice and a phototransistor put behind. The bubbles passing through the light beam give rise to an electrical signal which is fed directly to the Muirhead-Pametrada Wave Analyser where the frequency is measured. This frequency is doubled if the "double bubbling" mode is existing. The mean bubble volume is then calculated from the simple relation $v = \frac{Q}{F}$ where Q is the air volume flow and F the bubble emission frequency.

The method was checked by photographing the bubble chain. This also showed that the variation in volume between neighbouring bubbles was negligible.

7.5 THE PRODUCTION OF FOAMS OF CONSTANT DENSITY

1. The problem of foam drainage

As soon as a foam is formed the liquid contained in it drains through the bubble interstices at a rate which increases with the bubble size and foam density and decreases with the viscosity of the liquid (see for example reference (10) p. 98 ff.).

If the foam is allowed to stand, it will rapidly become non-uniform in density but if it is formed continuously there will be a steady state distribution whose shape will depend upon the experimental conditions.

Now the foam density is the second important foam parameter which must be controlled as closely as possible and for convenience it should also be variable at will.

In order to keep the spacial variation as small as possible the foam is made continuously and passed down the propagation tube by way of a connecting tube (see figs 7.1 and 7.2). This motion ensures that any portion of foam is not allowed time to drain to any great extent while in the measurement section and also that any drainage tends to smooth out the density variation, the heavier foam being removed continually from the bottom of the column and restored to the reservoir. The maximum time taken for a foam bubble to pass down the tube depends upon the density but, on an average, it is about 30 secs.

For very low densities, where the drainage rate is small, it is thought that the problem has been effectively solved, but for the higher values, where of course the conditions are much more stringent, the velocity of sound varies slightly with the position along the tube axis. It is reasonable to ascribe this to a non-uniform density distribution in the vertical direction.

2. The production of Foams of a Constant Density

The fact that foams drain, while a hindrance when uniform foams are required, become a help when a range of foam densities must be covered. All that is necessary is to sample a continually forming foam at a height above the liquid level in the bubbling tube which gives the required foam density. If the height is decreased the foam extracted will be denser, conversely if the height is increased the foam will be lighter.

If we continuously remove foam of a given density and also keep the air flow constant, as we must to ensure a fixed bubble size, the rate at which solution will be taken from the body of the liquid will change with the density required. The problem is therefore reduced to that of controlling the supply of solution so as to keep the top of the liquid, as precisely as this can be located, constant at any desired level under conditions where different flow rates may be required.

However, the supply of solution is also controlled to a great extent by the necessity to transport the foam once it has been made. The movement of a foam through a tube is opposed by a shear force which decreases with either the flow rate or the foam density. Thus for a given air flow and pressure inside the bubbling tube where the foam is formed, if the solution level rises by some chance, the sampled foam density increases and the drag is reduced. At constant pressure this means an increase in the foam flow rate and hence another decrease in the drag due to the foam motion. This results in a runaway action, rising foam flow rate leading to rising solution height and hence further increase in flow rate. We therefore have to deal with an unstable system.

Various methods to control the supply of solution have been tried. These include the simplest and most obvious, gravity feed; next a pressure feed from the air supply and then a manually controlled electric motor driving a gear pump. None of these methods however were satisfactory but the problems have been almost eliminated by using the servo system described below.

3. The Servo-System

The servo system was designed to eliminate the necessity to

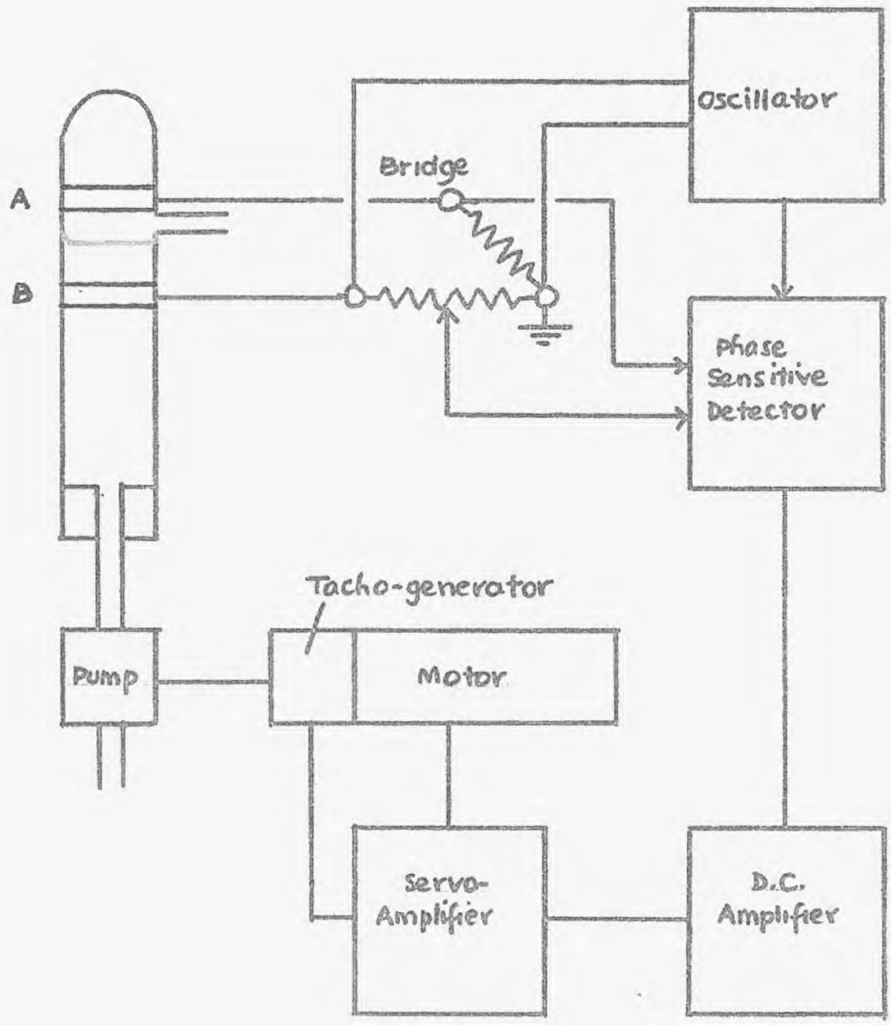

Fig 7.3 Block diagram of the Solution Supply System

check the solution level manually. Although there are still some problems associated with the device, at least the need for constant supervision has been eliminated.

The set-up is shown in the block diagram (fig 7.3). The solution-foam complex between the two platinum electrodes A and B on the bubbling tube form one resistance arm R_1 of a bridge. As the liquid level rises, this resistance decreases. R_2 is an ordinary carbon resistance (15 KΩ) for comparison. Provision has been made to replace this by the resistance of the solution between the electrodes B and F. This would eliminate drift of the balance due to variations of temperature or conductivity of the solution but it would be necessary to make special arrangements for starting up. The remaining arms of the bridge are formed by the two parts of the potentiometer used to set the standard solution level.

The bridge is supplied with an alternating voltage of 80 v at 50-200 c/s supplied from an oscillator (Mullard, BFO, Type E810). The error signal appearing when the bridge is out of balance is fed via a phase sensitive detector to a D.C. amplifier (Southern Instruments, Minirack MR 514 DC Pre-amplifier). The output from this is fed to the servo control unit (Feedback Ltd., SCIA).

A gear pump, driven by a servo motor supplies solution from the reservoir. The motor (Evershed and Vignoles type FAD 6 servo motor-generator) has a tachometer generator on the output drive shaft to provide a velocity feedback signal if it is required. The error signal is again amplified in the control unit and is fed to the field coils of the motor. When the error signal changes, the motor speed varies in unison; the system therefore, if connected the correct way round, will tend to stabilize so that there is a steady positive error signal, this signal corresponds to the loss of liquid into the foam.

If the foam required is dense, the system must not only raise the level to the appropriate one, but also stabilize at a higher pumping rate. The velocity feedback makes the system independent of changes of foam stiffness with density but also makes the system somewhat sluggish in reaction to changes. The only attention that the system needs during a run is the occasional balancing of the D.C. amplifiers which suffer from some drift which was probably the cause of a change in the stable position occurring over periods of a few hours even when the room temperature remained constant. As a further precaution against drift, all the control apparatus is fed from a constant voltage transformer to ensure that mains fluctuations are eliminated.

Apart from this, the system is an order of magnitude more stable than the previous manual control method, and it keeps the density constant to within $\pm$ 4%.

7.6 THE MEASUREMENT OF FOAM DENSITY

Having obtained a reasonably uniform foam that is also constant with time, then for accurate results, its density must be measured where the velocity measurements are to be carried out.

Clark (1948) (13) showed that the ratio of electrical conductivities of an aqueous foam to that of its solution, $\frac{\sigma_F}{\sigma_S}$, plotted against the ratio of the densities $\frac{\bar{\rho}}{\rho_S}$ lie on the same curve for a whole range of foams (see fig. 7.4). The parameters of this curve were shown to be independent of the chemical nature of the foaming agent, and of the bubble size.

This fact offers a simple method of measuring the density of the foam in situ without interfering with the acoustic measurements, provided that the calibration curve is first obtained.

Electrodes of platinum are baked onto the inner surfaces of the glass tubes and connections made to them by platinum 'tapes' sealed through the glass. Each electrode is 2 or 3 mm. in width and they are separated by more than 5 mm. (see figs. 7.1 and 7.2). Wires are soldered to silver electrodes painted and baked onto tapes. The outside of the tube is then painted with shellac or covered with Araldite to prevent external conduction due to dampness. Two electrodes G and H are placed inside the measurement tube and another three C, D and E are fixed well below solution level in the bubble tube. The three electrodes, A, B and F, at the top of the bubble tube are placed there for control purposes. Their function has already been described.

The conductivity ratio is measured directly by applying an alternating potential (of 50 to 80 volts at a frequency of 75 cps.)

across the potentiometer formed by the resistances (G to H) and (D to C (or E)) connected in series. The potential difference, V_s , across the solution electrodes (D to C (or E)) is measured. As the density of the foam increases so its resistance decreases and the voltage, V_s increases. When both tubes are filled with solution, this voltage is a maximum and this value is used to obtain the geometrical factor required to calculate the conductivity ratio. An alternating voltage is used to prevent polarization effects.

The system is calibrated using the set up as described but passing the foam into a measuring cylinder when a steady state has been reached. When a reasonable volume has been collected, the foam is weighed and the density calculated. The experiment is repeated for various densities and bubble sizes and the graph plotted. No variation with bubble size was found, but only a small range was covered. Consistent results have been obtained, but the curve differs slightly from that found by Clark (see fig. 7.4). However it is not claimed that this is an accurate absolute measurement of the conductivity ratio because errors due to surface conduction or pick-up are possible. It does give a calibration curve for the measurement of the density under the existing experimental conditions.

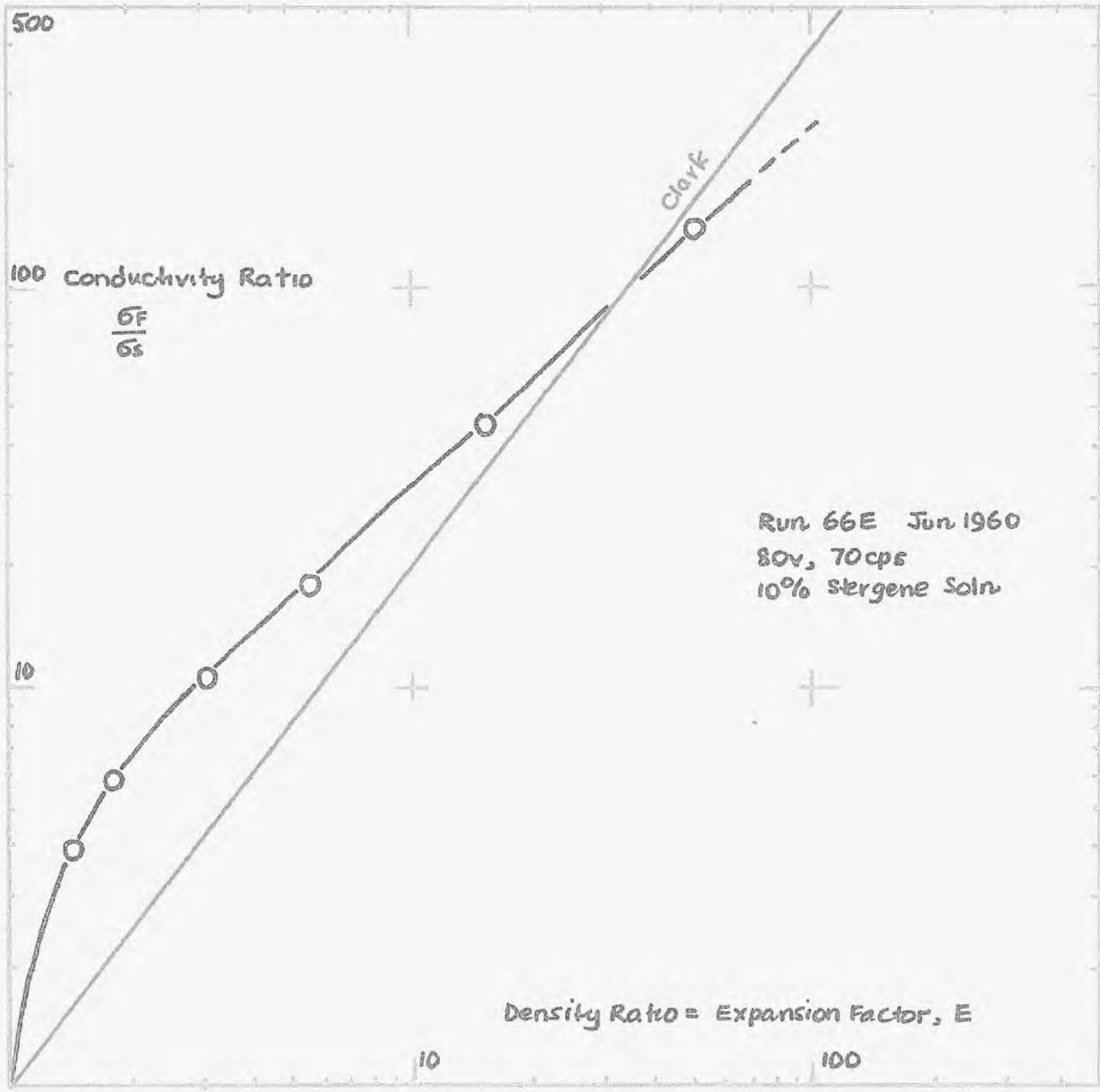

Fig 7.4 Calibration of the Conductivity Measurements

7.7 CONCLUSION

The apparatus described is able to make small quantities of a reasonable uniform density foam with a constant bubble size for periods of several hours.

Bubble sizes between $2\mu L$ to $12\mu L$ have been made with their volumes controlled within $\pm$ 10% over a few hours, and within $\pm$ 1% over periods of minutes.

Densities were automatically kept constant in time to within about $\pm$ 4% in the least favorable case, but there was often a slow change over a period of hours which meant that the density had to be checked and the control settings altered. Foam densities lying in the range 0.5 to 0.003 (gm/mL) ($2 < E < 300$) have been produced.

There is, however, some evidence of a small variation in density with height in the measurement tube. In order to eliminate this completely, greater rates of foam production must be used, than are possible with this apparatus (of the order of 100 mL per min.) so that the foam spends less time in the tube.

The mean bubble size is measured as they are produced from the orifice, and the foam density is measured at the position in the tube where the velocity and attenuation measurements are to take place.

It is these measurements that we shall deal with in the next chapter.

CHAPTER 8

ACOUSTIC DESIGN AND MEASUREMENTS

8.1 INTRODUCTION

The previous sections have dealt with the problems of forming a foam with constant and known parameters, and injecting it into the measuring chamber. We will now deal with the acoustic problems of measuring the sound velocity and attenuation in the foam.

The choice of the method of measurement is closely dependent upon an approximate knowledge of the attenuation in the foam and upon the frequencies at which it is desired and possible to work. After tests using resonant systems it was found that the attenuation in the foam was large and it was decided to use a continuous wave method and to work with frequencies between 1 and 20 kcs.

The method used is to measure the amplitude and the phase of the sound wave relative to the transducer as a function of distance along the axis of the measurement tube. At one time this was done by comparing the reference and the amplified sound amplitude picked up by a probe microphone directly on an oscilloscope by Lissajous figures. The positions at which a straight line was formed on the 'scope were measured. Since then a phasemeter has become available and this is now used exclusively.

8.2 THE MECHANICAL ARRANGEMENTS

Reference to figs. 7.1 and 7.2 will show the general design of the apparatus. Continuous sound waves are generated at the bottom of the measurement tube by a rubber diaphragm driven by a rod attached to a Goodman's vibrator. The vibrator is fed with the frequency required from a Bruel and Kjaer B.F. Oscillator (type 1012). The measurement tube (either 10 or 20 mm. diameter) is connected to the bubbling tube only by a narrow piece of rubber tubing to decrease the interference caused by the sound pulse emitted by the forming bubble. It is also mechanically isolated from the vibrating system by suspending the brass block in which it is embedded from a rubber sheet mounted upon the lower container. This reduces sound transmission by way of the glass, a factor that becomes important when vibrations are attenuated rapidly in the foam.

The measurement tube is also held in foam rubber higher up by a clamp fixed to another part of the frame. At very low frequencies this forms an alternative route for sound transmission and vibrations can be felt on the glass. In one version, with a narrow tube, a water jacket around the measurement tube loaded it as well as keeping the temperature constant.

To prevent standing waves in the foam the sound reaching the top of the measurement tube must be completely absorbed. This objective is partially achieved by the absorber used (fig. 8.1).

It consists of a tapered strip of metal foil coiled round a central hole left to allow the passage of the probe microphone. The coil is in the form of a spiral and its edge forms an internal cone narrowing towards the top. Behind this wedge absorber is a plug of glass wool and behind this an airtight joint with a neoprene ring which fits the microphone probe tube tightly. This is to retain the pressure which is forcing the foam down through the system. With very dense foams, at high flow rates, if this junction is not tight, there is a tendency for the foam column to break down, the top part of the tube containing no foam except that pouring down the side.

When used with air some standing waves can be detected in the tube but when it is filled with foam, which already has a high

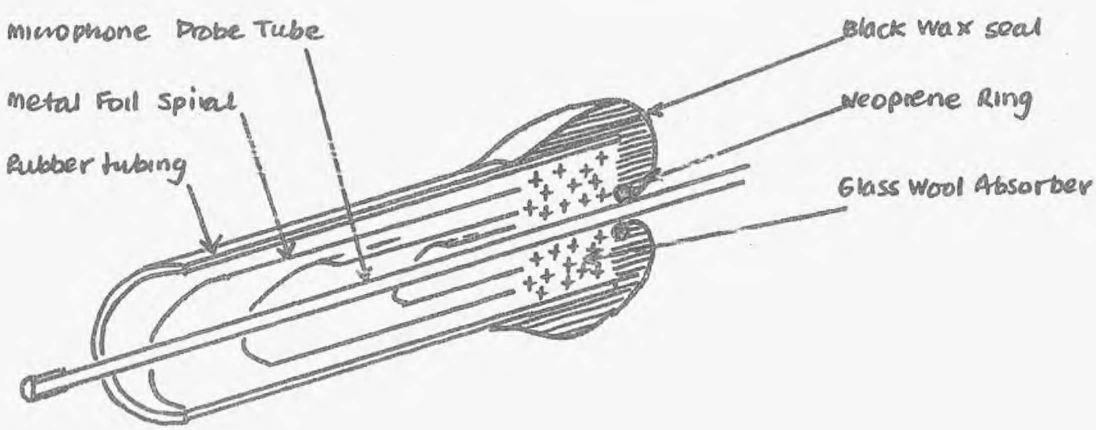

Fig 8·1 Sound Absorber fitted at the top of the Measurement tube attenuation, this simple absorber is quite effective over the frequency range used.

The pick-up device is a probe tube fitted to a Bruel and Kjaer condenser microphone. This is mounted upon a travelling microscope movement so that the height can be varied and measured accurately with a vernier scale. To prevent foam being forced up the probe tube the end is blocked with some $\frac{1}{4}$ thou. melinex sheeting fixed on with Durofix and wrapped with thin wire. This is effective at keeping out foam but highly attenuates sound transmission; no more satisfactory method seemed available however because of the small diameter of the probe tube (about 2 mm.).

8.3 THE ACOUSTIC MEASUREMENTS

A block diagram of the acoustic measurement system is shown in fig. 8.2.

The output from the microphone is amplified (B. and K. microphone amplifier type 2601) and then fed to the phasemeter together with a reference signal from the oscillator. The amplitude of the in-phase and in-quadrature components of the signal can be observed directly on the scales of the phasemeter (Solartron Resolved Component Indicator VP 250). The amplified sound output is also passed to the wave analyser which is here used to measure the amplitude. (Muirhead-Pametrada type D-489). A small 'Serviscope' oscilloscope monitors the output.

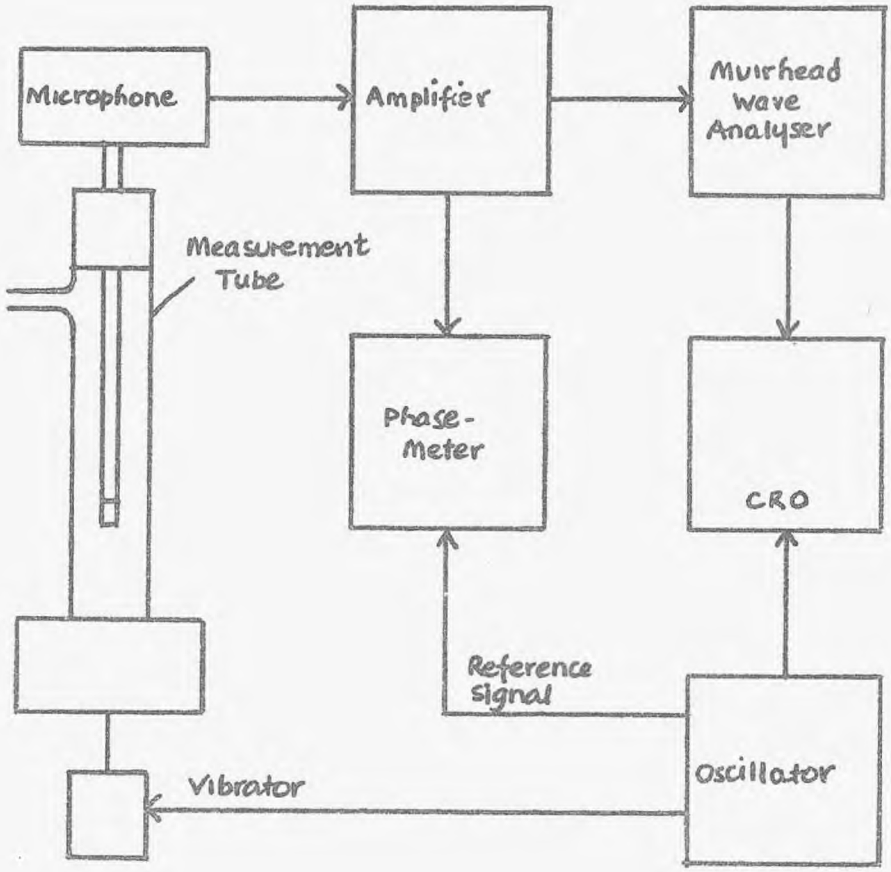

Fig 8.2 Block Diagram of the Sound Measurement system

The ratio of the in-quadrature to the in-phase components of the signal gives the tangent of the phase at the position of the probe end. The measurement is repeated for perhaps 10 positions over a range of a few centimetres, depending on the foam attenuation. The phase, in radians is calculated from the tangent by means of tables, and plotted against distance. The slope of this line to line together with the frequency, enables the phase velocity of the wave to be calculated. Similarly the amplitude, measured in decibels, is plotted against distance to give the attenuation.

The experiment is then repeated for each frequency to obtain the velocity and attenuation versus frequency curves.

Another technique was tried to deal with the attenuation peaks that were found and that will be discussed in the next chapter. It has here merely necessary to find the frequency at which maximum attenuation occurred, and this was done by keeping the microphone fixed and varying the frequency, The frequency corresponding to minimum sound amplitude was that of maximum attenuation. This was difficult to do in practice owing to spurious minima in the amplitude as the frequency was varied, possibly due to mode interference which it is suggested may occur in these regions.

CHAPTER 9

EXPERIMENTAL RESULTS

9.1 INTRODUCTION

The last two chapters have described the apparatus for producing uniform foams and for measuring the phase velocity and attenuation of sound waves passing through the sample. The results obtained from the measurements made with the apparatus are discussed now.

The analysis of the sound velocity at very long wavelengths, where the foam is assumed to be continuous, is tested first, and it is found that the measured velocity is always higher than that predicted by the theory for the particular foam density.

It is found that the measured phase velocity is a discontinuous function of frequency and that there are attenuation peaks near the discontinuities. The frequencies of these peaks depend upon the tube radius and their existence means that any change in the foam properties as a function of frequency cannot easily be determined using this type of apparatus. However, at low frequencies, below that of the first peak, the variations of velocity and attenuation can be measured.

In order to explain both the velocity discrepancy and the existence of the modes, a hypothesis in terms of the shear properties of the foam is put forward.

9.2 THE RELATION BETWEEN VELOCITY AND DENSITY

The first result to be established is that of the relation between the foam expansion factor and the "zero" compression wave velocity (i.e. the velocity at very long wavelength). The theoretical analysis of which is given in Chapter 3. It is however found that the compression wave velocity is a function of frequency and the zero value must be calculated by extrapolating from the velocity-frequency curve for each value of the density.

The values of these estimated zero velocities are plotted against the expansion ratio in the logarithmic graph (fig. 9.1) together with an indication of the estimated experimental errors.

Also drawn is the theoretical relation for a fluid foam, calculated from equation 3.3, assuming isothermal condition and standard temperature and pressure and that the media are pure air and water. This is a part of the curve drawn in fig. 3.1.

The measured points lie on a line that is displaced upwards by an amount significant compared with the errors. This displacement is equal to that produced by multiplying the calculated velocity by a constant factor of 1.5.

How can we explain this displacement of the measured points from the theoretical curve? We discuss first the possible effects due to temperature and pressure.

The temperature at which the measurements are made will have some effect upon the velocity by changing the compressibility of

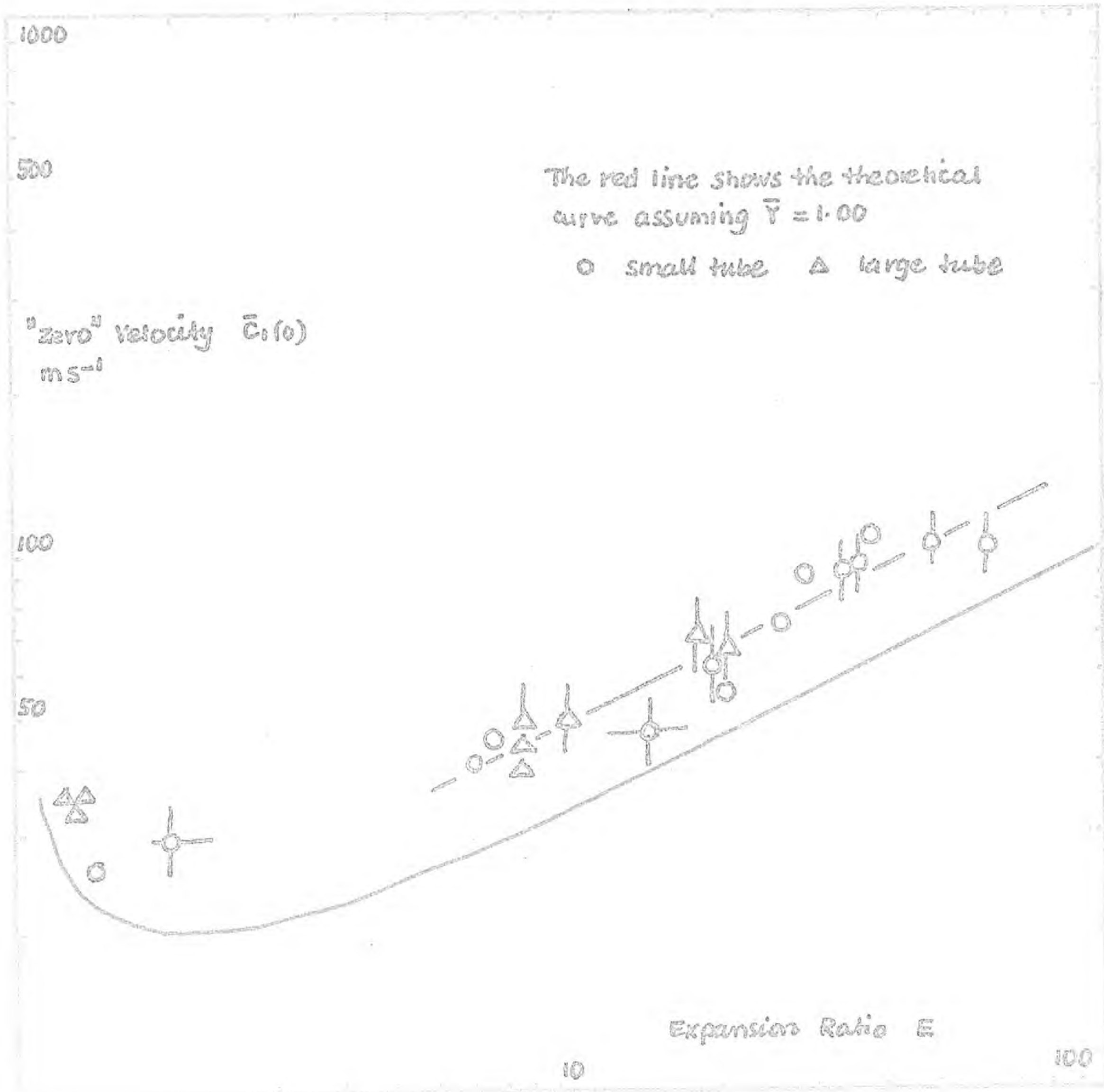

Fig 9.1 Compression wave velocities as a function of Expansion Ratio

the gas in the foam. The magnitude of this effect can be estimated simply by considering the maximum temperature, $26^{\circ}C$, at which measurements were made. Using this value, and assuming that the foam modulus is wholly dependent upon the air compressibility, the ratio of the maximum possible velocity to that calculated for $0^{\circ}C$ is given by $\sqrt{\frac{299}{273}} \simeq 1.05$ the difference being of the order of the errors and very small compared with the ratio actually observed.

It has already been pointed out that an increase in the static pressure in the system will give rise to an increase in compression wave velocity and this increase will be a maximum in the velocity minimum region $E \sim 2$, $\bar{\rho} \sim 0.5$. It is difficult to estimate the pressure increase that is obtained in the measurement tube during a run, but it is obviously less than that in the air system which was always smaller than 5 cm. Hg. The velocity ratio is therefore less, and in the critical region probably considerably less, than $\sqrt{\frac{81}{76}} \simeq 1.03$ which is of the same order as the maximum temperature effect.

It is clear that neither the temperature nor the pressure at which measurement is made can explain the departure from the theoretical curve.

However, if we allow the foam to have a shear modulus, and hence a shear velocity, it is possible to explain this large velocity increase by choosing the correct value and using the relations

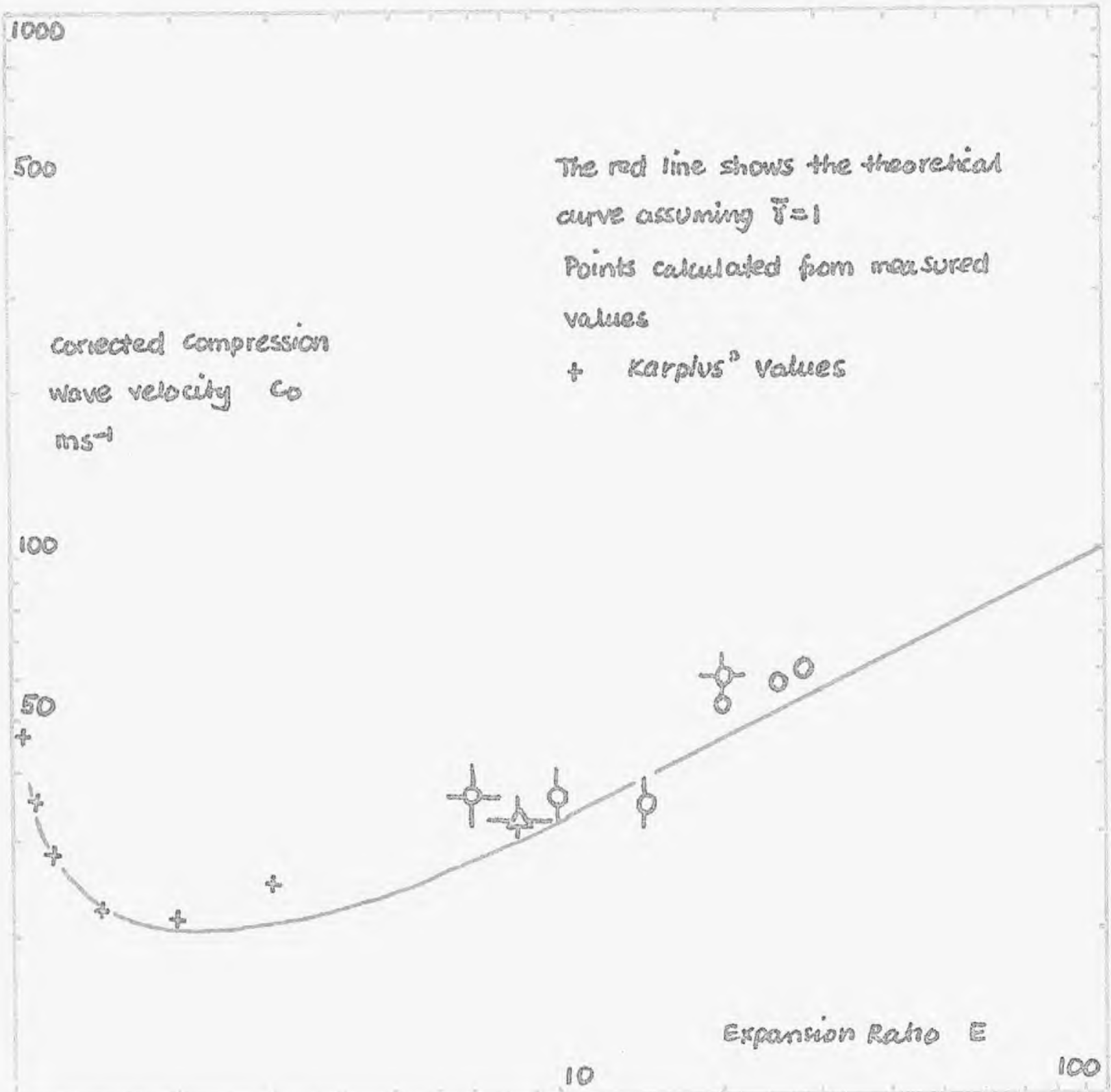

Fig 9.2 Calculated sound velocity as a function of Expansion Ratio

obtained in Chapter 3.

A more convincing demonstration would be to measure the shear velocity independently and then to correct the measured velocity using equation 3.4

$$\bar{c}_0^{\,2} = \bar{c}_1^{\,2} + 2\bar{c}_2^{\,2}$$

where $\bar{c}_1$ and $\bar{c}_2$ are the measured velocities and $\bar{c}_0$ is the calculated fluid zero velocity that would be given by equation 3.3. It has been found possible to do this for some of the runs by a method to be described later, and the corrected values are plotted in fig. 9.2 to show that, despite the meagre number of points and the large scatter, they lie on the theoretical line.

Also plotted are some of Karplus's values for the sound velocity in bubbly water which lie in the region of interest. His points have much less scatter and lie well on the theoretical line. The small scatter is probably due to the increased accuracy possible at the low frequencies that he used (250–1750 cps) and the consequent increase in wavelength. The precision with which they lie on the theoretical curve suggests that there is little or no shear modulus at these high densities.

9.3 MODE STRUCTURE AND SHEAR VELOCITY

1. Evidence for the existence of modes

We must first establish the evidence for the existence of modes in the tube at certain frequencies when compression waves are being propagated.

(a) When the measured attenuation is plotted against frequency it is found that peaks rising to values of the order of 20 db cm^{-1} occur at approximately regular frequency intervals. The position of these peaks vary with the foam density. (see figs 9.3 and 9.5).

(b) The velocity versus frequency curve shows marked discontinuities near the peak attenuation frequencies. In some cases the phase velocity appears to rise to 2000 ms^{-1} where one would expect velocities of the order of 75 ms^{-1}. It is only at frequencies below that of the first peak that velocities are near the expected values.

(c) At certain frequencies, in particular around the peak values, two waves are propagated with markedly different attenuations.

(d) In the regions just below the peak frequencies, interference effects occur, suggesting the propagation of two waves at the same frequency with slightly different velocities.

(e) If the peak frequencies are checked against the bubble size using dimensional equations, only a small degree of correlation is found, whereas they are very dependent upon the foam density. This suggests that the phenomenon is connected with the bulk properties of the foam rather than its structure.

(f) In order to check this conclusion the apparatus was rebuilt using a measurement tube of double the diameter. The peaks were found to occur at much lower frequencies than before and more peaks were now observable.

2. Alternative Explanations of the Observed Phenomena

It is necessary to consider alternative explanations for the peaks before going on to discuss the mode theory for their formation. There are three possibilities to investigate; that the peaks are due to bubble resonances or foam structure, that they are due to resonances in the apparatus, or that they are due to radiation effects from the diaphragm.

The observation that there is such a small correlation between the peak frequencies and the bubble volume indicates that they are not due to bubble resonances or to the foam structure. In addition to this, the frequencies are very much lower than expected theoretically from the simple theories, and the dispersion curves found are not of the type that would be given by the bubble resonance processes visualised.

The use of continuous waves leads inevitably to the possibility of the occurrence of resonances in the glass tube, or in the rubber diaphragm. In order to decrease the vibrations in the apparatus, the base of the measurement tube was set in a brass block and suspended from a rubber sheet fixed to the massive block holding the vibrator. In this way, the tube is isolated mechanically from the vibrating system, except through the foam. However apart from one resonance which was observed at about 1.4

Kcs., and which remained fixed in frequency, and is thought to be a resonance in the vibrator, all the measured peak frequencies are strongly affected by the foam density, indicating that they are due to the bulk properties of the foam. But they are also inversely proportional to the tube radius.

We are therefore left with two alternative hypothesis which are, in a way, closely connected, since they concern interference phenomena in the foam in the tube; i.e. that the peaks are due either to radiation effects from the diaphragm or to the cylindrical modes that are discussed later.

When a diaphragm of the same order of size or smaller than the sound wavelength is vibrated, a lobe radiation pattern is produced by interference between waves from different parts of the disc so that the intensity is stronger in some directions than in others. If the diaphragm is fitted at the end of a tube, as in our case, the waves will be reflected at the tube walls and interference between the beams will occur giving rise to a spacial interference pattern in the tube. This will have the form of peaks and troughs in the sound intensity as one moves along the tube axis. The variations will become smaller as the distance from the diaphragm increases until plane waves are propagated and the amplitude remains constant at very great distances.

In addition to these effects, the normal acoustic modes will be propagated; if by chance, the direction of the lobes correspond to

Runs 51-53 April 1960
$E \simeq 13 \pm 1$ $v = 3 \pm 0.2\ \mu L$
tube diameter 10mm

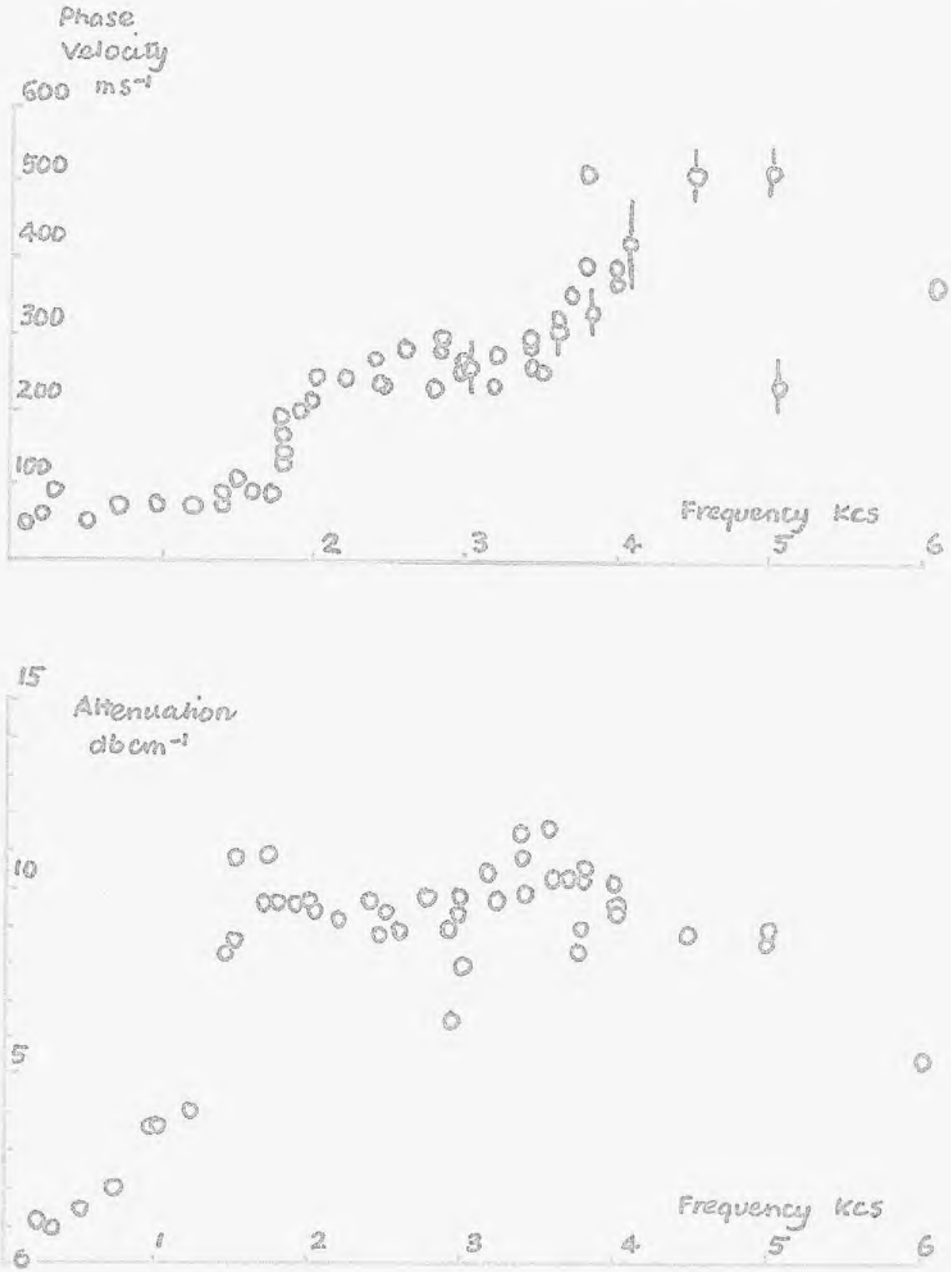

Fig 9·3 Attenuation and Phase Velocity as functions of Frequency

Fig 9.4 (a) Mode Diagram for Runs 51-53
based upon the measurements plotted in fig 9.3

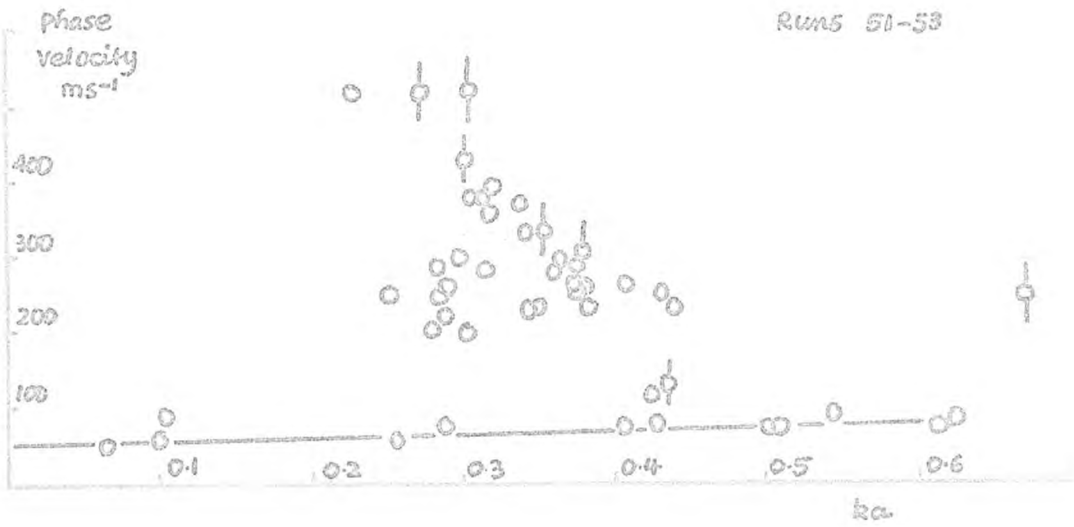

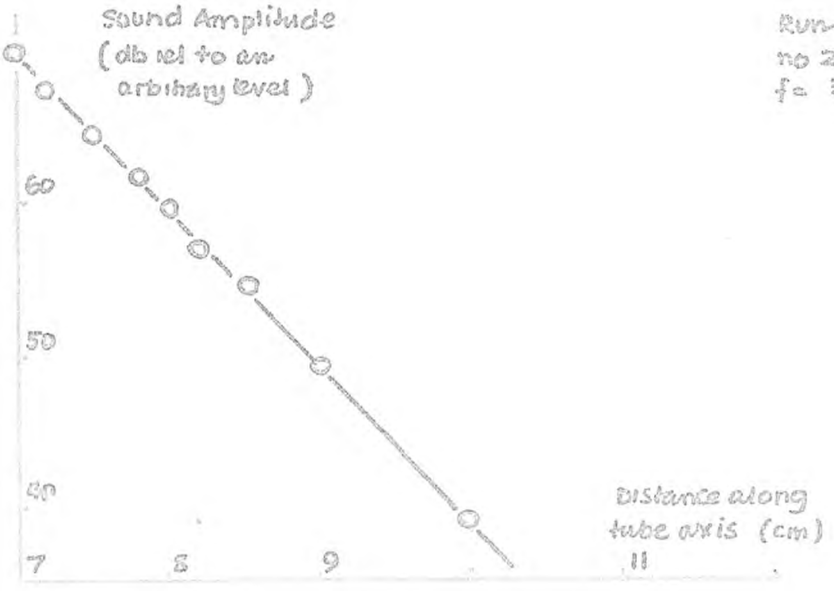

Fig 9.4 (b) Amplitude - distance curve
the diaphragm is at approximately 6 cm.

the propagation angles of the higher modes, these modes will be strongly excited and the amplitude curve altered accordingly.

However such diaphragm radiation effects will give neither the amplitude variation with distance nor the attenuation and phase velocity curves with frequency that have been observed. (see figs 9.3, 9.4 and 9.5).

These observations suggest that the peak frequencies depend upon the tube size and the bulk properties of the foam medium rather than upon its structure, and that they indicate the existence of a series of modes of wave propagation up the measurement tube. The theoretical argument for the formation of such modes is outlined in the next section.

3. Discussion of the Transverse Modes in the tube of foam

We deal here with purely elastic media although it has been pointed out (chapter 4) that foams are probably visco-elastic and waves therefore strongly attenuated. Nevertheless the simple theory should be reasonably close to the practical case particularly for light foams.

Transverse modes are, of course, to be expected in a perfectly rigid cylindrical tube containing a material that propagates waves, even if the waves are purely compressional and the medium is a perfect fluid. These "acoustic" modes occur at frequencies given by the solution to the equation

$$J_1(k_2 b) = 0 \qquad 9.01$$

where J_1 is the 1st order Bessel function

κ_2 is the wave number $= \frac{\omega}{c_1}$

c_1 is the velocity in the unconfined medium

and b is the internal tube radius

The frequencies at which new modes are allowed to propagate are given by

$$f_n = \frac{\xi_n c_1}{2\pi b} \qquad 9.02$$

where are the solutions to $J_1(\xi_n) = 0$

Each of these modes will have a phase velocity which is a function of the frequency, this velocity being infinite at the cut-off value. The form of the velocity curve depends upon the boundary conditions, for the simple case of a gas or liquid the phase velocity, V, is given by

$$\frac{V^2}{c_1^2} = \left[1 - \frac{\xi_n^2 c_1^2}{\omega^2 b^2}\right]^{-1} = \left[1 - \frac{f_n^2}{f^2}\right]^{-1} \qquad 9.03$$

Here we have considered only the purely symmetrical waves, but for each of the modes given by these equations there will be an infinite number of asymmetrical modes formed by different divisions of the tube cross-section by diametrical lines. Since the measurement system is axially symmetrical, these more complicated wave systems need not be considered here.

Now it is necessary to confirm that the mode structure is unexplainable in terms of these "acoustic" modes. This can be done from the estimated "zero" compression wave velocities measured at frequencies below that of the mode associated with the first peak. It is found that the measured velocities are much too high (often more than twice as great) to account for the observed mode frequencies.

Conversely we can estimate the velocity from the mode frequencies, using equation 9.02, and it is found that not only is it below the measured zero velocity but also usually well below the theoretically predicted value.

An alternative hypothesis is therefore proposed in which the existence of a foam shear modulus and shear velocity is postulated. In other words the foam is now to be considered as a solid-like elastic medium. The introduction of the shear velocity implies an additional wave equation and an additional set of boundary conditions which must be satisfied. A theoretical analysis of the propagation of waves in such an elastic material confined in a cylinder is presented in Appendix 5.

The conditions at the wall of the tube have an effect upon the propagation of the waves down it. The first, and most obvious boundary condition (apart from the proviso that the amplitudes do not reach infinity along the tube axis) is that the tube itself shall be perfectly rigid, i.e. the radial displacement shall be zero at the tube surface. This condition gives rise to the "acoustic" modes described above.

The second condition is that which describes the shear properties at the tube wall. The simplest case occurs when the elastic solid is rigidly glued into the tube so that it cannot move relative to the surface. Thus all components of displacement are zero at $r = b$. For light and therefore rigid foams, it is thought that this condition is probably most likely to be the case. Certainly at very low frequencies (about 50 cps), where high amplitudes could be obtained using the vibrator, the displacement (at maximum a few mm.) was similar to that predicted by the theory assuming this condition.

However, during the experiment, the foam is continuously flowing down the measurement tube in the form of a plug. Observation showed that at the tube wall there was a thin boundary layer of liquid. The existence of this layer means that there must be some possibility of vibratory motion of the foam parallel to the tube wall. Hence we get out second simple case of the shear condition by assuming complete shear freedom at the wall, i.e. that the shear stresses τ_{rz} and $\tau_{r\varphi}$ are both zero at $r = b$. (Appendix 5).

The intermediate case, where displacement is restricted but not completely prevented, gives the third type of the shear boundary condition, and it is examined in Appendix 5 by inserting a shear force proportional to the velocity of displacement parallel to the wall.

Now it is found that a second set of longitudinal wave modes can exist. They are here termed the "shear" type of mode to distinguish them from the "acoustic" type since they are dependent upon the shear properties of the medium. Nevertheless they are still compressional waves since they have an axial component of displacement and a dilatation term. In addition to these modes there is also a set of shear wave modes, purely torsional in character, the direction of displacement being around the tube axis.

The frequencies at which this set of "shear" type longitudinal wave modes can occur depend upon the shear velocity and upon the boundary conditions at the wall. For the rigid case, the mode frequencies are given by $f_n = \frac{\eta_n c_2}{2\pi b}$, $J_0(\eta_n) = 0$

where c_2 is the shear velocity

and for the freely sliding case ($\tau_{r\phi}, \tau_{rz} = 0 \quad r = b$)

$$f_m = \frac{\xi_m c_2}{2\pi b} \qquad J_1(\xi_m) = 0$$

The intermediate boundary condition give frequencies between these values, the actual positons depending upon the magnitude of the resistive force assumed (see Appendix 5).

Since the shear velocity is always lower than the longitudinal wave velocity, these mode frequencies will be lower than those of the acoustic type and will therefore assume a greater importance in practical work.

It may safely be assumed that the rubber diaphragm neither acts as a plane piston nor has a purely sinusoidal displacement over its diameter as it is held at the centre by the threaded rod connecting it to the vibrator. The displacement is transmitted into the foam and this can only be done by exciting all the transverse modes in the tube and adding their amplitudes is in a Fourier series. Thus, close to the diaphragm all the possible modes exist but most of them are very highly attenuated. As the frequency is increased, the propagation of new modes becomes possible, and the attenuation curve will exhibit attenuation peaks as each of the modes appears (see fig 9.5).

This discussion, together with the more detailed examination in Appendix 5, shows that "shear" type of modes are possible at frequencies much lower than the "acoustic" type in an elastic medium enclosed in a tube. This conclusion therefore presents us with a possible explanation for the modes found in practice. A comparison of these modes with those predicted by this hypothesis is undertaken in the next section.

4. Analysis of the modes found experimentally

First it is necessary to decide what, in fact, are the mode cut-off frequencies obtained in practice. We have two methods of estimating these, using the attenuation maxima or the phase velocity discontinuities. They give slightly different estimates, the peak attenuation frequencies being often a little lower than the associated velocity rise. In practice, therefore, the peak frequencies have been taken as the best estimate for the cut-off frequencies.

As an example, we will deal with the analysis of one set of readings, set 69-71, whose graph of attenuation against frequency

Fig 9.5 Attenuation versus Frequency Curve

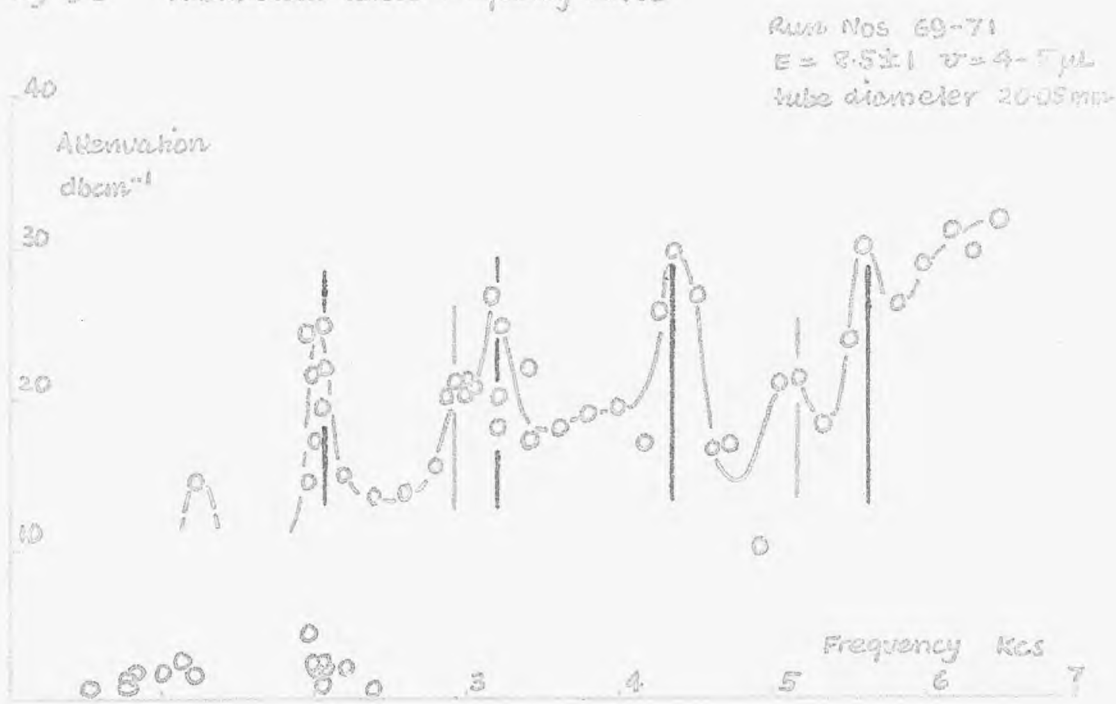

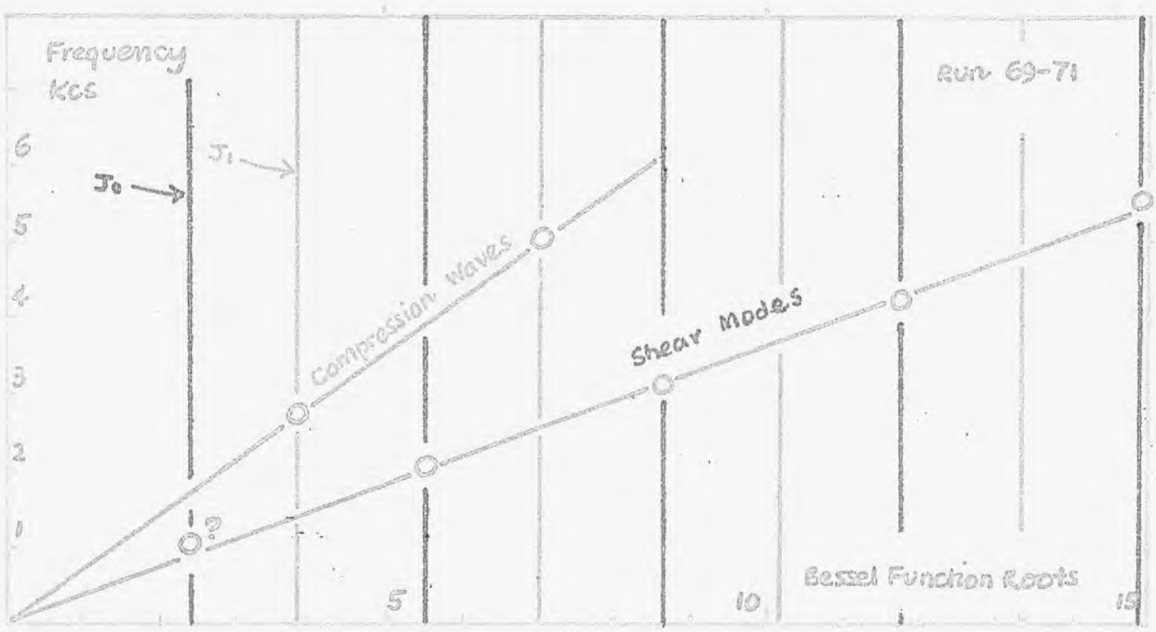

Fig 9.6 Mode Frequencies Plotted against the Bessel Function Roots

has already been given (fig 9.5). The parameters for this run are $E = 8.5 \pm 1$, $v = 4\text{–}5\ \mu L$, 5% Stergene foams, tube diameter $2b = 2.05$ cm.

The "acoustic" modes must first be recognised and this is done by estimation from the measured zero velocity which is given by estrapolation from the low frequency measurements as $47 \pm 10\ ms^{-1}$. The mode frequencies are given by the equations

$$f_n = \frac{\xi_n c_1}{2\pi b} \qquad J_1(\xi_n) = 0$$

thus the frequencies are plotted against the appropriate solutions of the Bessel functions (fig 9.6).

There are three combinations of frequencies that give approximately straight lines in this region. Of these only one gives a close fit and this is drawn, giving an estimated compression wave velocity of $45.9 \pm 0.6\ ms^{-1}$ being very close to the measured value. The peaks corresponding to these frequencies are, however, of small size and it might be felt that one of the other two lines (giving velocities of 52 and 38 ms^{-1} respectively) would be more reasonable since they include some of the larger peaks. However the line drawn has the advantage of close fit and the remaining frequencies coincide well with the shear mode line.

Having taken into account what we consider to be the "acoustic" modes, we plot the remainder of the peak frequencies on the same graph, but this time against the roots of $J_0(\eta_n) = 0$ corresponding to the solutions of the rigid case discussed in the last section.

The mode numbers are chosen knowing that the points should lie on a straight line passing through the origin.

It is seen that the points lie on a good straight line of slope corresponding to a velocity of $23.5 \pm 0.3\ ms^{-1}$ which from the hypothesis is taken to be the shear velocity. The accuracy with which the points lie on this line passing through zero is taken as the justification for the choice of the $J_0(\ )$ roots and hence for the assumption of the rigid boundary conditions.

Thus for the series of runs 69-71 we have as estimates for the velocities

$$\bar{c}_1 = 45.9 \pm 0.6\ ms^{-1} \qquad \bar{c}_2 = 23.5 \pm 0.3\ ms^{-1}$$

and from these we calculate the equivalent fluid velocity using equation 3.4

$$\bar{c}_0^{\,2} = \bar{c}_1^{\,2} - 2\bar{c}_2^{\,2}$$

giving $\bar{c}_0 = 31.6 \pm 0.7\ ms^{-1}$, a value that within the experimental errors lies close to the theoretical value $29.2 \pm 2.0\ ms^{-1}$.

5. The shear velocity as a function of density

Having a method for the estimation of what is taken to be the shear velocity from the mode diagram, the values obtained may be plotted against the expansion ratio E as has been done already for the compression wave velocity. The graph, fig 9.7 shows the result for the runs that have given such estimates. As can be seen they lie roughly on the straight line on the logarithmic graph, with slope of 0.5 corresponding well to the behaviour of the theoretical

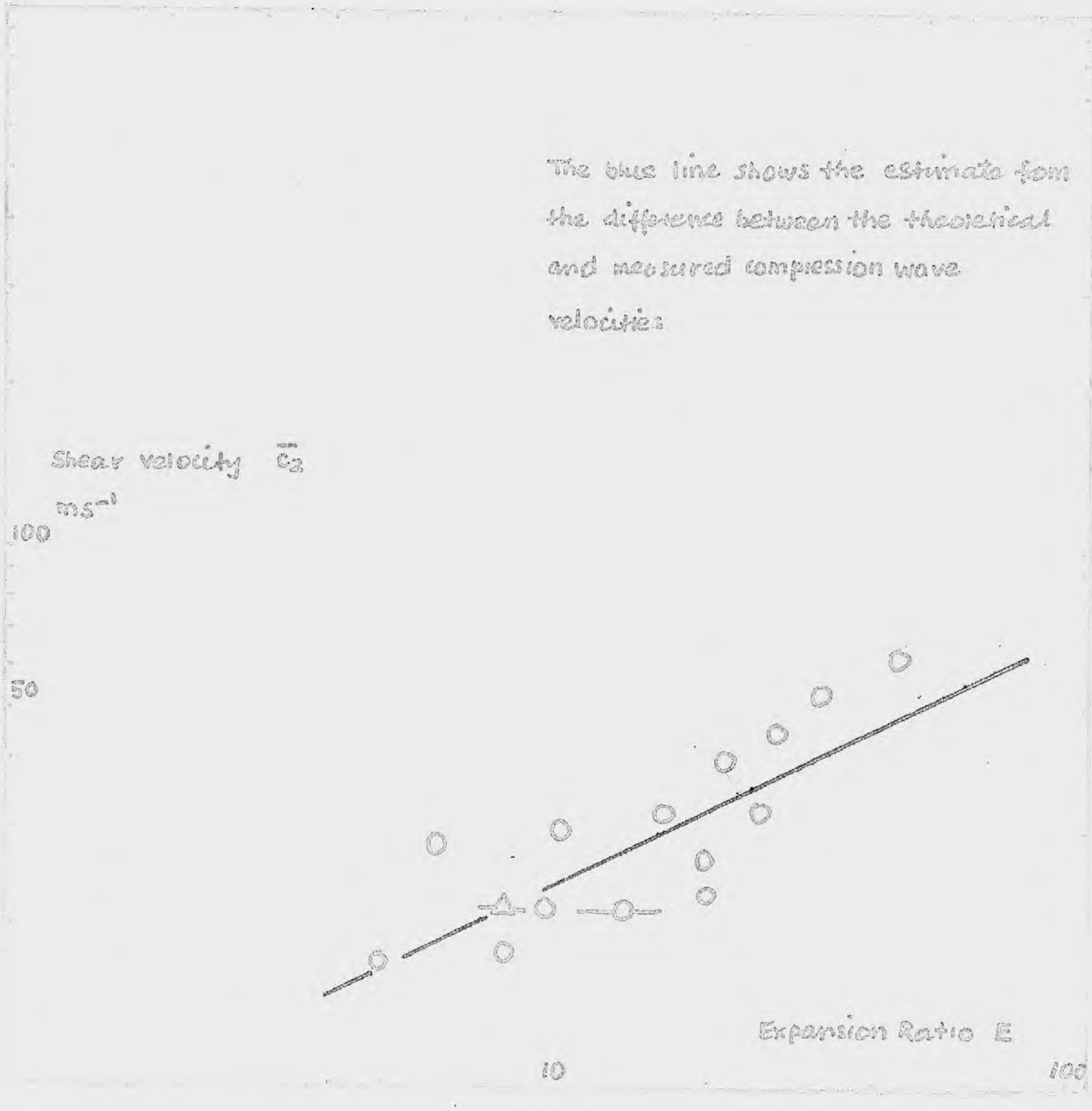

Fig 9.7 Shear Velocity Calculated from Peak Frequencies

equation

$$\bar{c}_2 = \left[\frac{\bar{\mu}}{\rho_L}\right]^{\frac{1}{2}} \epsilon^{1/2}$$

This slope would be found for any velocity which depends upon the density of the medium in the usual manner.

We have an independent way of establishing the shear velocity: from the discrepancy of the measured compression wave velocities from the theoretical expression. This is, of course, arguing round in a circle since we have postulated the existence of the shear modulus in order to explain this discrepancy. But the independent methods lead to very close agreement as the line drawn in fig 9.7 shows.

From the intercept of the best straight line through the points, we can estimate the shear modulus, since it appears to be independent of the foam density. The intercept is $8 \pm 1 \times 10^2$ (cms^{-1}) giving a shear modulus of

$$\bar{\mu} = 6.4 \pm 1 \times 10^5 \ [dyn\ cm^{-2}]$$

This value is very much higher (by a factor of 1000) than that calculated from Deryagin's theory (1933) (18) mentioned above in Chapter 4.2, using the mean bubble size and an estimate of the surface tension. But this measurement, for 5% stergene foams, is only about 30 times greater than his measured values of $\bar{\mu}$ for 0.1 % saponin foams; 22000 dyn cm^{-2}.

The points in fig 9.8 have been plotted neglecting any difference in bubble size between runs. Because of the high degree of

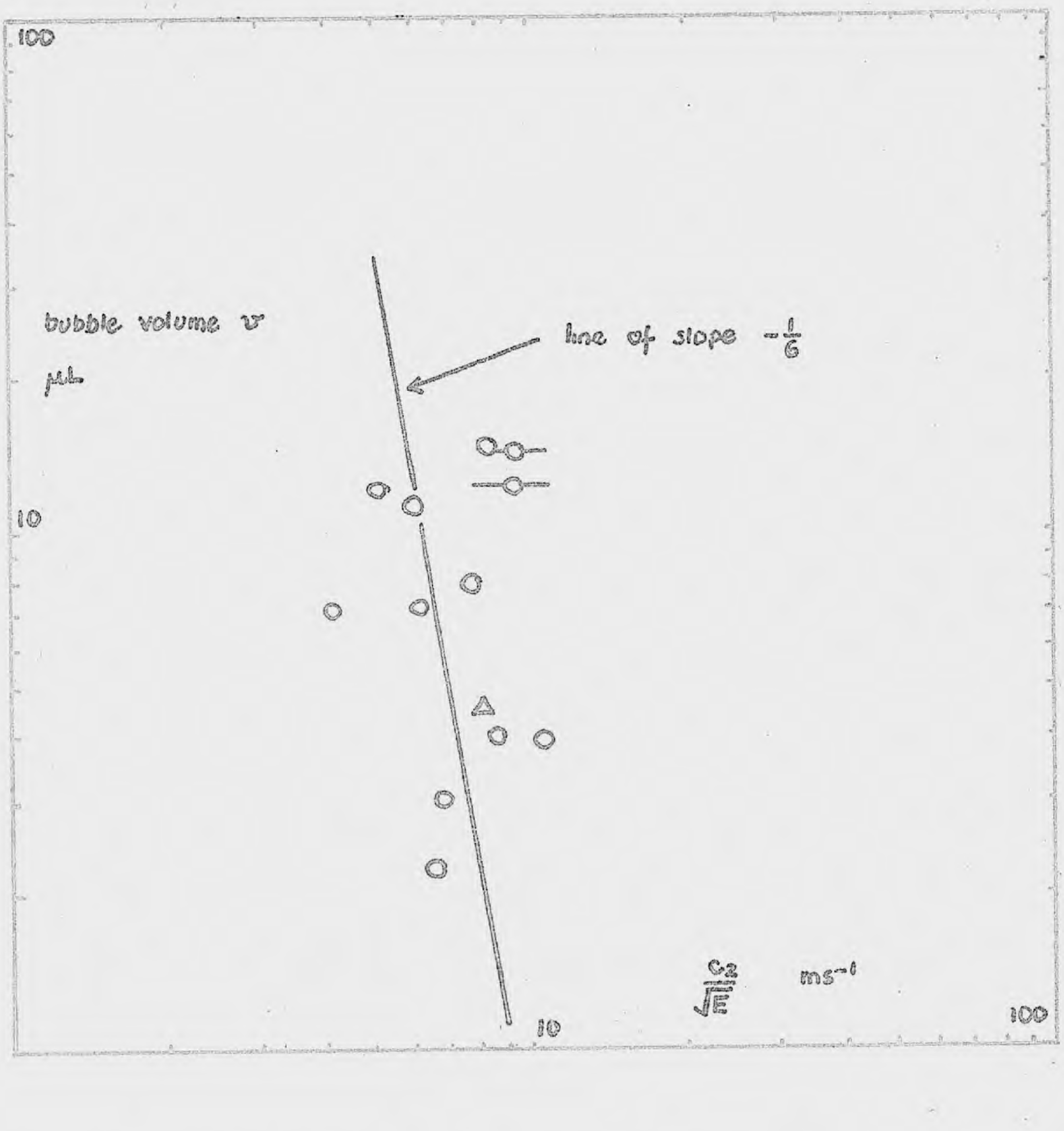

Fig 9.8 The effect of Bubble size on the Shear Velocity

scatter and since there is some suspicion that the capillary theory does not explain the experimental values it was felt necessary to test whether the shear modulus depended upon the bubble size.

We have from equation 5.11

$$\bar{c}_2 = \left[\frac{\bar{\mu}}{\rho_L} \right]^{\frac{1}{2}} E^{\frac{1}{2}}$$

and this relation is found to hold quite well as far as the variation with expansion ratio is concerned. The shear modulus will be given by

$$\bar{\mu} = \rho_L \frac{\bar{c}_2^{\,2}}{E}$$

now from Deryagin's theory

$$\bar{\mu} = \frac{B}{v^{1/3}}$$

where B is a constant. Thus plotting $\frac{c_2}{E^{1/2}}$ against v on a logarithmic graph should give a slope of $-\frac{1}{6}$. But as can be seen from the plotted values, fig 9.8, there is so much scatter that no useful conclusion can be drawn. The reason for the scatter is unknown, it seems to be independent of the temperature.

9.4 ATTENUATION AT LOW FREQUENCIES

The existence of the mode structure on the wave propagation means that measurement of the bulk properties of the foam, except for the shear velocity, becomes very difficult. However, we can examine the attenuation at frequencies below that of the first mode, so that pure plane waves of the zeroth symmetrical mode are propagated. In these measurements we must be careful that the frequency is not taken too low in case effects due to longitudinal resonances in the tube occur, since in these regions we cannot be sure that all the energy is absorbed at the attenuator.

With this proviso we can plot the attenuation, α , as a function of frequency on a logarithmic graph and we find that for each set of readings the measured values satisfy the expression

$$\alpha = A f^{n}$$

where A and n are constants.

We can recognise two regions:

(i) high densities, $E < 3$, $\bar{\rho} > 0.3$

where $n = 1$; thus from chapter 6

$$\Delta = \text{constant}$$

There are only two sets of readings in this region giving the following values of A

$E = 2.20 \pm 0.1$ $\quad$ $A = 6.0 \pm 0.5 \times 10^{-3}$ db cm^{-1} cps^{-1}

$E = 1.35 \pm 0.1$ $\quad$ $A = 2.9 \pm 0.3 \times 10^{-3}$

Apart from this, no more useful conclusions may be drawn because of the scarcity of data.

(ii) low densities $E > 3$ $\bar{\rho} < 0.3$

where $n = 2$ corresponding to the classical type of attenuation proportional to the square of the frequency.

Now plotting the measured values of A as a function of the expansion ratio E (fig 9.9) we find that a slope of -1.5 is

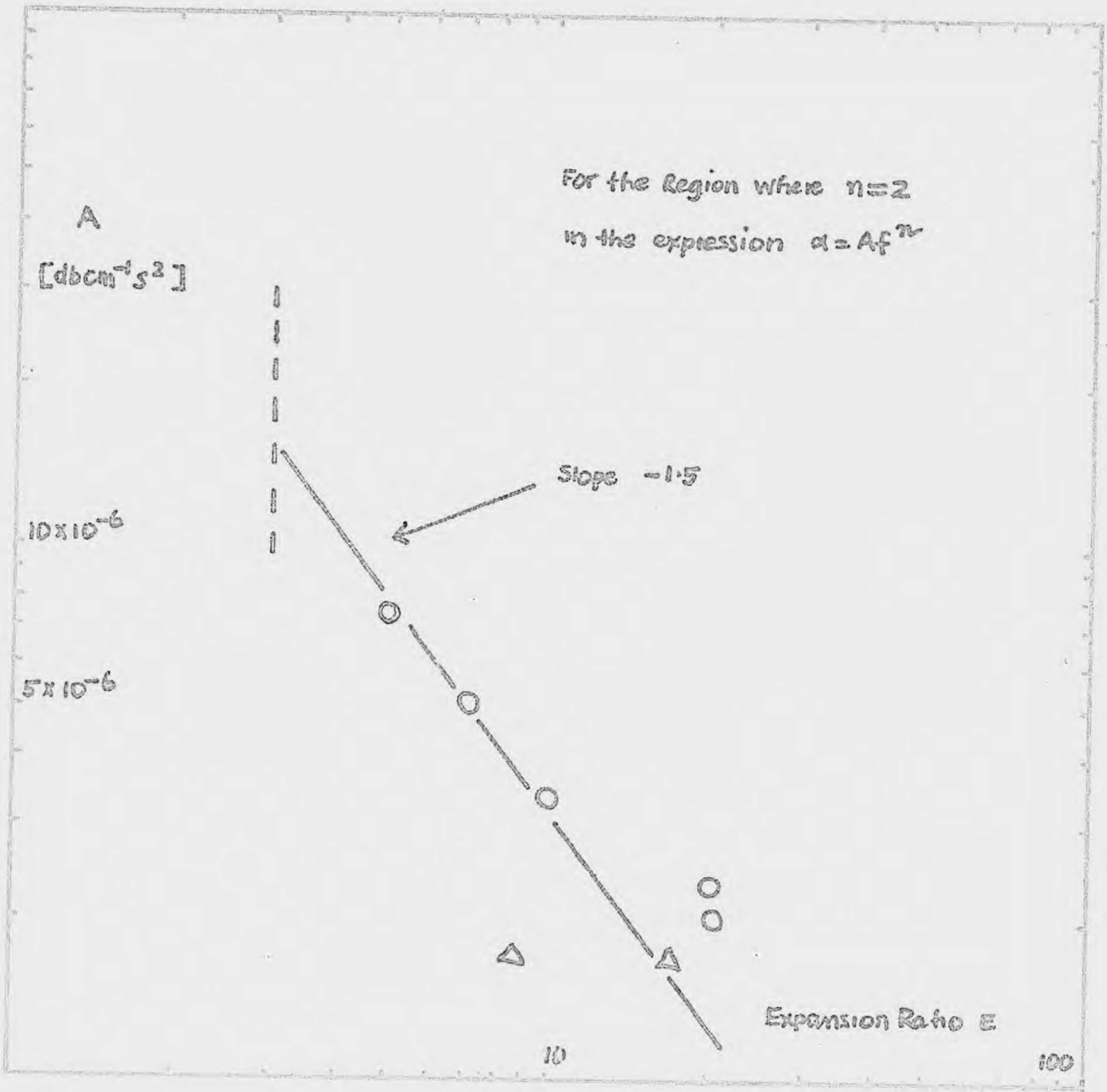

Fig 9.9 Values of A in the Expression $\alpha = Af^{n}$ against E.

reasonable. Thus within experimental error

$$A \propto E^{-1.5}$$

but from chapter 6 we have

$$A = \frac{2\pi^2}{\bar{c}_1} \cdot \frac{K''}{K} = \frac{\Delta}{\bar{c}_1 . f}$$

thus, since in the region considered we have established that $\bar{c}_1 \propto E^{1/2}$ we have

$$\frac{K''}{K} \propto \frac{1}{E}$$

now of the various types of damping mechanisms considered, only one, that of dilatational viscosity damping is similar to the observed values both in frequency dependence and dependence upon the expansion ratio.

From equation 6.10

$$\frac{K''}{K} = \frac{4}{3} \frac{\eta_L}{\gamma P} \frac{1}{E}$$

We can estimate, from these measurements that

$$\eta_L = 300 \pm 50 \quad \text{dyn cm}^{-2}\,\text{sec}$$

this large viscosity might be explained in terms of a 'surface viscosity' associated with the bubble surfaces. This is not unlikely since a large percentage of detergent is being used to make the foams.

We can therefore draw no strong conclusions from these observations beyond the different frequency behaviour of foams with $E < 3$ or $E > 3$. This transition actually corresponds to an observed change of foam structure from random bubbly liquid to a crystalline lattice.

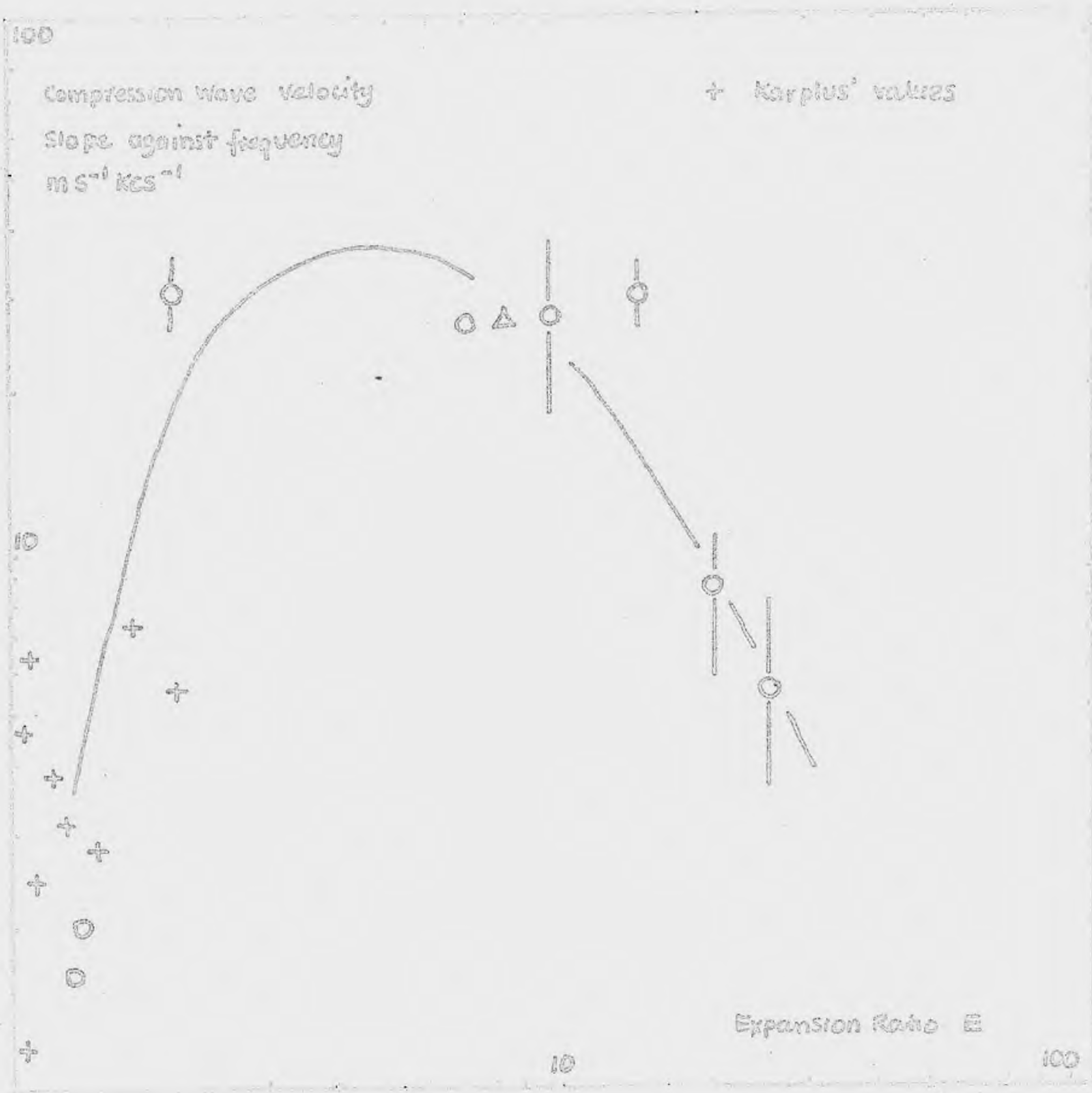

Fig 9.10 Velocity-Frequency Slope as a function of Expansion Ratio

9.5 VELOCITY DISPERSION AT LOW FREQUENCIES

With the same limitations as those described in section 9.4 we may examine the velocity as a function of frequency in the region below the first mode.

The velocity increased linearly with frequency in almost every case. The velocity-frequency slopes give the graph in fig 9.10 when plotted against expansion ratio together with the values found by Karplus (1958) (3). The maximum effect occurs in the region of $E \sim 4$ where it is likely that major structural changes occur in the medium as it turns from a bubbly liquid into a foam.

Karplus attributed the dispersion that he found wholly to the detergent in the water and this seems to be a reasonable hypothesis since any surface active agent will increase the surface viscosity of the interfaces.

9.6 CONCLUSION

We can conclude from the experimental results that the compressional wave velocity is predicted well by the theoretically derived equations only if a correction is made.

If this correction is made by postulating a shear modulus of about

$$\bar{\mu} = 6.4 \pm 1 \times 10^5 \quad [dyn\ cm^{-2}]$$

a value which is much higher than that predicted by the Deryagin theory, then the appearance of a mode structure in the propagation at higher frequencies is also explained.

The existence of these modes is as predicted by the theory of propagation of waves in an elastic medium contained in a cylindrical tube when there is no displacement at the wall (the Rigid case, see Appendix 5). In addition to the normal "acoustic" modes there exist "shear" type modes whose cut-off frequencies depend upon the shear wave velocity.

The existence of modes makes the investigation of bulk properties as a function of frequency very difficult, but at low frequencies some measurements have been made. In spite of a large scatter, the attenuation for light foams is similar to that predicted by the dilatational viscosity theory, using a very high value of the assumed liquid viscosity.

9.7 SUGGESTIONS FOR FURTHER WORK

The results of the present work suggest some possible lines of future research. It is quite obvious that further investigation of both velocity and attenuation in uniform foams and bubbly liquids should be made over as wide a range of bubble size and density as possible. Variations with frequency, bubble size and density at very low frequencies (below about 100 cps) and in the minimum velocity region ($\bar{\rho} \sim 0.5$ $\Xi \sim 2$) would confirm the existence of the predicted thermal and viscous relaxation processes.

It would seem best to make these measurements either in the free bulk medium or in an apparatus with easily interchangeable measurement tubes since the effect of the enclosure is so marked in the interesting regions. Problems due to the difficulty of forming and retaining large amount of uniform foam will be encountered but the present apparatus could in principle be altered so as to produce foams at much larger rates if the bubble making section could be improved. Multiple banks of precision fine capillary tubing or a mechanical bubble-forming system might be used. However the main difficulty would be the prevention of drainage in the foam, once formed. It may prove necessary to accept the density distribution as part of the experimental conditions.

The existence of a foam shear modulus, suggested in this work, should be confirmed, if possible in an apparatus specially designed to excite shear waves alone. The estimations of velocity that have been made would help in the design of such an apparatus. The variation of the shear velocity with frequency, density and bubble size would be the primary aim of such an investigation but changes in shear modulus due to foam structure and the properties of the surface layers in the foam would also be interesting problems.

The minimum compression wave velocity region is of interest particularly in the connection with the pumping of foams and gas-liquie mixtures at high speeds. If the mixture behaves as a fluid (i.e. there is no plug flow) then high amplitude variations in density would be expected if the pumping speed is higher than the sound speed. It would be interesting to see if this phenomenon in fact occurred and it could be easily studied using simple apparatus.

The bubbling process itself is still little understood, and as pointed out in Appendix 4, further fundamental work on the formation, growth and break-off of a bubble would be useful.

A P P E N D I C E S

APPENDIX 1

A GLOSSARY OF TERMS USED IN DESCRIBING FOAMS AND SOME OF THE PARAMETERS

1. GENERAL

Foams are agglomerations of gas bubbles separated from each other by thin liquid films (as defined by Bikerman (10))

Froth is a term used to describe light, stable foams.

Monodisperse Foam, one in which all the bubbles are the same size. most foams in practice are Polydisperse, having a wide range of bubble sizes. Monodisperse foams have certain distinct properties, in particular their crystalline structure.

Mechanical Foams are those generated by mechanical (e.g. bubbling or agitation) rather than chemical means.

2. FOAM DENSITY

Density, $\bar{\rho}$, the mass of unit volume of foam ($gm.ml^{-1}$)

Specific Gravity, the ratio

$$\frac{\text{mass of unit volume of foam}}{\text{mass of unit volume of water}} = \frac{\bar{\rho}}{\rho_w}$$

Expansion Defined by J.M. Perri (1953) ref (10) as (specific gravity)$^{-1}$.

Mass Ratio. z, (or Heinrich's Mixing Ratio, μ) defined by

Karplus (3) as the ratio

$$z = \frac{\text{mass of gas}}{\text{mass of liquid}} \quad \text{(in the foam)}$$

and in terms of the expansion factor, E, and the air volume factor, A:

$$z = \frac{\rho_G}{\rho_L}(E-1) = \frac{\rho_G}{\rho_L} A$$

Density ratio defined as

$$\xi = \frac{\text{density of soln}}{\text{density of foam}}$$

and is approximately equal to the expansion factor for normal foams.

3. DENSITY IN TERMS OF THE VOLUME EXPANSION

Expansion factor, E, defined by Clark (1947) (6). It is identical with Friedrich's (1943) Foam number

$$E = \frac{\text{Vol of foam}}{\text{Vol of soln}}$$

thus $\bar{\rho} = \frac{1}{E}(\rho_L + (E-1)\rho_G)$

and for most foams,

$$E \simeq \frac{\rho_L}{\bar{\rho}} = \xi$$

this quantity is used in this report because it leads to simple expressions for the mechanical properties in the regions of densities that are used.

Air (or gas) volume factor, A: Clark (1947), (6),

$$A = \frac{\text{vol of gas}}{\text{vol of liquid}} = E - 1$$

volume ratio, x, Heinrich (1942) (4)

$$x = \frac{\text{vol of gas}}{\text{vol of foam}} = \frac{E-1}{E} = \frac{A}{A+1}$$

frothing volume, the volume percentage of air (or gas); used by McBain and Ross (1949) (9) and is related to the volume ratio, x:

frothing volume = $100x = 100\frac{E-1}{E}$ %

foaming power, P, was defined by Bailey (1935) to compare different liquids used in the preparation of foams. It is the increase in volume upon foaming and is expressed as a percentage

$$P = 100E \%$$

relative foam density, d, is strictly an innacourate description since it was defined by McBain et al. (8) in terms of a volume ratio

$$d = \frac{\text{vol of soln}}{\text{vol of foam}} = \frac{1}{E}$$

but for normal foams it is approximately

$$d = \frac{\bar{\rho}}{\rho_L} = \text{specific gravity}$$

porosity, defined in the usual way as

$$\frac{\text{vol of continuous phase}}{\text{total vol}} = \frac{\text{vol of soln}}{\text{vol of foam}} = d = \frac{1}{E}$$

4. QUANTITIES DESCRIBING THE BUBBLE SIZE

bubble volume, v, is the volume of the gas contained in each cell of the foam, and it is this quantity which is measured experimentally and is used in the main body of this report.

bubble radius, a, the radius of the sphere which has the same volume as the gas in the cell

$$a = \left(\tfrac{4}{3}\pi\right)^{-\frac{1}{3}} v^{1/3}$$

cell volume, V, the total volume of each cell containing a bubble, including the liquid surrounding it. It can be expressed in terms of the bubble volume and the expansion factor

$$V = v \frac{E}{E-1}$$

inradius is the radius of the sphere that will fit inside the cell. It is used in particular in connection with the face centred cubic lattice mode for the foam. In this case it is approximately equal to the bubble radius, a.

specific surface, S, (or A), which was first used by Clark (1947) (6) is particularly useful in describing the characteristics of polydisperse foams, measuring the energy beaten into the foam in the form of increased surface area. It is defined as the area of interface between the disperse and the continuous phase included in unit volume of foam

$$S = \frac{\text{area of interface}}{\text{vol of foam}}$$

for a monodisperse foam, with bubble radius, a,

$$S = \frac{3}{a} \cdot \frac{E-1}{E}$$

dispersivity, was used by Deryagin (1933) and has the same meaning as _specific surface._

APPENDIX 2

A SIMPLE ANALYSIS OF THERMAL DAMPING WITHIN A FOAM

The model of the foam that we shall use is one where each cell is considered to be a liquid sphere, radius R containing a bubble of radius r. We are interested in the variation in temperature within the gas in this bubble, and how this is influenced by the liquid in the cell. In the following discussion the cell size is considered to be much smaller than the acoustic wavelength.

As the pressure in the cell increases so does the temperature of the gas but radial heat flow takes place to warm the liquid of the cell wall.

For low frequencies and very small bubbles, and for large volumes of liquid in the cell wall, the conditions are such that the temperature in the gas remains approximately constant, i.e. isothermal conditions exist.

For large bubbles and high frequencies when conditions in the infinite pure gas would be adiabatic, the rate of heat flow will be small and conditions at the centre of the bubble will be nearly independent of the cell walls. Towards the cell surface, however, conditions will be nearly isothermal since the liquid acts as a heat sink, thus keeping the temperature constant. The mean effect will therefore be intermediate between the two limiting cases.

At intermediate frequencies, the heat flow will be out of phase with the pressure variation; this out of phase effect will give rise to an imaginary part in the compressibility and hence to thermal damping.

We will now examine the thermal conditions more closely.

Some thermodynamic relations

There are two relations which we require. The equation of state of the gas

$$pv = R\theta \qquad (1)$$

when differentiated leads to the relation

$$p\,dv + v\,dp = R\,d\theta \qquad (1a)$$

where R is the Gas Constant and θ the temperature.

The second expression we need is the First Law of Thermodynamics

$$dQ = C_v d\theta + p\,dv \qquad (2)$$

substitution from (1a) gives the required relation

$$dQ = C_p d\theta - v\,dp \qquad (2a)$$

Now from (1a) we obtain the bulk modulus

$$\bar{K} = -v\frac{dp}{dv}$$

$$= p - R\left(\frac{d\theta}{dv}\right)$$

Now $\dfrac{d\theta}{dv} = \dfrac{d\theta}{dp}\cdot\dfrac{dp}{dv} = \left(-\dfrac{\bar{K}}{v}\right)\dfrac{d\theta}{dp}$

Substituting and rearranging we arrive at the result

$$\bar{K} = p\left\{1 - \frac{R}{v}\left(\frac{d\theta}{dp}\right)\right\}^{-1} \qquad (3)$$

The well-known relations for the compressibility of a gas can easily be found from this expression; thus for isothermal conditions, when $d\theta = 0$ equation (3) gives

$$\bar{k} = p$$

Under adiabatic conditions, $dQ = 0$ and calculating $\frac{d\theta}{dp}$ from (2a) we have

$$\frac{d\theta}{dp} = \frac{v}{c_p}$$

and substituting

$$\bar{k} = p\left\{1 - \frac{R}{v}\frac{v}{c_p}\right\}^{-1} = \gamma p$$

Now in order to determine the compressibility of the gas in the foam it is necessary to examine the heat flow to establish a value for the factor $\frac{d\theta}{dp}$.

<u>The heat flow in the gas</u>

The equation defining the thermal conductivity in a medium is

$$\frac{dQ}{dt} = -\lambda \operatorname{grad} \theta$$

where $\frac{dQ}{dt}$ is the rate of heat flow across unit area

and λ is the thermal conductivity (cal cm^{-1} sec^{-1} deg^{-1}C)

From this relation we obtain the equation for heat conduction in a medium in which there is a heat source A*.

$$\nabla^2\theta - \frac{1}{b}\frac{\partial\theta}{\partial t} = -\frac{A}{\lambda} \qquad (5)$$

where A is the heat produced per unit time per unit volume

---

* cf H.S. Carslaw and J.C. Jaeger
"Conduction of heat in solids"
2nd ed Oxford, Clarendon Press, 1959 p. 8.

b is the thermal diffusivity

$$b = \frac{\lambda}{c_p \rho} \tag{6}$$

which has a value of 18.2 10^{-2} (cm^2 sec^{-1}) for air.

Now from equation 2a we can put

$$A = \rho v \frac{\partial p}{\partial t} \tag{7}$$

Taking Laplace Transforms of (5) after substituting from (7),

$$\nabla^2\bar{\theta} - \frac{p}{b}\bar{\theta} = -\frac{\rho v}{\lambda}\overline{\frac{\partial p}{\partial t}} = -\bar{Z} \quad (say)$$

If we rewrite the equation in terms of $r\bar{\theta}$, for the spherically symmetrical case, we arrive at a simple expression for $\nabla^2(r\bar{\theta})$.

The general solution for this equation is

$$r\bar{\theta} = C e^{+sr} + D e^{-sr} + \frac{\bar{Z}}{s^2} r \tag{8}$$

where $$s^2 = \frac{p}{b} \tag{9}$$

The boundary conditions are that

B.C. 1) at $r = 0$ $\quad \bar{\theta} \neq \infty$ $\quad$ thus $\bar{D} = -\bar{C}$ (10)

B.C. 2) at $r = a$ $\quad \bar{\theta} = \bar{\theta}_a$

$$\bar{\theta}_a = \frac{\bar{C}}{a}\left(e^{sa} - e^{-sa}\right) + \frac{\bar{Z}}{s^2}$$
$$= 2\frac{\bar{C}}{a}\sinh sa + \frac{\bar{Z}}{s^2} \tag{11}$$

Now we must consider the heat exchange at the cell boundary. We assume that the heat flow into the cell wall merely raises the temperature of the liquid which we assume to be constant across the wall thickness; there is, of course, no heat flow from one cell to another, except when the sound wavelength is of the order of the cell size. We do not consider this case here.

For unit area of the cell wall

B.C. 3) at $r = a$

$$\left(\frac{dQ}{dt}\right)_{r=a} = \rho_L c_L d \left(\frac{d\theta}{dt}\right)_{r=a} \tag{12}$$

where d is the wall thickness for low density foams. It would be more accurate to put d as the ratio of the volume of liquid in the cell to the area of interface between the gas and liquid.

$$d = \frac{a}{3}\left(\frac{R^3}{a^3} - 1\right) = \frac{a}{3}\,\frac{1}{E-1} \tag{13}$$

from the definition of the expansion ratio, E.

Thus at $r = a$ we have, from (12) and equation (4)

$$-\lambda\left(\frac{\partial\bar{\theta}}{\partial r}\right)_a = \rho_L c_L d\, p\, \bar{\theta}_a$$

or

$$\left(\frac{\partial\bar{\theta}}{\partial r}\right)_a = \Upsilon p\, \bar{\theta}_a \tag{14}$$

where we have put $\Upsilon = \dfrac{\rho_L c_L d}{\lambda}$ (15)

Now differentiating (8) and substituting, we have, at $r = a$

$$a\left(\frac{\partial\bar{\theta}}{\partial r}\right)_a + \bar{\theta}_a = 2s\,\bar{C}\cosh sa + \frac{\bar{Z}}{s^2} \tag{16}$$

Substituting for $\left(\frac{d\bar{\theta}}{dr}\right)_a$ and for $\bar{\theta}_a$, we obtain a relation for the amplitude, $\bar{C}$ as a function of the exciting value $\bar{Z}$

$$\bar{C} = \frac{\bar{Z}\,\frac{a}{s^2}\,(pa\Upsilon)}{2\left\{(1 - pa\Upsilon)\sinh sa - sa\cosh sa\right\}} \tag{17}$$

Hence upon substitution into the solution 8, we have an expression for the Laplace Transform of the temperature in space and time, viz.

$$\bar{\theta} = \frac{\bar{Z}}{s^2}\left\{1 + \frac{a}{r}\,\frac{(pa\gamma)\sinh sr}{\{(1-pa\gamma)\sinh sa - sa\cosh sa\}}\right\} \qquad (18)$$

If we invert this expression we would have the variation in temperature θ in the bubble for a given heat input function Z. However, for our purpose, we need only the mean temperature in the bubble θ_m as a function of time.

Taking the mean of $\bar{\theta}$ by integrating over the sphere from $r = 0$ to a, we arrive at the expression

$$\bar{\theta}_m = \frac{\bar{Z}}{s^2}\left\{1 - \frac{3p\gamma}{as^2}\,\frac{\sinh sa - sa\cosh sa}{(1-pa\gamma)\sinh sa - sa\cosh sa}\right\} \qquad (19)$$

In order to invert this expression we apply the Inversion Theorem whereby

$$\theta_m = \frac{1}{2\pi i}\int_{c-i\infty}^{c+i\infty} \frac{b\rho v}{\lambda}\,\frac{p}{p^2+\omega^2}\,\Delta p\left(1 - \frac{3pa\gamma}{(as)^2}\,\frac{\sinh sa - sa\cosh sa}{\{(1-pa\gamma)\sinh sa - sa\cosh sa\}}\right)e^{-pt}.dp \qquad (20)$$

where we have put

$$\frac{\bar{Z}}{s^2} = \frac{\rho_6 v b}{\lambda}\,\frac{p}{p^2+\omega^2}\,\Delta p \qquad (21)$$

assuming a sinusoidal pressure variation

$$dp = \Delta p \cos\omega t \qquad (22)$$

Now we are interested only in the residues of this expression at the poles $p \pm i\omega$ since these will give the periodic rather than the transient solutions.

These residues will be given by the relation

$$\theta_m = \frac{v}{c_p}\left(1 - X\,\frac{\sinh sa - sa\cosh sa}{(1-pa\gamma)\sinh sa - sa\cosh sa}\right)\Delta p\, e^{-i\omega t} + \text{conjugate} \qquad (23)$$

where

$$Sa = a\sqrt{\frac{i\omega}{b}} = x(1+i) \;, \quad x = a\sqrt{\frac{\omega}{2b}} \tag{24}$$

and

$$X = \frac{3bY}{a} \tag{25}$$

substituting for Y we have

$$X = 3b\,\frac{d}{a}\,\frac{\rho_L c_L}{\lambda} \tag{26}$$

and hence from equations (6) (13)

$$X = \frac{\rho_L c_L}{\rho_G c_p}\cdot\frac{1}{E-1} \tag{27}$$

Upon substituting for Sa from equation (24) the expression for $\dfrac{\theta_m}{\Delta p}$ may be expanded to derive, by substitution in equation (3), the following relations for bulk modulus $\overline{K}$ and logarithmic decrement Δ_T:

$$\overline{\gamma} = \frac{\overline{K}}{P} = \frac{\gamma}{1+X(\gamma-1)}\;\frac{AC+BD}{C^2+D^2} \tag{28}$$

and

$$\Delta_T = \pi\,\frac{AD-CB}{AC+BD} \tag{29}$$

where

$$A = 2x\,(\cosh 2x + \cos 2x) - 2\sinh 2x - f_a(2x)^2\sin 2x$$

$$B = 2x\,(\cosh 2x + \cos 2x) - 2\sin 2x + f_a(2x)^2\sinh 2x$$

$$C = 2x\,(\cosh 2x + \cos 2x) - 2\sinh 2x - f_b(2x)^2\sin 2x$$

$$D = 2x\,(\cosh 2x + \cos 2x) - 2\sin 2x + f_b(2x)^2\sinh 2x$$

$$f_a = \tfrac{1}{3}X$$

$$f_b = \frac{\frac{1}{3}X}{1+(\gamma-1)X} \tag{30}$$

Now these equations can be simplified for the cases where $2x \ll 1$

and $2x$ is large. We now derive analytical expressions for these cases.

Case 1 Bubble size and frequency small

The expression reduces to

$$\frac{\theta_m}{\Delta p} = \frac{\rho_G v b}{\lambda}\left\{1 - \frac{X}{1+X} - \left(\frac{X}{1+X}\right)^2\left(\frac{\omega a}{b}\right)^2 \cdot \frac{1}{210} + i\omega \frac{a^2}{15b}\left(\frac{X}{1+X}\right)^2\right\} \tag{31}$$

substituting for $\frac{\theta_m}{\Delta p}$ in equation (3) we have

$$\left(\frac{\bar{K}}{P}\right)^{-1} = 1 - \frac{R}{C_p}\left(\frac{C_p \rho_G b}{\lambda}\right)\left\{\frac{1}{1+X} - \left(\frac{X}{1+X}\right)^2\left(\frac{\omega a}{b}\right)^2 \frac{1}{210} + i\omega \frac{a^2}{15b}\left(\frac{X}{1+X}\right)^2\right\} \tag{32}$$

thus for small ω inverting this gives

$$\frac{\bar{K}}{P} \simeq \frac{\gamma(1+X)}{\gamma X + 1}\left\{1 + \frac{\gamma-1}{\gamma}\,\frac{\omega^2}{210}\left(\frac{a^2}{b}\right)^2 \frac{\gamma X^2}{(1+X)(1+\gamma X)} + i\omega \frac{\gamma-1}{15\gamma}\left(\frac{a^2}{b}\right)\frac{\gamma X^2}{(1+X)(1+\gamma X)}\right\} \tag{33}$$

now writing $\bar{K} = \bar{K}' + i\omega \bar{K}''$

consider the real part first giving the <u>bulk modulus at low frequencies</u>

$$\bar{K}' = P\,\frac{\gamma(1+X)}{\gamma X + 1}\left\{1 + \frac{\gamma-1}{\gamma}\,\frac{\omega^2}{210}\left(\frac{a^2}{b}\right)^2 \frac{\gamma X^2}{(1+X)(1+\gamma X)}\right\} \tag{34}$$

now substituting for X from the definition and multiplying out

$$\bar{K}' = P\left[\frac{\frac{\rho_G}{\rho_L}(E-1)C_p + C_L}{\frac{\rho_G}{\rho_L}(E-1)C_v + C_L}\right] \qquad \omega \to 0 \tag{35}$$

Now the factor in the bracket is identical with the expression derived by Heinrich (4)* for the effective value of $\bar{\gamma}$ for the foam. This identity is easily recognised by substitution for Z, Heinrich's mixing ratio, from the definition

---

* (4) Heinrich, G. Z. Angew Math. Mech 22 1942, 117.

$$Z = \frac{\rho_G}{\rho_L}(E - 1) \tag{36}$$

i.e.

$$\bar{\gamma} = \frac{ZC_p + C_L}{ZC_V + C_L} \tag{37}$$

This, of course, is the limit at low frequencies: we have isothermal conditions as assumed by Heinrich.

The imaginary part of expression (33) gives a relation for the thermal damping of vibrations at low frequencies. We write

$$\frac{\bar{K}''}{\bar{K}'} \simeq \frac{1}{15}\ \frac{\gamma - 1}{\gamma}\ \frac{a^2}{b}\ \frac{\gamma X^2}{(1+X)(1+\gamma X)} \tag{38}$$

or alternatively, in terms of the decrement

$$\Delta_T \simeq \frac{\omega\pi}{15}\ \frac{\gamma - 1}{\gamma}\ \frac{a^2}{b}\ \frac{\gamma X^2}{(1+X)(1+\gamma X)} \tag{39}$$

This may be compared with the relation obtained by Pfriem* for the damping in a single bubble in an infinite medium. For large values of X the boundary conditions become identical in the two cases and the temperature at the bubble walls remains constant.

Case 2 Bubble size and frequency large

The expression reduces to

$$\left(\frac{\bar{K}}{P}\right)^{-1} = 1 - \frac{R}{C_p}\left(1 - \frac{X}{\Upsilon}\frac{1}{\sqrt{2b\omega}} + i\frac{X}{\omega\Upsilon}\sqrt{\frac{\omega}{2b}}\right) \tag{40}$$

thus we obtain for the real part of the bulk modulus of the gas in the foam

$$\frac{\bar{K}'}{\gamma P} = 1 - 3\,\frac{\gamma - 1}{a}\sqrt{\frac{b}{2\omega}} \tag{41}$$

---

* Pfriem H. Akust Z. 5 202 1940.

as a or $\omega \to \infty$ this expression reduces to the well known value for the adiabatic case

$$\bar{K}' \to \gamma P$$

The imaginary part gives

$$\Delta_T = \pi \frac{3\frac{\gamma-1}{a}\sqrt{\frac{b}{2\omega}}}{1+3\frac{\gamma-1}{a}\sqrt{\frac{b}{2\omega}}} \qquad (42)$$

which also reduces to the expression derived by Pfriem at high frequencies.

Case 3 Intermediate Values of Bubble Size and Frequency

We have derived analytical expressions for the variation of bulk modulus and logarithmic decrement for the two limiting cases of high and low frequency: but for the intermediate regions the whole expression, i.e. equations 28, 29 and 30, must be used. These have been calculated for certain values of the expansion factor; they are tabulated below (tables 1 and 2) and are plotted in the diagrams (figs 1). The curves also show the variation of decrement and effective specific heat ratio with both the parameter $2a\sqrt{\frac{\omega}{2b}}$ and the expansion factor E. They show that for foams of expansion factor less than about 100, the damping and bulk modulus are approximately as predicted by Pfriem for bubbles in an infinite liquid. This is to be expected since the effect of the mass of water is very marked and it is only in very light foams that it becomes of the same order of magnitude as the thermal capacity of the air.

Conclusion

Using a simple model of a cell in a mass of foam, we have derived expressions for the bulk modulus and logarithmic decrement for the gas in a foam. The complete analysis gives values equal to those obtained by Pfriem for the single bubble in an infinite medium, when the foam is assumed to be very dense.

It is concluded that the variation in bulk modulus and the thermal damping decrement Δ_T , are greatest for dense foams. The decrement has a maximum value of about 0.35 at $2a\sqrt{\frac{\omega}{2b}} \simeq \frac{3\pi}{2}$. For foams with expansion factor less than about 100, there is little change from this case; but as foams become lighter the variation in bulk modulus lessens and the decrement also becomes smaller.

TABLE 1

Effective Specific Heat Ratio, $\bar{\gamma}$ for the gas in a foam for various densities of foam.

E^*	1	100	1000	5000	10,000
$2x = 0^{**}$	1.0	1.008	1.070	1.205	1.272
$\frac{\pi}{2}$	1.002	1.010	1.069	1.207	1.2735
π	1.029	1.030	1.089	1.2125	1.2760
$\frac{3\pi}{2}$	1.0985	1.104	1.1365	1.2255	1.2820
$2\pi^{***}$	1.1745	1.178	1.200	1.260	1.300
3π	1.241	1.243	1.255	1.2895	1.3165
4π	1.2785	1.278	1.287	1.309	1.328
5π	1.3015	1.299	1.306	1.322	1.338
6π	1.3175	1.317	1.321	1.331	1.344
7π	1.3270	1.327	1.331	1.339	1.351
8π	1.3355	1.336	1.3405	1.346	1.355

* E, the foam expansion factor

** values calculated using Heinrich's Formula

*** values for $2x \geq 2\pi$ are calculated from an approximate formula

$$\bar{\gamma} = \frac{\gamma}{1 + X(\gamma - 1)} \frac{(1 + 2x f_a)}{(1 + 2x f_b)}$$

TABLE 2

Values of logarithmic decrement, Δ_T for foams of various densities

E^*	1	100	1000	5000	10,000
$2x = \frac{\pi}{2}$	.0746	.0710	.0501	.0139	.0052
π	.2514	.2404	.1663	.0540	.0233
$\frac{3\pi}{2}$	.3534	.3428	.2548	.0942	.0472
2π**	.3438	.3349	.2692	.1287	.0573
3π	.2795	.2745	.2356	.1244	.0683
4π	.2305	.2273	.2023	.1242	.0744
5π	.1946	.1922	.1750	.1153	.0758
6π	.1682	.1667	.1508	.1073	.0742
7π	.1478	.1465	.1370	.1000	.0727
8π	.1319	.1310	.1233	.0937	.0700

** for values of $2x \geq 2\pi$ the values have been calculated by the approximate formula:

$$\Delta_T \simeq \pi \frac{x(x-1)\left[(1+2xf_b)-(1+2xf_a)\right]}{(x-1)^2 + x^2(1+2xf_b)(1+2xf_a)}$$

* E, the foam expansion factor is related to the density by the formula

$$\bar{\rho} = \frac{\rho_L}{E}\left[1 + (E-1)\frac{\rho_b}{\rho_L}\right]$$

Effective Specific Heat Ratio $\bar{\gamma}$ For the gas in a Foam

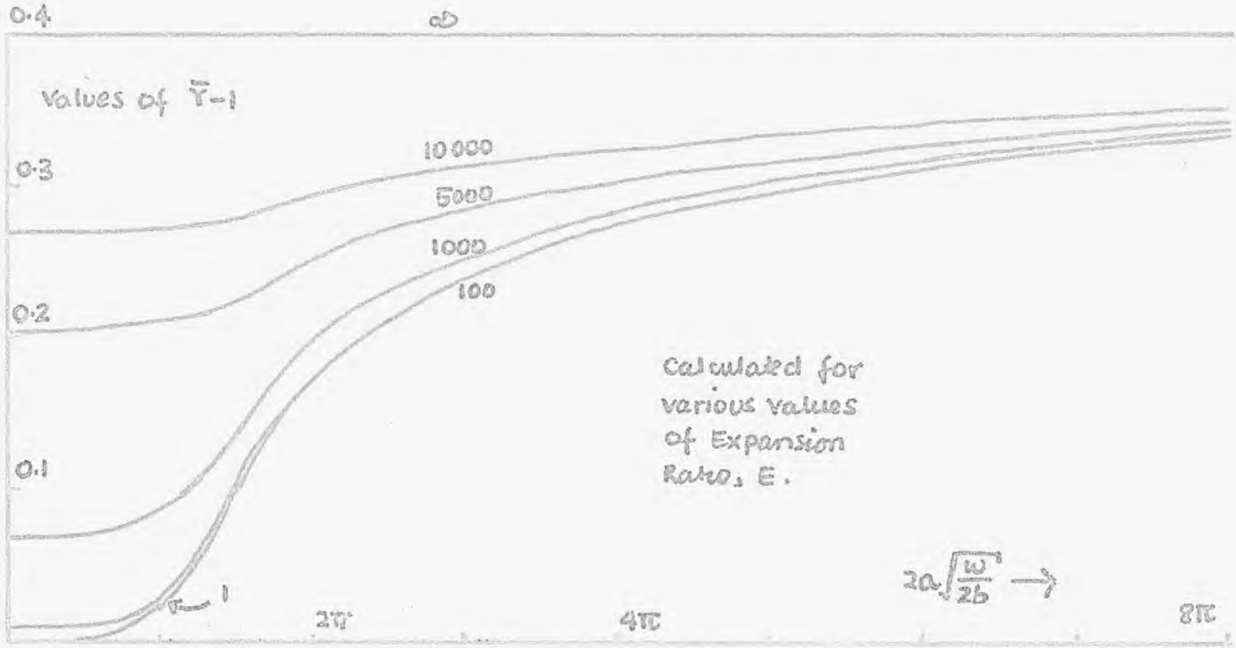

Logarithmic damping decrement Δ_T

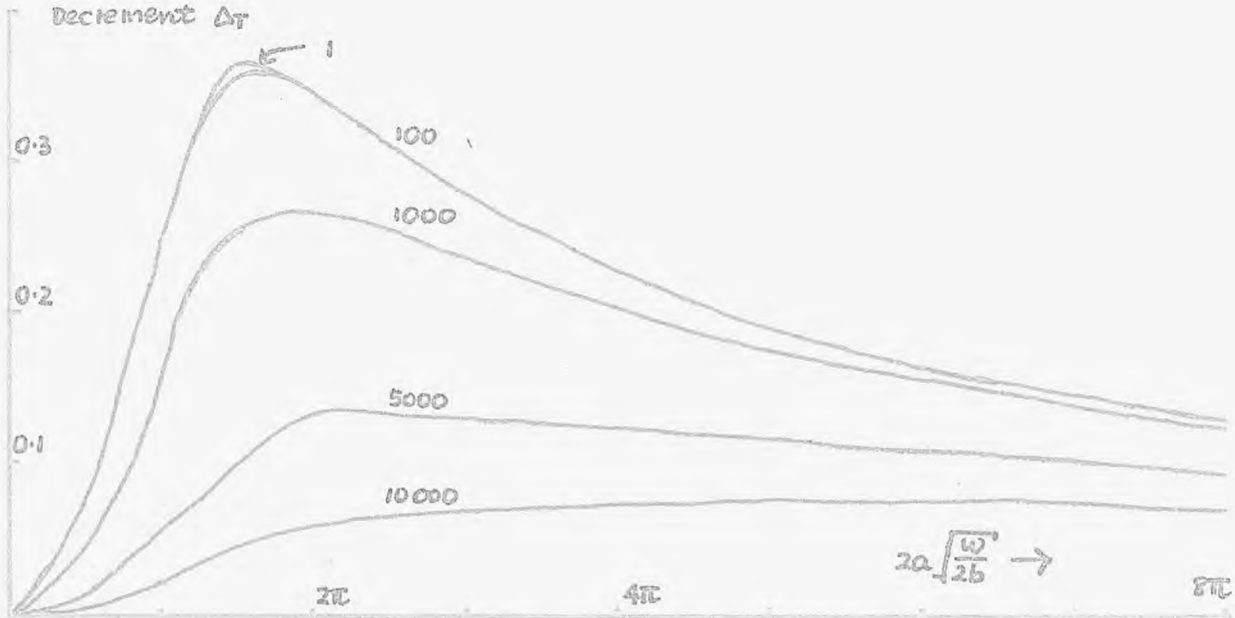

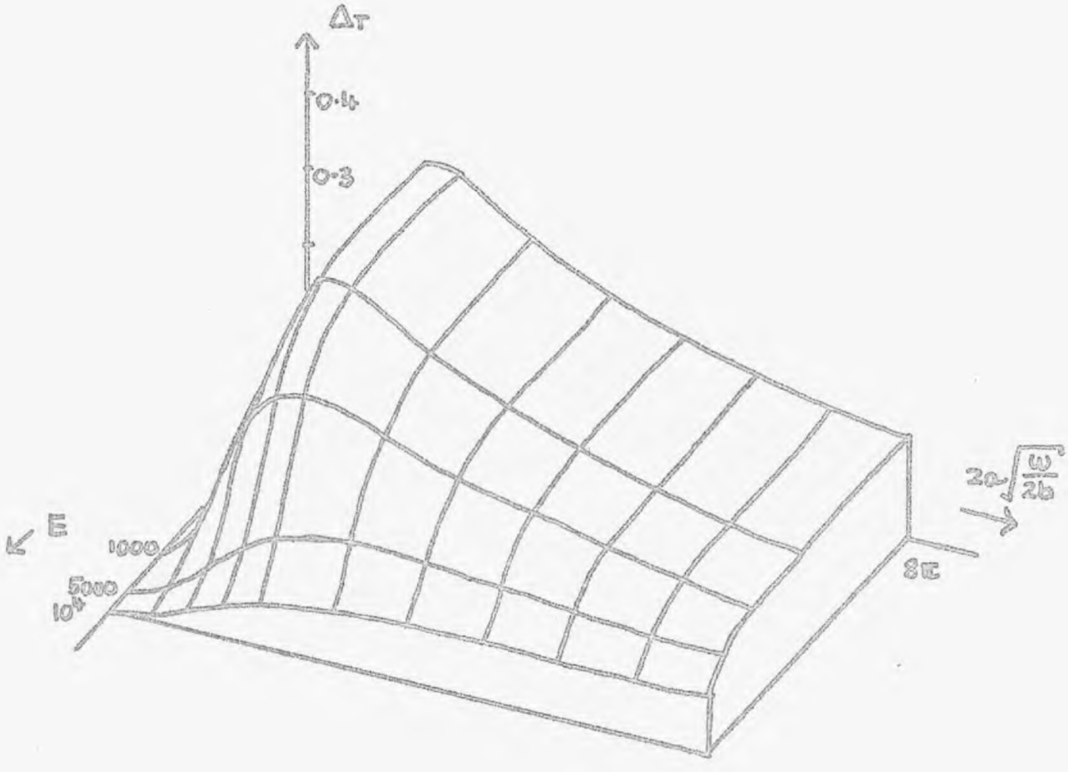

Variation of Damping Decrement Δ_T with $2a\sqrt{\frac{\omega}{2b}}$ and E

APPENDIX 3

A SIMPLE THEORY FOR THE DILATATIONAL VISCOSITY OF A CELL IN A FOAM

The dilatational viscosity of a medium is that viscosity which opposes pure expansion or compression of the material, apart from that due to the shear viscosity. The viscosity, in the case of a foam, will depend upon the flow conditions around the bubble in each cell. Because the cell shape is so complicated, any attempt to describe the liquid flow accurately will be mathematically very difficult. We therefore have to use a much simplified model, a spherical bubble radius a, contained in a spherical cell of liquid, radius R.

As our starting point we take the Navier-Stokes equation for the pressure opposing expansion under conditions of spherical symmetry.

$$dp(r) = \frac{2}{3}\frac{\eta_L}{r^2}\frac{\partial}{\partial r}(r^2 u_r) + 2\eta_L \frac{\partial u_r}{\partial r} \qquad (1)$$

We assume that the motion of the liquid shell is purely radial and also that the wavelength of vibrations in the foam is much larger than the cell diameter. Then the radial velocity of the liquid can be given by the following equations

$$r^2 u_r = R^2 u_R = \text{constant} \qquad (2)$$

$$u_r = \frac{R^2}{r^2} u_R$$

Thus the first term on the R.H.S. of (1) reduces to zero and

$$\frac{\partial u_r}{\partial r} = -2\frac{R^2}{r^3}u_R \tag{3}$$

Then putting

rate of change of cell volume = $\frac{dV}{dt} = 4\pi R^2 u_R$ (4)

and substituting into(1)we have

$$\partial p(r) = -4\eta_L R^2\frac{u_R}{r^3} = -\frac{\eta_L}{\pi}\frac{1}{r^3}\frac{dV}{dt} \tag{5}$$

hence the bulk modulus of the cell, neglecting any shear modulus, is

$$\bar{K} = \bar{\lambda} = -V\frac{dp}{dV} = \bar{\gamma}P\frac{V}{v} + i\omega\frac{\eta_L V}{\pi a^3}\left(1-\frac{a^3}{R^3}\right) \tag{6}$$

assuming sinusoidal volume pulsations.

This expression can be simplified because

bubble volume = $v = \frac{4}{3}\pi a^3$

and $\frac{V}{v} = \frac{E}{E-1}$ $\left(1-\frac{a^3}{R^3}\right) = \frac{1}{E}$ (7)

Thus we arrive at the following expression for the bulk modulus (or Lamé's first constant if we neglect the shear modulus) of the foam medium

$$\bar{\lambda} = \bar{\gamma}P\frac{E}{E-1} + i\omega\frac{4\eta_L}{3}\frac{1}{E-1} \tag{8}$$

The logarithmic decrement due to the dilatational viscosity is therefore

$$\Delta_V = \frac{4\pi\omega}{3}\cdot\frac{\eta_L}{\bar{\gamma}P}\cdot\frac{1}{E} = \pi\omega\frac{\lambda''}{\bar{\lambda}} \tag{9}$$

Comparison with Taylor's Theory

G. Taylor (1954) gave an analysis of the dilatational viscosity of a liquid containing many tiny, widely spaced bubbles. The basic assumptions were that the bubbles could be considered independently of each other. His value for the dilatation viscosity (which he denoted by $\mathcal{K}$) for an incompressible liquid is

$$\mathcal{K} = \lambda'' = \frac{4}{3}\frac{\eta_L}{x} = \frac{4}{3}\eta_L\frac{E}{E-1} \tag{10}$$

where x is the air (or gas) volume ratio

η_L is the liquid viscosity.

Now equation 10 differs from equation 8, particularly at the limits of the density range.

Taylor's assumption of sparse bubble distribution suggests that for very light foams (i.e. E large) the theory based upon cell structure is likely to be more accurate. Even so in this range the assumption of a spherical cell is likely to be invalid. We should expect, then, that as $E \to \infty$ then $\lambda'' \to 0$. This is not unexpected since in this range the amount of liquid is very small. Taylor's theory predicts that λ'' should tend to a constant value under these conditions.

For bubbly liquids, (i.e. $E < 2$), Taylor's theory is likely to be more accurate than that of the author since the assumption of a cell structure is no longer valid. He predicts that λ'' tends to an infinite value for an incompressible liquid but passes through a maximum and then goes to zero if the liquid is compressible. Our theory suggests that it would tend to a constant value at $E = 1$.

For dense foams, where the assumptions of the author's theory are valid, the theoretical predictions would seem to be more correct than those due to Taylor.

Conclusion

The theory presented supplements Taylor's theory in the regions where his assumptions are invalid. For bubbly liquids Taylor's theory is probably more accurate. The value of dilatational viscosity obtained is

$$\lambda' = \frac{4}{3}\eta_L \frac{1}{E} \qquad (E > 2)$$

and hence the logarithmic decrement for compressional waves in the foam is

$$\Delta = \frac{4\pi}{3}\omega \frac{\eta_L}{\gamma p}\cdot\frac{1}{E} \qquad (E > 2)$$

APPENDIX 4

THE PRODUCTION OF BUBBLES FROM AN ORIFICE

Introduction

This note is based upon work done to establish whether the bubbling method could produce large numbers of bubbles of sufficiently constant size for the foam experiments. It was felt that it might be useful to investigate the problem theoretically as well as experimentally.

For small gas flows the size of a bubble produced from a small circular orifice is given approximately by the well-known relation

$$R = \frac{3}{2}\left[\frac{r T}{(\rho_L - \rho_G) g}\right]^{\frac{1}{3}} \tag{1}$$

where R is the (spherical) bubble radius

r is the orifice radius

T is the surface tension of the bubble liquid

$\rho_L \; \rho_G$ are the liquid and gas densities

and g is the acceleration due to gravity.

The assumptions made are that the contact angle is zero, that a very small flow rate is used and that a spherical bubble is formed, whence the relation follows by equating the buoyancy and surface tension forces at break-off.

For air bubbles in water at 20°C this relation reduces to

$$R = 0.48 \; r^{1/3} \quad cm \tag{2}$$

or

$$\frac{v}{2r} = 0.231 \quad [cm^2] \qquad (3)$$

where v is the bubble volume.

Maier (1927) reported that not only did the above equation have to be modified by a constant factor in practical cases (e.g. measurements gave an average value of $\frac{v}{2r} = 0.33\ cm^2$ but as would be expected from the stated assumptions, at larger flow rates, the equation was virtually useless.

Datta (et. al.) (1950) collected data from previous work on the subject and showed that as the gas flow increased, the radius of bubbles produced decreased to a minimum and then gradually increased to a point where the bubble size became random.

Some workers tried to produce theories to explain this variation. Most of them have considered the question from the static point of view, attempting to calculate the shape and surface area as a function of the bubble volume. The bubble shape is important in evaluating the surface tension forces at the neck of the bubble as it breaks away, but the mathematical problem involved even in the static case is formidable. Null and Johnson (1958) approximated the shape by equating it to a sphere standing on a right truncated cone whereas Poutanen and Hohnson (1960) used an empirical formula in polar coordinates to simplify the calculation.

Krevelen and Hoftijzer (1950) tackled the problem from a different direction. They pointed out that the maximum production of bubbles would occur when they formed a chain, each bubble touching the one formed before it. The bubble diameter produced for a given flow rate would then be independent of the orifice size but would depend upon the rise velocity of the chain of bubbles away from the orifice. This will not be the same as that for single bubbles and so these workers examined dimensional formulae to establish this quantity as a function of bubble size.

No satisfactory theory which accounts for bubble size at high flow rates has yet been produced. Any such theory must take into account the effects of orifice size, surface tension, density, viscosity and gas flow rate. Since the gas flow rate (or the bubble expansion rate) plays such an important part, it was thought that study of the expansion process from the dynamic point of view might augment the considerable knowledge that we have about the static problem. We deal with this approach in the next section.

Bubble Formation

The process of bubble formation may conveniently be divided into three phases; the expansion of the bubble, its eventual separation from the orifice and hence from the supply of gas, and its acceleration and ascent from the orifice region as a free (and possibly oscillating) body.

We will consider some points about these stages separately

(i) the expansion of a bubble.

The simple case chosen for theoretical examination had the following features.

The bubble was produced at a point in an infinite liquid of density ρ and viscosity η . The gas-liquid surface tension was T and the gas was passed to the bubble via a very long thin tube so that the conditions for spherical symmetry could be satisfied.

The differential equation to be satisfied was found to be

$$\underset{1.}{P_i(t)} = \underset{2.}{P_O} + \underset{3.}{\frac{3}{2}\rho\left(\frac{dR}{dt}\right)^2} + \underset{4.}{\rho R\frac{d^2R}{dt^2}} + \underset{5.}{\frac{2T}{R}} + \underset{6.}{\frac{4\eta}{R}\frac{dR}{dt}} \qquad (4)$$

where the term

1. is the pressure inside the bubble which may be a function of the gas flow rate.
2. is the hydrostatic pressure in the liquid.
3. the effect of production of kinetic energy of expansion.
4. the effect of inertia of the fluid.
5. the effect of surface tension.
6. the "excess pressure" or viscosity effect.

Inspection shows that the solution of this equation would be difficult as it stands, but some approximations are possible.

Let us assume first that we are supplying the gas from a source of very large capacity so that the pressure difference between the gas and the liquid remains constant, i.e. $P = P_i - P_O$. It is quite likely that this assumption will prove to be invalid since bubbles are usually produced from long thin capillaries across which there would be pressure differences depending upon the gas flow rate. The question of the effect of a sound wave on the process is also interesting, under these conditions the pressure would contain a periodic term. However such complexities may be left until the simple problem has been solved.

We can make another assumption, that of reasonably slow expansion where we can assume that the inertial terms are negligible but where the viscous terms are still important. We may then neglect terms 3. and 4. in equation (4), giving us

$$P = \frac{2T}{R} + \frac{4\eta}{R}\frac{dR}{dt} \qquad (5)$$

integrating this leads to the solution for the radius R as a function of time.

$$R = \frac{2T}{R} + \left(R_0 - \frac{2T}{P}\right) \exp\left\{\frac{Pt}{4\eta}\right\} \qquad (6)$$

where $R = R_0$ at $t = 0$

upon rearranging this gives

$$\frac{P - \frac{2T}{R}}{P - \frac{2T}{R_0}} \cdot \frac{R}{R_0} = \exp\left\{\frac{Pt}{4\eta}\right\}$$

now the expression $P - \frac{2T}{R_0}$ is the pressure excess on the bubble over that needed to force the bubble out of the orifice against surface tension forces. (The surface tension can be measured using the critical pressure under "zero flow" conditions). This pressure difference is termed the excess pressure P_E. If it is positive, the bubble can expand; if it is negative the bubble of course will contract.

But the rate at which it will expand depends, in this theory, also upon the absolute pressure difference (the difference between the gas and the liquid). It is this that will determine the frequency at which bubbles are produced, together with the conditions for breakaway. We consider these in the next section.

(ii) The Mechanism of Break-away

The bubble grows and moves away from the orifice until the film connecting it to the surface breaks and it is cut off from the gas supply.

Whether the film breaks due to mechanical rupture or because of instability in the cylindrical tube is in doubt. In the static case, the break occurs as soon as the buoyancy overcomes the surface tension; but as flow rates increase other effects come into play. Among these may be

(a) Buoyancy. An upward force of $\frac{4}{3}\pi R^3 \rho_L g$ with R varying with time according to the expansion process.

(b) Surface Tension. An approximately constant downward force of $2\pi r' T$ where r' is the smallest radius of the neck.

(c) Drag due to the upward motion of the bubble in the viscous liquid. For low speeds this will be proportional to the upward velocity relative to the fluid (by Stokes' Law).

(d) Upward Drag due to the movement of preceding bubbles.

They may be considered as carrying with them, a column of liquid moving at a lower velocity. This then reduces the effective velocity of the bubbles in term (c).

(e) Inertial Force due to the acceleration of the liquid surrounding the bubble. One can imagine a mass associated with each bubble - the "accession to inertia", which has been calculated as $\frac{2}{3}\pi R^3 \rho_L$ for solid spheres.

(f) Repulsion from a surface due to the rapid expansion of the bubble. This will be most marked at high gas pressures and at small distances from the surface but under most conditions it will be small.

(g) Gas impact due to the upward momentum of the gas flowing into the bubble.

It will be appreciated that if all the terms are included the problem will become very difficult, especially since most of the terms involve the solution to the first problem, that of the expansion of the bubble.

(iii) The movement away from the orifice

Once it is free of the restraining surface tension forces, the bubble can accelerate to the terminal velocity in the liquid and move away from the growth region. The terminal velocity depends mainly upon the buoyancy and the viscous drag, but also to a marked extent upon the motion of others in the chain of bubbles.

It is this latter dependence that is most difficult to estimate. Krevelen and Hoftijzer (1950) produced a dimensional equation to estimate the most this effect could have.

As the bubble rises it oscillates both in volume and in shape. This oscillation produces a pulse of sound as each bubble is produced, and this can cause interference in acoustic experiments.

The frequency of Bubble Emission

We can use some of the points discussed in the last section to estimate the frequency of bubble emission. The maximum bubble radius is given by the break-off conditions. In order to simplify the equations still further, let us assume that this is given by the static formula of equation (1). Then we can estimate the time needed for expansion from a small sphere assumed to have the same radius as the orifice.

$$t = \frac{1}{f} = \frac{4\eta}{P} \ln_e \left\{ \frac{R}{R_0} \left(P - \frac{2T}{R} \right) \frac{1}{P_E} \right\}$$

where f is the frequency of bubble emission.

It will be noticed that this frequency is very dependent upon the injection pressure and especially upon the excess pressure over the critical.

Practical Observations

The bubbling process was observed using a stroboscope and travelling microscope and bubbling through glass capillary tubing. The following points were noted:

(i) It was easier to keep bubbling going than to start it initially. This consistent with the hypothesis that the motion of other bubbles plays an important role in the bubbling process. This effect seemed to be more important in pure water than in water containing Stergene, which has a much smaller surface tension.

(ii) The bubble is attached to the glass at some distance down the tube. The narrowest part of the stalk is therefore smaller than the capillary diameter.

(iii) It grows from an approximately hemispherical cap situated inside the tube and rises as it grows until it is joined to the glass only by a long stalk. The stalk is then suddenly pinched in, and the bubble rises from the surface.

(iv) Soon after cut-off the bubble still has the vestige of a stalk and it executes surface oscillations due to this initial distortion. This may be the primary cause of the noise produced since the sound intensity decreases when Stergene is added to the water to decrease the surface tension. The sound spectrum also contains more than one frequency.

(v) An approximately linear relation between pressure and volume flow was found except at low excess pressures.

(vi) The bubble size remained sensibly constant under constant pressure within a limited pressure region.

(vii) The frequency of bubble emission, measured with a stop-watch at low frequencies and with a stroboscope at high frequencies, remains constant and independent of the pressure over the same region described in (vi).

(viii) The between-bubble size variation, i.e. the difference in volume between bubbles produced within a short time of each other, was shown by photographs to be less than 1%.

Conclusions from the Investigation

Any solution to the theoretical problem is handicapped by too little information about specific points such as the effect of the motion of other bubbles, the shape of the growing bubble and even the conditions of the break away. It is felt that more work must be done to elucidate these specific points before the theoretical problem can be tackled with any hope of success.

The formation of a bubble apparently depends to a marked extent upon the motion of other bubbles in the chain.

The bubbling method can be used to produce small quantities (of the order of 100 mL per minute) of air bubbles of constant (within a few percent) and reasonable ($\sim$ 10 μL volume) size for the foam experiments.

Constant size can, however, be expected only if the pressure is kept constant and much higher than the critical pressure. But if it is taken too high, turbulance sets in and random bubble sizes are produced. There is therefore a safe pressure region where conditions can be stable.

Acoustic measurements showed that the sound pulse produced upon emission of a bubble was of high enough amplitude to require that the measurement area be kept separate from the foam-making part of the apparatus.

APPENDIX 5

THE PROPAGATION OF ELASTIC WAVES IN A MEDIUM ENCLOSED IN A CYLINDER

1. INTRODUCTION

The problem of propagation in a free elastic cylinder is an old problem and the general behaviour of the modes found is well understood (Mott* (1960) has discussed this and similar problems). The complementary case, that of the cylinder whose surface is rigidly fixed, has, however, not received much attention. We are interested not only in this latter case but also in the intermediate case where the elastic medium is able to slide quite freely in the tube but cannot expand radially.

2. THE GENERAL EQUATIONS

The components of displacement of the elastic medium, in cylindrical coordinates are written

$$\underline{u} = (u_r \;\; u_\varphi \;\; u_z) \tag{1}$$

and from these the ROTATION $\underline{\omega}$ is given by

$$2\underline{\omega} = \operatorname{curl} \underline{u} = \left(\frac{1}{r}\frac{\partial u_z}{\partial \varphi} - \frac{\partial u_\varphi}{\partial z}, \frac{\partial u_r}{\partial z} - \frac{\partial u_z}{\partial r}, \frac{1}{r}\frac{\partial (r u_\varphi)}{\partial r} - \frac{1}{r}\frac{\partial u_r}{\partial \varphi} \right) \tag{2}$$

and the DILATATION Δ by

$$\Delta = \operatorname{div} \underline{u} = \frac{1}{r}\frac{\partial}{\partial r}(r u_r) + \frac{1}{r}\frac{\partial u_\varphi}{\partial \varphi} + \frac{\partial u_z}{\partial z} \tag{3}$$

---

* G. Mott, A study of wave propagation in thin sheets, University of London Thesis, Jan, 960.

The equations of motion of the elastic medium, in vector notation are written

$$(\lambda + 2\mu)\ \mathrm{grad}\ \Delta \ - \ \mu\ \mathrm{curl}\ \mathrm{curl}\ \underline{\underline{u}} \ = \ \rho\ \frac{\partial^2 \underline{u}}{\partial t^2} \tag{4}$$

where we have neglected the body forces. In cylindrical coordinates they become

$$(\lambda + 2\mu)\frac{\partial \Delta}{\partial r} - \frac{2\mu}{r}\frac{\partial \omega_z}{\partial \varphi} + 2\mu \frac{\partial \omega_\varphi}{\partial z} = \rho \frac{\partial^2 u_r}{\partial t^2} \tag{5}$$

$$(\lambda + 2\mu)\frac{1}{r}\frac{\partial \Delta}{\partial \varphi} - 2\mu \frac{\partial \omega_r}{\partial z} + 2\mu \frac{\partial \omega_z}{\partial r} = \rho \frac{\partial^2 u_\varphi}{\partial t^2} \tag{6}$$

$$(\lambda + 2\mu)\frac{\partial \Delta}{\partial z} - \frac{2\mu}{r}\frac{\partial}{\partial r}(r\omega_\varphi) + 2\mu \frac{1}{r}\frac{\partial \omega_r}{\partial \varphi} = \rho \frac{\partial^2 u_z}{\partial t^2} \tag{7}$$

Now this set of equations gives the properties of all waves that may be propagated in the medium. We simplify the problem by examining some of the waves separately.

3. THE THREE TYPES OF WAVE

(A) Torsional Waves

The wave is assumed to be purely distortional and also there is no radial displacement

i.e. $$\Delta = 0$$

$$u_r \ u_z = 0$$

We further assume that u_φ is independent of φ

Then

$$\omega_r = -\frac{1}{2}\frac{\partial u_\varphi}{\partial z} \qquad \omega_\varphi = 0 \qquad \omega_z = \frac{1}{2}\left(\frac{\partial u_\varphi}{\partial r} + \frac{u_\varphi}{r}\right)$$

The equations (5) and (7) are satisfied identically and equation (6) reduces to

$$\frac{\partial^2 u_\varphi}{\partial r^2} + \frac{1}{r}\frac{\partial u_\varphi}{\partial r} - \frac{u_\varphi}{r^2} + \frac{\partial^2 u_\varphi}{\partial z^2} = \frac{1}{c_2^2}\frac{\partial^2 u_\varphi}{\partial t^2} \tag{8}$$

where

$$c_2^2 = \frac{\mu}{\rho} \tag{9}$$

(B) Longitudinal waves

We assume here that $u_\varphi = 0$ and u_r and u_z are independent of φ. Then

$$\Delta \neq 0$$
$$u_\varphi = 0$$

it follows that equation (6) is satisfied identically and that (4) and (7) become

$$c_1^2 \frac{\partial \Delta}{\partial r} + 2c_2^2 \frac{\partial \omega_\varphi}{\partial z} = \frac{\partial^2 u_r}{\partial t^2} \tag{10}$$

$$c_1^2 \frac{\partial \Delta}{\partial z} - 2\frac{c_2^2}{r}\frac{\partial (r\omega_\varphi)}{\partial r} = \frac{\partial^2 u_z}{\partial t^2} \tag{11}$$

where

$$c_1^2 = \frac{\lambda + 2\mu}{\rho} \tag{12}$$

(C) "Flexural" waves

These are waves which have all components non-zero. In the free cylinder case these are flexural waves since the cylinder actually bends, in our case this is impossible by the boundary conditions to be discussed below. We might introduce the term "Pseudo-flexural waves" for this case, we have

$$\Delta \neq 0$$
$$u_r, u_\varphi, u_z \neq 0$$

4. THE BOUNDARY CONDITIONS

The first condition is that the amplitude is always finite at the axis of the cylinder and is always assumed to be satisfied in the discussion to follow.

The second set of conditions is given by those existing at the surface of the cylinder. Since we are particularly concerned with an elastic medium enclosed in a rigid tube, it is first assumed that the radial displacement is zero at the surface, i.e.

$$u_r = 0 \qquad (r = b)$$

where b is the tube radius.

We are now left with a choice of the value of the z and φ components of stress or displacement at the surface. We choose three of the possible combinations:

Case 1. that the elastic medium is held rigidly at the surface (the material is glued into the tube)

$$u_z \,,\, u_\varphi = 0 \qquad (r = b)$$

Case 2. that the medium is completely free to move as a plug inside the tube

$$\tau_{rz} \,,\, \tau_{r\varphi} = 0 \qquad (r = b) \qquad \text{where}$$

$$\left.\begin{aligned} \tau_{rz} &= \mu\left(\frac{\partial u_r}{\partial z} + \frac{\partial u_z}{\partial r}\right) \\ \tau_{r\varphi} &= \mu\left(\frac{1}{r}\frac{\partial u_\varphi}{\partial r} + r\frac{\partial}{\partial r}\left(\frac{u_\varphi}{r}\right)\right) \end{aligned}\right\} \qquad (13)$$

Case 3. that the material is constrained by a viscous force at the edge of the tube. We may represent this force by a friction term

S where

$$\tau_{rz} = -i\omega S u_z \qquad (r=b) \tag{14}$$
$$\tau_{r\varphi} = -i\omega S u_\varphi$$

We now consider the various waves possible under these conditions.

5. CASE 1. MATERIAL HELD RIGIDLY

Case 1.A) Torsional Waves $\Delta = 0 \quad u_r, u_z = 0$

We assume that the displacement u_φ is given by

$$u_\varphi = \Phi(r)\, e^{ikz - i\omega t} \tag{15}$$

this leads to the equation

$$\frac{\partial^2 \Phi}{\partial r^2} + \frac{1}{r}\frac{\partial \Phi}{\partial r} + \left(\kappa_1^2 - \frac{1}{r^2}\right)\Phi = 0 \tag{16}$$

where $$\kappa_1^2 = \frac{\omega^2}{c_2^2} - k^2 \tag{17}$$

a solution of this is

$$\Phi(r) = A\, J_1(\kappa_1 r) \tag{18}$$

and to satisfy the boundary condition,

$$J_1(\kappa_1 b) = 0 \tag{19}$$

i.e. $$\kappa_1 b = \xi_n$$

where ξ_n are the solutions of the equations

$$J_1(\xi_n) = 0 \tag{20}$$

Substituting from (17) we get an equation for the phase velocity V as a function of wavelength Λ.

$$(kb)^2\left(\frac{V^2}{c_2^2}-1\right) = \xi_n^2$$

$$\frac{V^2}{c_2^2} = 1+\frac{\xi_n^2}{(kb)^2} \tag{21}$$

$$\frac{V^2}{c_2^2} = 1+\frac{\xi_n^2}{\left(\frac{2\pi b}{\Lambda}\right)^2} \tag{22}$$

where

$$k = \frac{2\pi}{\Lambda} = \frac{\omega}{V} \tag{23}$$

the frequencies at which new modes are allowed are given by the relation

$$\frac{\omega_n a}{c_2} = \xi_n$$

$$f_n = \frac{\xi_n c_2}{2\pi b} \tag{24}$$

Case 1.b) Longitudinal Waves

We must satisfy the two equations (10) and (11) and we substitute

$$u_r = R(r)e^{ikz-i\omega t} \qquad u_z = Z(r)e^{ikz-i\omega t} \tag{25}$$

then it can be shown by substitution that we obtain the following expressions for R and Z

$$R = -A k_2 J_1(k_2 r) + B k J_1(k_3 r) \tag{26}$$

$$Z = A ik J_0(k_2 r) + B ik_3 J_0(k_3 r) \tag{27}$$

where

$$k_2^2 = \frac{\omega^2}{c_1^2} - k^2 \tag{28}$$

$$k_3^2 = \frac{\omega^2}{c_2^2} - k^2 \tag{29}$$

now at $r = b$, the following determinant must equal zero.

$$\begin{vmatrix} -k_2 J_1(k_2 b) & k J_1(k_3 b) \\ ik J_0(k_2 b) & ik_3 J_0(k_3 b) \end{vmatrix} = 0 \qquad (30)$$

this gives the relation

$$\frac{(kb)^2}{k_2 b}\frac{J_0(k_2 b)}{J_1(k_2 b)} + (k_3 b)\frac{J_0(k_3 b)}{J_1(k_3 b)} = 0 \qquad (31)$$

We can find the frequencies at which new modes are possible by putting $V = \infty$

We find that the necessary conditions are either

(i) $$J_1(k_2 b) = 0$$

and thus $$f_m = \frac{\xi_m}{2\pi b} c_1 \qquad (32a)$$

or

(ii) $J_0(k_3 b) = 0$ $$f_m = \frac{\eta_m}{2\pi b} c_2 \qquad (32b)$$

but the velocity equation is very complicated at other values of frequency.

Case 1.c) "Flexural" Waves

We consider here only the first type of asymmetrical wave, however, the work of Mott suggests that there should be a whole series of these waves each of which will have an infinite series of modes.

We put

$$\underline{u} = (V\cos\phi, V\sin\phi, W\cos\phi)e^{ikz - i\omega t} \qquad (33)$$

and, using these we must satisfy the three wave equations (5), (6) and (7). We find that the following solutions are necessary:

$$\left.\begin{aligned} U &= A k_2 J_1'(k_2 r) + B k k_3 J_1'(k_3 r) + C \frac{1}{r} J_1(k_3 r) \\ V &= -A \frac{1}{r} J_1(k_2 r) - B \frac{k}{r} J_1(k_3 r) - C k_3 J_1'(k_3 r) \\ W &= A ik J_1(k_2 r) - B i k_3^2 J_1(k_3 r) \end{aligned}\right\} \quad (34)$$

since the boundary conditions are that $u_z, u_r, u_\phi = 0 \quad (r=b)$ the following determinant must become zero

$$\begin{vmatrix} k_2 J_1'(k_2 b) & k k_3 J_1'(k_3 b) & \frac{1}{a} J_1(k_3 b) \\ -\frac{1}{a} J_1(k_2 b) & -\frac{k}{a} J_1(k_3 b) & -k_3 J_1'(k_3 b) \\ ik J_1(k_2 b) & i k_3^2 J_1(k_3 b) & 0 \end{vmatrix} = 0 \qquad (35)$$

and upon rearrangement this reduces to

$$\begin{vmatrix} 1 - \phi(k_2 b) & 1 - \phi(k_3 b) & 1 \\ 1 & 1 & 1 - \phi(k_3 b) \\ kb & \frac{(k_3 b)^2}{kb} & 0 \end{vmatrix} = 0 \qquad (36)$$

where

$$\phi(y) = y \frac{J_2(y)}{J_1(y)} \qquad (37)$$

New modes come in at those frequencies given when $V = \infty$

This leads to the relation

$$\frac{1}{\phi\left(\frac{\omega b}{c_1}\right)} + \frac{1}{\phi\left(\frac{\omega b}{c_2}\right)} = 1 \qquad (38)$$

which is an expression which can give the frequencies if the velocity ratio $\frac{c_1}{c_2}$ is known. If this ratio is very large, then we may write

$$J_2\left(\frac{\omega b}{c_2}\right) \simeq 0$$

or

$$f_n \simeq \frac{\gamma_n c_2}{2\pi b} \qquad (39)$$

where γ_n are the solutions of the equation $J_2(\gamma_n) = 0$

Case 1: Conclusions for the Rigid Case

We find that the actual phase velocity - frequency curve for the three types of wave are very difficult to analyse; but the cut-off frequencies for the different modes can be estimated. Particularly when the shear velocity is small, these frequencies are dependent only upon the shear properties of the material.

6. CASE 2. MATERIAL FREE TO SLIDE AT THE SURFACE

Case 2.A) Torsional Waves $\Delta = 0 \quad u_r, u_z = 0$

We have only the φ component to deal with. The equation for the displacement is the same as equation (16) and the solution must be

$$u_\varphi = \Phi(r)\, e^{ikz - i\omega t}$$

$$\Phi = A\, J_1(k_1 r)$$

the boundary condition is that $\tau_{rz} = 0 \quad \tau_{r\varphi} = 0 \quad (r = b)$

The first of these is satisfied by the assumption that $u_r, u_z = 0$ and the second reduces to

$$(r = b) \qquad \tau_{r\varphi} = \mu\left\{\frac{1}{r}\frac{\partial \Phi}{\partial r} + r\frac{\partial}{\partial r}\left(\frac{\Phi}{r}\right)\right\} = 0 \qquad (40)$$

This leads to the condition that $\frac{\partial}{\partial b}\left[\frac{J_1(k_1 b)}{b} \right] = 0$

i.e. $k_1 b = \beta_n$ where β_n are the roots of the equation

$$\beta\, J_0(\beta) = 2J_1(\beta)$$

Hence
$$\frac{V^2}{C_2^2} = 1 + \frac{\beta_n^2}{\left(\frac{2\pi b}{\lambda}\right)^2}, \qquad (41)$$

which is a similar equation to that in the "rigid" case, although the cut-off frequencies differ, viz:

$$f_n = \frac{\beta_n}{2\pi b}\, c_2 \qquad (42)$$

Case 2.B) Longitudinal Waves $\quad u_\varphi = 0$

Equations (26) and (27) hold but we have to adjust the boundary conditions. They are $R(b) = 0$ and $\tau_{rz} = 0$.
These lead to the following

$$R = 0 = -A k_2 J_1(k_2 b) + B\, k\, J_1(k_3 b) \qquad (43)$$

$$\tau_{rz} = 0 = -2A k k_2 J_1(k_2 b) + B\left(2k^2 - \frac{\omega^2}{c_2^2}\right) J_1(k_3 b) \qquad (44)$$

Solutions to these equations are immediately obvious, we may have

(i) $\quad J_1(k_2 b) = 0 \qquad B = 0$

$$k_2 b = \xi_n$$

$$\frac{V^2}{c_1^2} = 1 + \frac{\xi_n^2}{\left(\frac{2\pi b}{\lambda}\right)^2} \qquad f_n = \frac{\xi_n c_1}{2\pi b} \qquad (45)$$

These modes correspond to the normal acoustic modes in a tube, occurring at frequencies governed only by the compression wave velocity. These waves are here designated by the subscript C.

The second obvious solution is

Fig A1 Case 2B Radially Symmetrical Longitudinal Waves in a Medium Freely held in a Tube

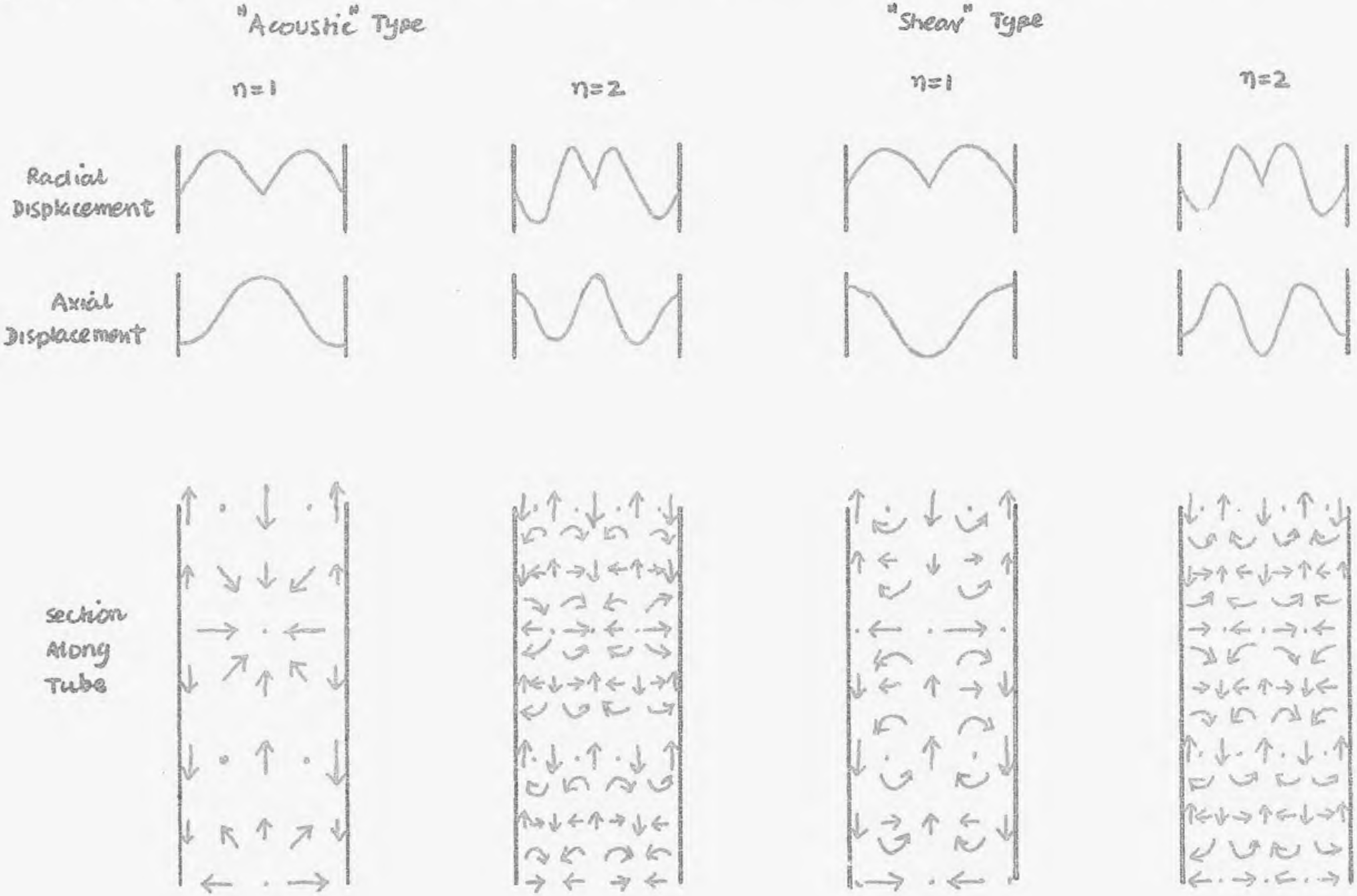

(ii) $\quad J_1(\kappa_3 b) = 0 \qquad (A = 0)$

$$\kappa_3 b = \xi_n$$

$$\frac{V^2}{c_2^2} = 1 + \frac{\xi_n^2}{\left(\frac{2\pi a}{\lambda}\right)^2} \qquad f_{Sn} = \frac{\xi_n c_2}{2\pi b} \tag{46}$$

the frequencies are governed entirely by the shear velocity, and are designated by the subscript S.

(iii) the third solution is that $V = c_1$, a case that is already covered by (i) and is, in fact, mode (CO).

The first modes of each type of longitudinal wave, the zero mode, $n = 0$, have an r and z displacement as a constant function ofthe radius vèctor. They propagate with velocities c_1 or c_2. The higher modes , ${}^{C}_{S}n = 1,2,3,4$, have a more complicated displacement function. Graphs of these are drawn in fig. A1. for frequencies somewhat higher than the cut-off so that the wavelength is small.

The compression types have a distinct dilatation which gives rise to a pressure wave propagating down the tube: whereas the shear types of wave do not display such a dilatation. These shear types of mode are possible at lower frequencies than the equivalent compression modes.

Case 2.C) "Flexural" Waves

Again we consider only the first type of asymmetrical wave. Equations (34) hold, but under the boundary conditions

$$u_r = 0 \quad \tau_{rz} = 0 \quad \text{and} \quad \tau_{r\varphi} = 0 \quad (r = b).$$

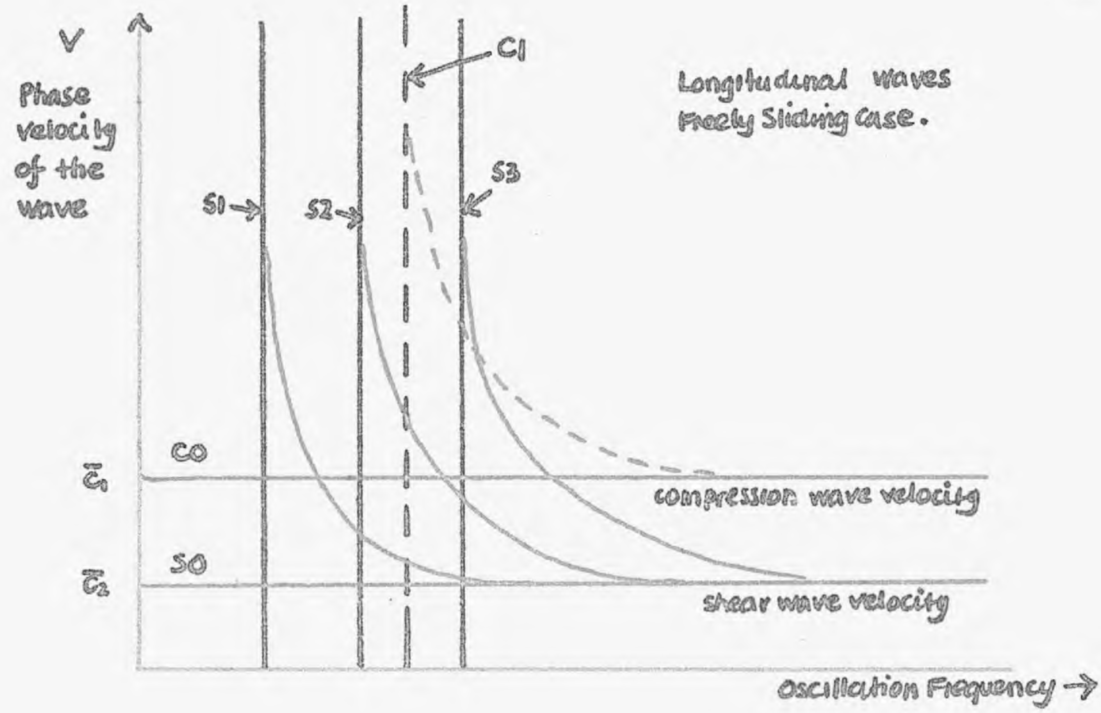

Diagram showing the modes in case 2B, Freely sliding case longitudinal waves

Table showing some results for the simpler cases.

	A Pure shear waves $\Delta = 0$	B Longitudinal waves $u_\varphi = 0$	
		"compressional" or "Acoustic"	"shear"
case 1 Rigidly Fixed	$f_n = \frac{\xi_n}{2\pi b} c_2$ $\frac{V^2}{c_2^2} = 1 + \xi_n^2 \left(\frac{\Lambda}{2\pi b}\right)^2$ $V_0 = c_2$	$f_{cn} = \frac{\xi_n c_1}{2\pi b}$	$f_{sn} = \frac{\eta_n c_2}{2\pi b}$
case 2 sliding	$f_n = \frac{\beta_n}{2\pi b} c_2$ $\frac{V^2}{c_2^2} = 1 + \beta_n^2 \left(\frac{\Lambda}{2\pi b}\right)^2$ $V_0 = c_2$	$f_{cn} = \frac{\xi_n c_1}{2\pi b}$ $\frac{V^2}{c_1^2} = 1 + \xi_n^2 \left(\frac{\Lambda}{2\pi b}\right)^2$ $V_0 = c_1$	$f_{sn} = \frac{\xi_n c_2}{2\pi b}$ $\frac{V^2}{c_2^2} = 1 + \xi_n^2 \left(\frac{\Lambda}{2\pi b}\right)^2$ $V_0 = c_2$

Using similar methods to Case 1.C, we arrive at the following necessary condition

$$\begin{vmatrix} \phi(k_2b)-1 & k\{\phi(k_3b)-1\} & 1 \\ 2\{\phi(k_2b)-2\} & 2k\{\phi(k_3b)-2\} & 2\{\phi(k_3b)-1\}-(k_3b)^2 \\ 2k\{\phi(k_2b)-1\} & (k^2-k_3^2)(k_3b) & k \end{vmatrix} = 0. \tag{47}$$

where $\phi(y) = y\,\dfrac{J_0(y)}{J_1(y)}$ and the other symbols have been previously defined. We can easily obtain the expression giving the conditions for new modes by putting $V = \infty$. We obtain

$$2\left(\phi(k_3b)-1\right) - (k_3b)^2 = 2\,\frac{\phi(k_2b)-2}{\phi(k_2b)-1} \tag{48}$$

which is rather a complicated function of frequency and the two velocities.

Case 2. Conclusion for the Free-sliding Case

The propagation of various waves is shown to be theoretically possible under these conditions. Both pure shear and asymmetrical waves are possible but for our particular needs the most interesting type is Case 2.B, the propagation of longitudinal waves. Two types or classes of waves are predicted; the compressional class, where dilatation is more important than rotation and the shear class where these are reversed in importance. Various modes of each of them satisfy the conditions, and these have velocities decreasing to c_1 and c_2 respectively at infinite frequency (see fig).

For a given tube the shear class of modes will occur at lower frequencies than the compression class, and they will therefore be of more practical importance.

7. CASE 3. MATERIAL RETARDED BY A FRICTIONAL FORCE AT THE EDGE OF THE TUBE

The material is assumed to have a retarding force proportional to the velocity of displacement at the tube surface. This, in fact, will lead to an attenuation if the force is truly viscous, but we deal here with the general case without choosing a particular form of force constant.

Case 3.A) Torsional Waves $\quad \Delta = 0 \quad u_r, u_z = 0$

We deal here with the φ component of displacement, giving as before the equations

$$u_\varphi = \Phi(r)\, e^{ikz - i\omega t} \tag{15}$$

$$\Phi(r) = A\, J_1(k_1 r) \tag{18}$$

now $\tau_{r\varphi} = -i\omega S\, u_\varphi$ is the boundary condition, and thus, since

$$\tau_{r\varphi} = \mu A\, r \frac{\partial}{\partial r}\left(\frac{J_1(k_1 r)}{r} \right) \tag{49}$$

the condition for propagation is that

$$\mu b \frac{\partial}{\partial b}\left(\frac{J_1(k_1 b)}{b} \right) + i\omega S\, J_1(k_1 b) = 0 \tag{50}$$

or more simply

$$\frac{\partial}{\partial b}\left(\frac{J_1(k_1 b)}{b} \right) + \frac{i\omega S}{\mu}\left(\frac{J_1(k_1 b)}{b} \right) = 0 \tag{51}$$

The mode cut-off frequencies are given by the roots of this equation.

Case 3.B) Longitudinal Waves

Equations (26) and (27) together with the new boundary conditions give

$$k = 0 = -A\, k_2 J_1(k_2 b) + B\, k J_1(k_3 b)$$

$$0 = -A\left\{\begin{matrix} 2kk_2 J_1(k_2 b) \\ -i\omega k S J_0(k_2 b) \end{matrix}\right\} + B\left\{\begin{matrix} (2k^2 - \frac{\omega^2}{c_2^2}) J_1(k_3 b) \\ -i\omega k_3 S J_0(k_3 b) \end{matrix}\right\} \quad (52)$$

then the frequencies at which $V = \infty$ are given by putting $k = 0$ giving the conditions:-

(i) Compression type of mode

$$J_1(k_2 b) = 0 \qquad f_n = \frac{\xi_n c_1}{2\pi b} \quad (53)$$

as found before cases 1B and 2B

(ii) Shear type of mode

$$-\frac{\omega^2}{c_2^2} J_1(k_3 b) - i\omega S k_3 J_0(k_3 b) = 0$$

$$\frac{(k_3 b) J_0(k_3 b)}{J_1(k_3 b)} = -\frac{\omega^2}{c_2^2}\frac{b}{i\omega S} \quad (54)$$

This result can be checked by putting $i\omega S$, the resistive term, equal to either infinity, equivalent to the rigid case, or to zero, equivalent to the freely sliding case.

Rigid Case

$$i\omega S = \infty$$

$$J_0(k_3 b) = 0$$

as equation (32) case 1B

Freely Sliding Case

$$i\omega S = 0$$

$$J_1(k_3 b) = 0$$

as equation (46) case 2B

For intermediate values the mode numbers lie between those given for the limits, the values determined by the magnitude of the resistive term $i\omega S$.

Case 3.C). Flexural Waves

The formulae in this case become very complicated. The solution will be given by a determinant of the form of equation (35) but containing the resistive term. These solutions will be very tedious to find except with the aid of a computor and will therefore not be further considered here.

Case 3. Conclusion for the Frictionally Controlled Case

Again two sets of modes are found for longitudinal waves. The compressional or "acoustic" type is given by the same equation $J_0(k_2 b) = 0$ as found before, but the shear type have different equations depending upon the magnitude of the restoring force constant. At the limits, these equations tend to those for cases 1 and 2 as would be expected.

For shear and flexural waves, the equations found become too complicated for simple analytical solution.

8. CONCLUSION

We have considered the propagation of different types of wave in an elastic medium constrained in a rigid tube, under boundary conditions varying from the completely rigid to the completely free except for radial displacement.

Different phase velocities of propagation and different cut-off frequencies for the various types of wave and conditions have been found.

In particular, we are interested in the propagation of longitudinal waves. It has been found that for all cases, the same compressional wave modes occur at the same frequencies independently of the shear boundary conditions. These waves correspond to the acoustic modes found in a cylindrical tube when the medium has no shear modulus.

A second set of modes, called here the shear type, also occur with longitudinal waves. The mode frequencies change with the boundary conditions, for the completely rigid case they correspond to the roots of $J_0(\eta_n)=0$, and for the freely sliding case to the roots of $J_1(\xi_n)=0$; for intermediate boundary conditions where the material can slide against a viscous force, the roots lie between those limits. Because the shear velocity is necessarily lower than the compression wave velocity, these frequencies are lower than those of the acoustic type of mode, and they will therefore be encountered sooner than the latter as the frequency of the vibrations is gradually increased.

These modes will therefore be more important from the point of view of measurements upon the medium enclosed in the cylinder and in principle it should be possible to find the shear velocity and the boundary conditions from the mode frequencies.

APPENDIX 6

COMPRESSIONAL WAVE PROPAGATION IN FOAMS

Using a method similar to that of Frohlich and Sack (see Chapter 5)

The model for the foam is a mass of spherical cells, radius R each containing a gas bubble, radius a. We shall consider the impedance of one of these cells to compressional vibrations, arising from a compressional wave of wavelength very much greater than the cell size.

From the gas equation, at the bubble surface,

$$\frac{dp}{dv} = -\frac{\bar{\gamma}P}{v} \qquad (1)$$

where P is the static pressure and v the bubble volume.
In terms of the bubble radius, a,

$$\frac{dp}{da} = -\frac{3\bar{\gamma}P}{a} \qquad (2)$$

Now the bubble is loaded with a certain mass of liquid per unit area of surface. Then at the cell surface, the reaction to a sinusoidal pressure input

$$\frac{P_R}{V_R} = -i\omega\frac{M}{A} + \frac{3\bar{\gamma}P}{-i\omega a} \qquad (3)$$

where M is the liquid mass per cell,

A is the bubble surface area, and

V_R is the radial velocity.

We can rewrite this expression in terms of the expansion ratio, E

$$\frac{P_R}{V_R} = \frac{3\bar{\gamma}P}{-i\omega a}\left[1 - \frac{\omega^2}{\omega_1^2}\right] \qquad (4)$$

where

$$\omega_1^2 = \frac{3\bar{\gamma}P}{a^2\rho_L}(E-1) \tag{5}$$

Now the calculation is repeated assuming that the cell has no structure but contains a continuous medium of bulk modulus $\bar{\kappa}$ and density $\bar{\rho}$. We set up a wave system in this cell where the velocity potential ϕ is given by

$$r\phi(r) = Ae^{-i\omega t - ikr} + Be^{-i\omega t + ikr} \tag{6}$$

k is the wave number of the assumed wave

and $$v_r = -\frac{\partial\phi}{\partial r} \qquad p_r = -i\omega\bar{\rho}\phi \tag{7}$$

From this, and from the assumption that the pressure $\neq \infty$ at $r = 0$ we find the ratio p_R/v_R as before:

$$\frac{p_R}{v_R} = \frac{-i\omega\bar{\rho}R \sin kR}{\sin kR - kR\cos kR} \tag{8}$$

A comparison of eqns 4 and 8

$$\frac{3\bar{\gamma}P}{-i\omega a}\left[1 - \frac{\omega^2}{\omega_1^2}\right] = \frac{-i\omega\bar{\rho}R \sin kR}{\sin kR - kR\cos kR}$$

gives

$$kR\cot kR = 1 - \frac{\omega^2\bar{\rho}\,aR}{3\bar{\gamma}P(1 - \omega^2/\omega_1^2)} \tag{9}$$

Three particular cases can be recognised, viz:-

(i) low frequencies $kR \ll 1$

$$c_0 = \frac{R}{\sqrt{2}}\omega_1\left(\frac{E}{E-1}\right)^{\frac{1}{3}} \qquad \text{or} \qquad \omega_1 = \frac{\sqrt{2}}{R}\left(\frac{E-1}{E}\right)^{\frac{1}{3}}.c_0$$

(ii) when $kR = \frac{\pi}{2}$, then $\cot kR = 0$

$$\frac{c}{c_0} = \frac{2}{\pi}\frac{\sqrt{2}}{\left[1 + \left(\frac{E}{E-1}\right)^{2/3}\right]^{1/2}} \simeq \frac{2}{\pi} \quad (E \text{ large})$$

and this is the limit of the first zone

(iii) when $kR = \pi$ then $\cot kR = -\infty$

$$\omega = \omega_1$$

$$\frac{c}{c_0} = \frac{\sqrt{2}}{\pi}\left(\frac{E-1}{E}\right)^{\frac{1}{3}} \simeq \frac{\sqrt{2}}{\pi} \quad (E \text{ large})$$

Thus the general behaviour is of gradually decreasing velocity as the frequency is increased. Conclusions about the actual cut-off frequency and behaviour beyond this cannot be drawn since the assumption of long wavelength is no longer strictly valid.

REFERENCES

1. Mallock Proc. Roy. Soc. A 84, 391-395 (1910)

2. Wood, A.B. A Textbook of Sound (1955) P.361

3. Karplus, H.B. The velocity of Sound in a Liquid containing Bubbles. Armour Research Foundation, Rep. No. COO-248 (1958)

4. Heinrich, G. Z. Angew Math. Mech. 22, (1942), 117.

5. Mason, W.P. Physical Acoustics and the Properties of Solids (1958)

6. Clark, N.O. A Study of Mechanically produced foam for combating Petrol Fires, London D.S.I.R. (1947)

7. Bailey, M.I. Ind. Eng. Chem., 27, 973 (1935)

8. McBain, J.W., Ross, S. and Brady, A.A., U.S.A., NACA 1840 (1949)

9. McBain, J.W. and Ross. NACA 1841.

10. Bikerman, J.J. Foams (1953)

11. Clark, N.O. and Blackman, M., Trans. Farad. Soc. 44, 1, (1948).

12. Matelon, R. Flow properties of Disperse systems, J.J. Hermans (ed) (1953) p.323.

13. Clark, N.O. Trans. Farad. Soc., 44, 13 (1948)

14. Penney, W.G. and Blackman, M., Ministry of Home Security Research and Experiments Department, Report No. 282 (1943) "Flow of foam through pipes"

15. Siehr Kolloid-Z. 85, 70 (1938)

16. Pfriem Akust. Z., 5, 202 (1940)

17. NavShips 900, 164 vol. 1 "Sound absorption and sound absorbers in water" Dept. of the Navy, Bureau of Ships Wash. DC. (1950).

18. Deryagin (or Derjaguin) B., Kolloid Z. 64, 1, (1933)

19. Bingham, E.C. U.S. Bur. of Standards Bull. 13, 309, (1961)

20. Reiner, M. Rheology, Handbuch der Physik, 6, p.457 (1958)

21. Blackman, M. Trans. Faraday Soc., No. 304 XLIV, p.205 (1948)

22. Deryagin, B. and Ogukhov, E. Kolloid Z., 68, 243 (1934)

23. Blackman, M. Ministry of Home Security REN 420

24. Sibree, J.O. Trans. Faraday Soc., 30, 325 (1934)

25. Hatschek, E. Kolloid, Z. 8, 34, (1911).

26. Frohlich, H. and Sack, R. Proc. Roy. Soc. A., 185, 415 (1946)

27. Guth, E. and Mark, H. Ergebn exact Naturw., 12, 115 (1933)

28. Mooney, M. J. Colloid Sc., 6, 162 (1951)

29. Minnaert, M. Phil. Mag., 16, 235 (1933)

30. Meyer, E. and Skudrzyk, E. Akustica, 3, 434 (1953)

31. Nesterov, V.S. Acoustics, J. (USSR) 5, No. 3, 337, (1959)

32. Foldy, L.L. Phys. Rev., p.107, (Feb. 15, 1945)

33. Macpherson, J.D. Proc. Phys. Soc. B. LXX, p.85 (1956)

34. Rosenhead L., et al. Proc. Roy Soc. A., 226, p.1 (1954)

35. Cambell, I.J. and Pitcher, A.S. Proc. Roy. Soc. A. 243 p.534 (1958)

36. Mott, G. "A Study of wave propagation in thin sheets" U. of London PhD. Thesis (1960).

37. Lethersich W. J. Soc Chem Ind 61 101 (1942)

LIST OF COMMON SYMBOLS

The symbols used in the appendices are defined separately

- a bubble radius
- b tube radius
- c_1 compression wave velocity
- c_2 shear wave velocity
- c_p specific heat at constant pressure
- c_v specific heat at constant volume
- E expansion factor (see App. 1)
- f frequency
- J_n Bessel function of order n
- K bulk modulus
- P Hydrostatic pressure
- x volume ratio (see App. 1)
- Z Heinrich's mixing ratio (see App. 1)
- α attenuation coefficient
- γ specific heat ratio
- Δ logarithmic decrement
- λ Lame's first constant
- μ Lame's second constant, the shear modulus
- ρ density
- τ relaxation or retardation time
- η viscosity

subscripts: G gas, usually air; L liquid, water

the bar (eg $\bar{\rho}$) refers to a mean value and hence to a characteristic of the <u>foam</u>